



Calhoun: The NPS Institutional Archive
DSpace Repository

Theses and Dissertations

1. Thesis and Dissertation Collection, all items

2007-06

Performance analysis of a variable data rate
TCM waveform transmitted over a channel
with AWGN and pulse-noise interference.

Katzourakis, Ioannis

Monterey California. Naval Postgraduate School

<http://hdl.handle.net/10945/3464>

Downloaded from NPS Archive: Calhoun



<http://www.nps.edu/library>

Calhoun is the Naval Postgraduate School's public access digital repository for research materials and institutional publications created by the NPS community.

Calhoun is named for Professor of Mathematics Guy K. Calhoun, NPS's first appointed -- and published -- scholarly author.

Dudley Knox Library / Naval Postgraduate School
411 Dyer Road / 1 University Circle
Monterey, California USA 93943



**NAVAL
POSTGRADUATE
SCHOOL**

MONTEREY, CALIFORNIA

THESIS

**PERFORMANCE ANALYSIS OF A VARIABLE DATA
RATE TCM WAVEFORM TRANSMITTED OVER A
CHANNEL WITH AWGN AND PULSE-NOISE
INTERFERENCE**

by

Ioannis Katzourakis

June 2007

Thesis Advisor:
Second Reader:

Clark Robertson
Tri Ha

Approved for public release; distribution is unlimited

THIS PAGE INTENTIONALLY LEFT BLANK

REPORT DOCUMENTATION PAGE

Form Approved OMB No. 0704-0188

Public reporting burden for this collection of information is estimated to average 1 hour per response, including the time for reviewing instruction, searching existing data sources, gathering and maintaining the data needed, and completing and reviewing the collection of information. Send comments regarding this burden estimate or any other aspect of this collection of information, including suggestions for reducing this burden, to Washington headquarters Services, Directorate for Information Operations and Reports, 1215 Jefferson Davis Highway, Suite 1204, Arlington, VA 22202-4302, and to the Office of Management and Budget, Paperwork Reduction Project (0704-0188) Washington DC 20503.

1. AGENCY USE ONLY (Leave blank)	2. REPORT DATE June 2007	3. REPORT TYPE AND DATES COVERED Master's Thesis	
4. TITLE AND SUBTITLE: Performance Analysis of a Variable Data Rate TCM Waveform Transmitted Over a Channel with AWGN and Pulse-Noise Interference.		5. FUNDING NUMBERS	
6. AUTHOR Ioannis Katzourakis			
7. PERFORMING ORGANIZATION NAME(S) AND ADDRESS(ES) Naval Postgraduate School Monterey, CA 93943-5000		8. PERFORMING ORGANIZATION REPORT NUMBER	
9. SPONSORING /MONITORING AGENCY NAME(S) AND ADDRESS(ES) N/A		10. SPONSORING/MONITORING AGENCY REPORT NUMBER	
11. SUPPLEMENTARY NOTES The views expressed in this thesis are those of the author and do not reflect the official policy or position of the Department of Defense or the U.S. Government.			
12a. DISTRIBUTION / AVAILABILITY STATEMENT Approved for public release; distribution is unlimited		12b. DISTRIBUTION CODE A	
13. ABSTRACT (maximum 200 words) Trellis-coded modulation (TCM) is a technique where forward error correction coding and modulation are treated in a single operation without increasing the channel bandwidth. In this thesis the performance of a variable data rate TCM waveform transmitted over a channel is investigated. In general, TCM systems with rate 1/2 and rate 2/3 convolutional codes and Quadrature-shift keying (QPSK) and 8-phase-shift keying (PSK) modulation, respectively, are considered for two cases. In the first case, the number of memory elements K remains constant as the code rate increases. In the second case, the number of memory elements increases linearly with code rate, so that the total number of memory elements for 8-PSK, r=2/3 TCM is given by $K = 2K_{1/2}$, where $K_{1/2}$ is the number of memory elements for the QPSK, r=1/2 convolutionally encoded TCM. The effects of pulse-noise interference (PNI) in addition to additive white Gaussian noise (AWGN) are considered. It was found that TCM systems have significant resistance to PNI when K is large enough.			
14. SUBJECT TERMS TCM, Trellis code Modulation, code rate 1/2 and 2/3, AWGN, Pulse Noise Interference, QPSK, 8-PSK.		15. NUMBER OF PAGES 121	
16. PRICE CODE			
17. SECURITY CLASSIFICATION OF REPORT Unclassified	18. SECURITY CLASSIFICATION OF THIS PAGE Unclassified	19. SECURITY CLASSIFICATION OF ABSTRACT Unclassified	20. LIMITATION OF ABSTRACT UL

NSN 7540-01-280-5500

Standard Form 298 (Rev. 2-89)
Prescribed by ANSI Std. Z39-18

THIS PAGE INTENTIONALLY LEFT BLANK

Approved for public release; distribution is unlimited

**PERFORMANCE ANALYSIS OF A VARIABLE DATA RATE TCM
WAVEFORM TRANSMITTED OVER A CHANNEL WITH AWGN AND
PULSE-NOISE INTERFERENCE**

Ioannis Katzourakis
Lieutenant, Hellenic Navy
Bachelor of Science, Hellenic Naval Academy, 1996

Submitted in partial fulfillment of the
requirements for the degree of

MASTER OF SCIENCE IN ELECTRICAL ENGINEERING

from the

NAVAL POSTGRADUATE SCHOOL
June 2007

Author: Ioannis Katzourakis

Approved by: Clark Robertson
Thesis Advisor

Tri Ha
Second Reader

Jeffrey Knorr
Chairman, Department of Electrical and Computer Engineering

THIS PAGE INTENTIONALLY LEFT BLANK

ABSTRACT

Trellis-coded modulation (TCM) is a technique where forward error correction coding and modulation are treated in a single operation without increasing the channel bandwidth. In this thesis the performance of a variable data rate TCM waveform transmitted over a channel is investigated. In general, TCM systems with rate 1/2 and rate 2/3 convolutional codes and quadrature-shift keying (QPSK) and 8-phase-shift keying (PSK) modulation, respectively, are considered. The data rate of the later TCM system is 50% faster than that of the former. Two cases are considered. In the first case, the number of memory elements K remains constant as the code rate increases. In the second case, the number of memory elements increases linearly with code rate, so that the total number of memory elements for 8-PSK, $r=2/3$ TCM is given by $K = 2K_{1/2}$, where $K_{1/2}$ is the number of memory elements for the QPSK, $r=1/2$ convolutionally encoded TCM system. The effects of pulse-noise interference (PNI) in addition to additive white Gaussian noise (AWGN) are considered. It was found that both TCM systems have significant resistance to PNI when K is large enough.

THIS PAGE INTENTIONALLY LEFT BLANK

TABLE OF CONTENTS

I.	INTRODUCTION.....	1
A.	BACKGROUND AND RELATED WORK	1
B.	OBJECTIVES	2
C.	THESIS ORAGNIZATION.....	3
II.	TCM BACKGROUND.....	5
A.	TCM	5
1.	General Introduction.....	5
2.	Set Partitioning.....	8
B.	TCM ENCODER	12
C.	TCM PERFORMANCE.....	13
D.	PROBABILITY OF BIT ERROR.....	18
E.	SUMMARY	19
III.	PERFORMANCE OF TCM SYSTEMS IN AWGN	21
A.	INTRODUCTION.....	21
B.	PROBABILITY OF BIT ERROR.....	21
C.	PERFORMANCE WITH CODE RATE 1/2 IN AWGN.....	23
D.	PERFORMANCE OF ENCODER WITH CODE RATE 2/3 IN AWGN.....	27
1.	Encoder with $r=2/3$ and $K=2$	27
2.	Encoder with $r=2/3$ and $K=3$	31
3.	Encoder with $r=2/3$ and $K=4$	34
E.	COMPARISON BETWEEN TCM SYSTEMS WITH DIFFERENT CODE RATES AND AN EQUAL NUMBER OF MEMORY ELEMENTS IN AWGN.....	38
1.	Comparison between Different TCM Systems with $K=2$ in AWGN.....	38
2.	Comparison between Different TCM Systems with $K=3$ in AWGN.....	39
3.	Comparison between Different TCM Systems with $K=4$ in AWGN.....	39
F.	COMPARISON BETWEEN TCM SYSTEMS WITH DIFFERENT CODE RATES AND NUMBERS OF MEMORY ELEMENTS IN AWGN.....	41
1.	Comparison between TCM Systems with $r=1/2$, $K=1$ and $r=2/3$, $K=2$	41
2.	Comparison between TCM Systems with QPSK, $r=1/2$, $K=2$ and 8-PSK, $r=2/3$, $K=4$	42
3.	Comparison between TCM Systems with QPSK, $r=1/2$, $K=2$ and $r=2/3$, $K=8$	43
G.	SUMMARY	44

IV.	PERFORMANCE OF TCM SYSTEMS WITH PULSE NOISE	
	INTERFERENCE.....	45
A.	INTRODUCTION.....	45
B.	PERFORMANCE BOUNDS ON TCM WITH PNI.....	45
C.	PERFORMANCE OF TCM WITH QPSK AND RATE 1/2 ENCODING WITH PNI	46
D.	PERFORMANCE OF TCM WITH 8-PSK AND RATE 2/3 ENCODING WITH PNI	49
1.	Encoder with $K=2$	49
2.	Encoder with $K=3$	53
3.	Encoder with $K=4$	59
E.	COMPARISON BETWEEN QPSK AND 8-PSK TCM SYSTEMS.....	72
1.	Comparison between QPSK, $r=1/2$ and 8-PSK, $r=2/3$ TCM with $K=2$	72
2.	Comparison between QPSK, $r=1/2$ and 8-PSK, $r=2/3$, TCM with $K=3$	74
3.	Comparison between QPSK, $r=1/2$ and 8-PSK, $r=2/3$ TCM with $K=4$	77
4.	Comparison between TCM with QPSK, $r=1/2$, $K=1$ and 8-PSK, $r=2/3$, $K=2$	80
5.	Comparison between TCM with QPSK, $r=1/2$, $K=1$ and 8-PSK, $r=2/3$, $K=3$	82
6.	Comparison between TCM with QPSK, $r=1/2$, $K=1$ and 8-PSK, $r=2/3$, $K=4$	84
7.	Comparison between TCM with QPSK, $r=1/2$, $K=2$ and 8-PSK, $r=2/3$, $K=3$	87
8.	Comparison between TCM with QPSK, $r=1/2$, $K=2$ and 8-PSK $r=2/3$, $K=4$	89
F.	SUMMARY.....	94
V.	CONCLUSIONS AND RECOMMENDATIONS.....	97
A.	CONCLUSIONS	97
B.	RECOMMENDATIONS.....	98
	LIST OF REFERENCES.....	99
	INITIAL DISTRIBUTION LIST	101

LIST OF FIGURES

Figure 1.	One-dimensional, or pulse-amplitude modulation signal, constellation. The 2-PAM signal is equivalent to BPSK.	5
Figure 2.	Two-dimensional amplitude modulation signal constellation.	6
Figure 3.	Two-dimensional phase modulation signal constellation.	6
Figure 4.	(a) Uncoded transmission transmitting 2 bits every T seconds using 4-PSK modulation. (b) Convolutional encoder transmitting with rate $2/3$ and 4-PSK modulation with bandwidth expansion. (c) Convolutional encoder transmitting with rate $2/3$ and 8-PSK modulation with no bandwidth expansion. From [2].	7
Figure 5.	Partitioning of the 8-PSK constellation.	9
Figure 6.	Partition 2 and 3 of 8-PSK with $r=1/2$ and $r=2/3$ encoders, respectively.	10
Figure 7.	TCM encoder with a single parallel transition/branch for 8-PSK signaling. From [6].	11
Figure 8.	Error trellis diagram for TCM encoder with 8-PSK signaling and parallel transitions. From [6].	11
Figure 9.	TCM encoder with no parallel transition using 8-PSK signaling. From [6]....	12
Figure 10.	General structure of Underboeck encoder. From [7].	13
Figure 11.	Gray mapping rule for 4-PSK signal constellation.	15
Figure 12.	Code rate $r=1/2, v=3$ convolutional encoder. After [6].	16
Figure 13.	Signal flow graph for $r=1/2, v=3$ convolutional encoder with Gray mapped QPSK/TCM. From [6].....	17
Figure 14.	Convolutional encoder with code rate $1/2$ and $K=1$	23
Figure 15.	State diagram for the $r=1/2, K=1$ convolutional encoder.....	23
Figure 16.	Signal flow graph for the $r=1/2, K=1$ convolutional encoder with Gray mapping.....	24
Figure 17.	TCM system performance with QPSK modulation and a $r=1/2$ encoder with $K=1$ and Gray mapping in AWGN.	27
Figure 18.	Convolutional encoder with $r=2/3$ and $K=2$. From [6].	28
Figure 19.	State diagram of the $r=2/3, K=2$ encoder shown in Figure 18. From [6]. ..	29
Figure 20.	Trellis diagram of the code generated by the rate $r=2/3, K=2$ encoder shown in Figure 18. From [6].	29
Figure 21.	The probability of bit error for TCM with a $r=2/3, K=2$ encoder and 8-PSK.	31
Figure 22.	Convolutional encoder with $r=2/3$ and $K=3$. From [6].	32
Figure 23.	Trellis diagram of the code generated by the $r=2/3, K=3$ encoder shown in Figure 22. From [6].....	32
Figure 24.	TCM system performance with 8-PSK modulation and a $r=2/3$ encoder with $K=3$ and natural mapping in AWGN	34
Figure 25.	Encoder with code rate $r=2/3$ and $K=4$	35

Figure 26.	Trellis diagram of Encoder with code rate $r = 2/3$ and four memory elements.....	36
Figure 27.	TCM system performance with 8-PSK modulation and a $r = 2/3$ encoder with $K=4$ and natural mapping in AWGN.....	37
Figure 28.	Comparison between TCM with $r=1/2$ and $r=2/3$ encoders for $K=2$	38
Figure 29.	Comparison between TCM with $r=1/2$ and $r=2/3$ encoders for $K=3$	39
Figure 30.	Comparison between TCM with $r=1/2$ and $r=2/3$ encoders for $K=4$	40
Figure 31.	Comparison between TCM with QPSK, $r=1/2$, $K=1$ and 8-PSK, $r=2/3$, $K=2$	41
Figure 32.	Comparison between TCM with QPSK, $r=1/2$, $K=2$ and 8-PSK, $r=2/3$, $K=4$	42
Figure 33.	Comparison between TCM with QPSK, $r=1/2$, $K=2$ and 8-PSK, $r=2/3$, $K=8$	43
Figure 34.	Performance of QPSK, $r=1/2$ TCM system with $K=1$ and PNI with $E_b / N_o = 10.2$ dB.....	48
Figure 35.	Performance of 8-PSK, $r=2/3$ TCM with $K=2$ and PNI with $E_b / N_o = 12.2$ dB.....	53
Figure 36.	Performance of 8-PSK, $r=2/3$, TCM with $K=3$ and PNI with $E_b / N_o = 8.6$ dB.....	59
Figure 37.	Performance of 8-PSK, $r=2/3$, TCM with $K=4$ and PNI with $E_b / N_o = 7.8$ dB.....	70
Figure 38.	Comparison between QPSK, $r=1/2$ and 8-PSK, $r=2/3$ TCM with $K=2$ in PNI for $\rho = 1$ with $E_b / N_o = 8$ dB and $E_b / N_o = 12.2$ dB, respectively.....	72
Figure 39.	Comparison between QPSK, $r=1/2$ and 8-PSK, $r=2/3$ TCM with $K=2$ in PNI for $\rho = 0.2$ with $E_b / N_o = 8$ dB and $E_b / N_o = 12.2$ dB, respectively.....	73
Figure 40.	Comparison between QPSK, $r=1/2$ and 8-PSK, $r=2/3$ TCM with $K=2$ in PNI for $\rho = 0.01$ with $E_b / N_o = 8$ dB and $E_b / N_o = 12.2$ dB, respectively.....	74
Figure 41.	Comparison between QPSK, $r=1/2$ and 8-PSK, $r=2/3$ TCM with $K=3$ for $\rho = 1$ in PNI with $E_b / N_o = 7.4$ dB and $E_b / N_o = 8.6$ dB, respectively.....	75
Figure 42.	Comparison between QPSK, $r=1/2$ and 8-PSK, $r=2/3$ TCM with $K=3$ for $\rho = 0.2$ in PNI with $E_b / N_o = 7.4$ dB and $E_b / N_o = 8.6$ dB, respectively.....	76
Figure 43.	Comparison between QPSK, $r=1/2$ and 8-PSK, $r=2/3$ TCM with $K=3$ for $\rho = 0.01$ in PNI with $E_b / N_o = 7.4$ dB and $E_b / N_o = 8.6$ dB, respectively.....	77
Figure 44.	Comparison between QPSK, $r=1/2$ and 8-PSK, $r=2/3$ TCM with $K=4$ for $\rho = 1$ in PNI with $E_b / N_o = 7.1$ dB and $E_b / N_o = 7.8$ dB, respectively.....	78
Figure 45.	Comparison between QPSK, $r=1/2$ and 8-PSK, $r=2/3$ TCM with $K=4$ for $\rho = 0.2$ in PNI with $E_b / N_o = 7.1$ dB and $E_b / N_o = 7.8$ dB, respectively.....	79
Figure 46.	Comparison between QPSK, $r=1/2$ and 8-PSK, $r=2/3$ TCM with $K=4$ for $\rho = 0.01$ in PNI with $E_b / N_o = 7.1$ dB and $E_b / N_o = 7.8$ dB, respectively.....	80

Figure 47.	Comparison between QPSK, $r=1/2$, $K=1$ TCM and 8-PSK, $r=2/3$, $K=2$ TCM for $\rho=1$ and $\rho=0.2$ with $E_b/N_o=10.2$ dB and $E_b/N_o=12.2$ dB, respectively.....	81
Figure 48.	Comparison between QPSK, $r=1/2$, $K=1$ TCM and 8-PSK, $r=2/3$, $K=2$ TCM for $\rho=0.01$ with $E_b/N_o=10.2$ dB and $E_b/N_o=12.2$ dB, respectively.....	82
Figure 49.	Comparison between QPSK, $r=1/2$, $K=1$ and 8-PSK, $r=2/3$, $K=3$ TCM for $\rho=1$ and $\rho=0.2$ with $E_b/N_o=10.2$ dB and $E_b/N_o=8.6$ dB, respectively.....	83
Figure 50.	Comparison between QPSK, $r=1/2$, $K=1$ and 8-PSK, $r=2/3$, $K=3$ TCM for $\rho=0.01$ with $E_b/N_o=10.2$ dB and $E_b/N_o=8.6$ dB, respectively.....	84
Figure 51.	Comparison between TCM with QPSK, $r=1/2$, $K=1$ and 8-PSK, $r=2/3$, $K=4$ for $\rho=1$ with $E_b/N_o=10.2$ dB and $E_b/N_o=7.8$ dB, respectively.....	85
Figure 52.	Comparison between TCM with QPSK, $r=1/2$, $K=1$ and 8-PSK, $r=2/3$, $K=4$ for $\rho=0.2$ with $E_b/N_o=10.2$ dB and $E_b/N_o=7.8$ dB, respectively.....	86
Figure 53.	Comparison between TCM with QPSK, $r=1/2$, $K=1$ and 8-PSK, $r=2/3$, $K=4$ for $\rho=0.01$ with $E_b/N_o=10.2$ dB and $E_b/N_o=7.8$ dB, respectively....	87
Figure 54.	Comparison between TCM with QPSK, $r=1/2$, $K=2$ and 8-PSK, $r=2/3$, $K=3$ for $\rho=1$ and $\rho=0.2$ with $E_b/N_o=8.1$ dB and $E_b/N_o=8.6$ dB, respectively.....	88
Figure 55.	Comparison between TCM with QPSK, $r=1/2$, $K=2$ and 8-PSK, $r=2/3$, $K=3$ for $\rho=0.01$ with $E_b/N_o=8.1$ dB and $E_b/N_o=8.6$ dB, respectively.....	89
Figure 56.	Comparison between TCM with QPSK, $r=1/2$, $K=2$ and 8-PSK, $r=2/3$, $K=4$ for $\rho=1$ with $E_b/N_o=8.1$ dB and $E_b/N_o=7.8$ dB, respectively.....	90
Figure 57.	Comparison between TCM with QPSK, $r=1/2$, $K=2$ and 8-PSK, $r=2/3$, $K=4$ for $\rho=1$ with $E_b/N_o=8.1$ dB and $E_b/N_o=7.8$ dB, respectively.....	91

THIS PAGE INTENTIONALLY LEFT BLANK

LIST OF TABLES

Table 1.	Average Euclidean weight enumerator for 4-PSK with Gray mapping.	16
Table 2.	Squared-Euclidean distance for naturally mapped 8-PSK.....	28
Table 3.	Performance of 8-PSK, $r=2/3$ TCM with $K=2, 3, 4$ for $P_b = 10^{-5}$ in PNI.	71
Table 4.	Performance of 8-PSK, $r=2/3$, TCM with $K=2, 3, 4$ for $P_b = 10^{-6}$ in PNI.	71
Table 5.	Comparison between QPSK, $r=1/2$ and 8-PSK, $r=2/3$ TCM, each having the same number memory elements for $P_b = 10^{-5}$ in PNI.	92
Table 6.	Comparison between QPSK, $r=1/2$ with $K=1$ and 8-PSK, $r=2/3$ TCM with $K=2, 3,$ and 4 for $P_b = 10^{-5}$ in PNI.....	93
Table 7.	Comparison between QPSK, $r=1/2$ with $K=2$ and 8-PSK, $r=2/3$, TCM with $K=3$ and 4 for $P_b = 10^{-5}$ in PNI.	94

THIS PAGE INTENTIONALLY LEFT BLANK

ACKNOWLEDGMENTS

The author would like to thank his country, Greece, and the Hellenic Navy for giving him the opportunity to be student at NPS.

THIS PAGE INTENTIONALLY LEFT BLANK

EXECUTIVE SUMMARY

Trellis-coded modulation (TCM) is a technique where forward error correction coding and modulation are treated in a single operation without increasing the channel bandwidth. In this thesis the performance of a variable data rate TCM waveform transmitted over a channel is investigated. TCM was initially proposed by Ungerboeck [1] and combines binary convolutional codes with an M -ary signal constellation $M = 2^{m+1}$.

In this thesis, TCM systems with rate 1/2 and rate 2/3 convolutional codes and quadrature-shift keying (QPSK) and 8-phase-shift keying (PSK) modulation, respectively, are examined when additive white Gaussian noise (AWGN) as well as both AWGN and pulse-noise interference (PNI) are present. The data rate of the latter system is 50% faster than that of the former given the same channel bandwidth.

In the first case, where only AWGN is considered and the number of memory elements K remains constant as the code rate increases, the QPSK, $r=1/2$ system performs better than the 8-PSK, $r=2/3$ system. This was expected since using a higher code rate yields higher data rates at the cost of a loss in performance.

A comparison between the two systems was made when the number of memory elements increased linearly with code rate, so that the total number of memory elements for 8-PSK, $r=2/3$ TCM is given by $K = 2K_{1/2}$, where $K_{1/2}$ is the number of memory elements for the QPSK, $r=1/2$ TCM. Initially, only AWGN was taken into consideration. A QPSK, $r=1/2$, $K=1$ system has better performance than a 8-PSK, $r=2/3$, $K=2$ system. Increasing the number of memory elements in both encoders by a factor of two, we obtain an overall improvement, but for $P_b > 10^{-5}$, the QPSK, $r=1/2$ system still has better performance. For $P_b < 10^{-5}$, the 8-PSK, $r=2/3$ system had a slightly better performance, on the order of 0.5 dB.

When the 8-PSK, $r=2/3$ system has four times as many encoder memory elements as the QPSK, $r=1/2$ system, the 8-PSK, $r=2/3$ system has better performance. In this case, we obtain both a higher data rate and better performance, but the complexity of the decoder is increased significantly.

In the second case, the effect of both AWGN and PNI were considered. Both TCM systems exhibit significant resistance to PNI when K is large enough and when K increases, the degradation of the system due to PNI decreases, increasing the robustness of the system in PNI. Even small K results in some immunity from the degradation caused by PNI.

The two systems were compared for the same total number of encoder memory elements. The QPSK, $r=1/2$ system has better performance than the 8-PSK, $r=2/3$ TCM system for $K=2$, but as K increases and ρ decreases, the 8-PSK, $r=2/3$ system performs better than QPSK, $r=1/2$ system when E_b / N_o is chosen for each system such that P_b is the same for both systems when $E_b / N_i >> 1$.

Finally, a comparison between the QPSK, $r=1/2$ and the 8-PSK, $r=2/3$ systems were made with the latter system having more memory elements than QPSK, $r=1/2$ system. Under these conditions the performance of the 8-PSK, $r=2/3$ system is better than that of the QPSK, $r=1/2$ system, and the difference between the two systems increases when the fraction of the time the PNI is on decreases.

I. INTRODUCTION

A. BACKGROUND AND RELATED WORK

Communications are vital in modern society. The transmission of information increases everyday, and data rates as high as possible are needed. In addition, reliable communication systems must receive data with the minimum probability data bit error, the minimum transmitted signal power, and the minimum possible channel bandwidth.

Shannon's noisy channel coding theorem states that if the channel bit rate is greater than channel capacity, then error free communication is not possible. When the channel bit rate is less than channel capacity, we can approach the Shannon limit by implementing an error control code. *Automatic repeat request* (ARQ) and *forward error correction* (FEC) coding are two basic error control strategies.

ARQ is used for a two-way transmission system. When errors are detected, the receiver sends a request to the transmitter requesting a repeat of the message. The request is repeated until the message is received correctly.

On the other hand, FEC coding is used for a one-way communication link and employs error-correcting codes that attempt to correct the errors detected at the receiver. Although many communication systems today employ some form of FEC coding, FEC coding requires more sophisticated decoding equipment than ARQ.

Error correction coding both detects and corrects errors and is implemented by transmitting redundant bits. The total number of coded bits exceed the number of information bits, which means that the effective information rate is lower when the channel bandwidth is the same. On the other hand, keeping the same information rate implies that FEC requires more bandwidth than for the uncoded signal. Using a code rate $r = k / n$, FEC requires a bandwidth expansion of $1/r$ where $r < 1$.

Trellis-coded modulation (TCM) is a technique that introduces FEC coding without decreasing data rate or increasing the channel signal bandwidth. With TCM, channel coding and modulation take place in a single operation in the transmitter. Trellis-code modulation was introduced by Ungerboeck [1], in 1982 and is used in band-limited

channels where bandwidth expansion is not desirable. Although the number of transmitted bits are increased in order to achieve error correction coding, the information bit rate and the bandwidth remain constant.

The redundant bits which are transmitted with TCM are obtained by expanding the size of the signal constellation with respect to uncoded systems. Using the technique of *mapping by set partitioning*,[1, 2, 3] Ungerboeck introduced error correction coding, expanding the signal set rather than increasing the bandwidth.

B. OBJECTIVES

TCM has been examined extensively for additive white Gaussian noise (AWGN), but the effects of pulse-noise interference (PNI) on TCM systems have previously been evaluated only for TCM systems with quadrature phase-shift keying (QPSK) [4]. Because of the importance of high data rate communications to modern military systems as well as the necessity for military systems to potentially operate in a hostile electronic environment, it is important to understand the effects of narrowband noise interference on TCM systems. The effect of both AWGN and PNI on TCM systems are examined in this thesis.

The performance of two specific TCM systems are examined, the first with QPSK modulation and rate $r = 1/2$ convolutional coding and the second with 8-phase-shift keying (8-PSK) modulation and $r = 2/3$ convolutional coding both for different numbers of encoder memory elements $K=1, 2, 3$, and 4. Two types of comparison are also made. First, the number of memory elements K is kept constant as the code rate is increased, and the performance between TCM with code rate $r = 1/2$ and QPSK modulation and TCM with code rate $r = 2/3$ and 8-PSK is compared. Second, the number of memory elements is increased linearly with code rate, so the QPSK, $r=1/2$ system has half as many memory elements as the 8-PSK, $r=2/3$ system.

The approach taken to evaluate the effects of PNI on TCM systems is model the channel and the noise in such a manner as to allow analytic expressions to be derived for the probability of bit error. As previously mentioned, to the best of the author's knowledge, this has only been done previously for the special case of TCM with QPSK

modulation [4]. The results derived in this thesis for 8-PSK TCM and the general bound developed in Chapter IV are novel. The data have been produced using Mathcad, transferred into Excel and reproduced as graphs using Matlab.

C. THESIS ORAGNIZATION

Apart from Chapter I, which is the introduction and includes the objective of this thesis, there are four more chapters. In Chapter II, some background theory on TCM is presented, in particular the basic theory of TCM and set partitioning. TCM systems with code rate $r = 1/2$, QPSK modulation and code rate $r = 2/3$, 8-PSK modulation in AWGN for encoders with $K=1, 2, 3, 4$ memory elements are examined in Chapter III. For the same channel bandwidth, the latter TCM system can transmit data 50% faster than the former TCM system. The effect on the bound on the probability of bit error P_b with forward error correction coding of the number of summation terms that are used to compute P_b is also examined. In Chapter IV, the performance of the two TCM systems examined in Chapter III are examined when both AWGN and pulse-noise interference (PNI) are present. Chapter V summarizes the thesis conclusions and makes recommendations for future work.

THIS PAGE INTENTIONALLY LEFT BLANK

II. TCM BACKGROUND

A. TCM

1. General Introduction

Trellis-coded modulation is a method that combines binary convolutional codes with code rate $r = m/(m+1)$ with M -ary signal constellations. With TCM forward error correction coding can be achieved without increasing the bandwidth compared to the corresponding uncoded modulation with the same data rate.

The M -ary signal constellation may be in one or two dimensions as shown in Figures 1, 2, and 3, where the horizontal axis in each figure corresponds to the normalized in-phase baseband signal amplitude, and the vertical axis corresponds to the normalized quadrature baseband signal amplitude. Each black dot represents an M -ary symbol, where each symbol represents q bits and $M = 2^q$.

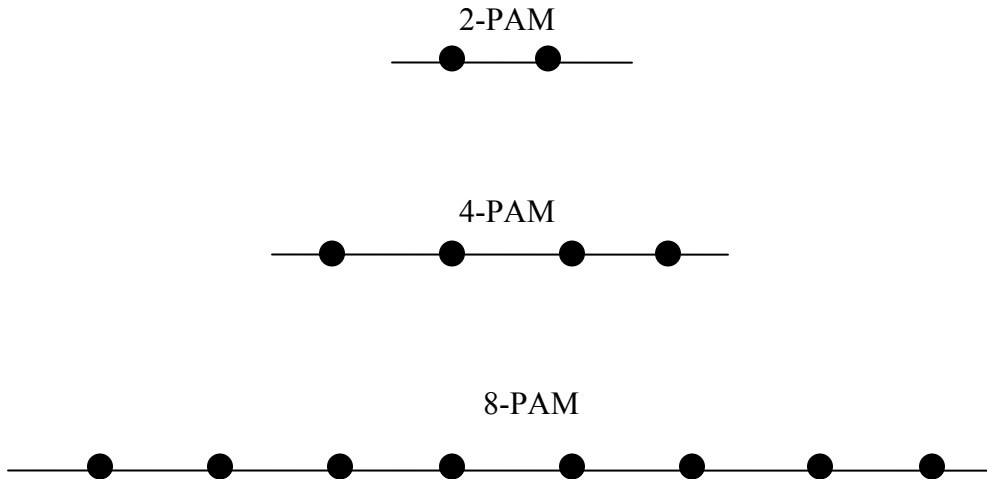


Figure 1. One-dimensional, or pulse-amplitude modulation signal, constellation.
The 2-PAM signal is equivalent to BPSK.

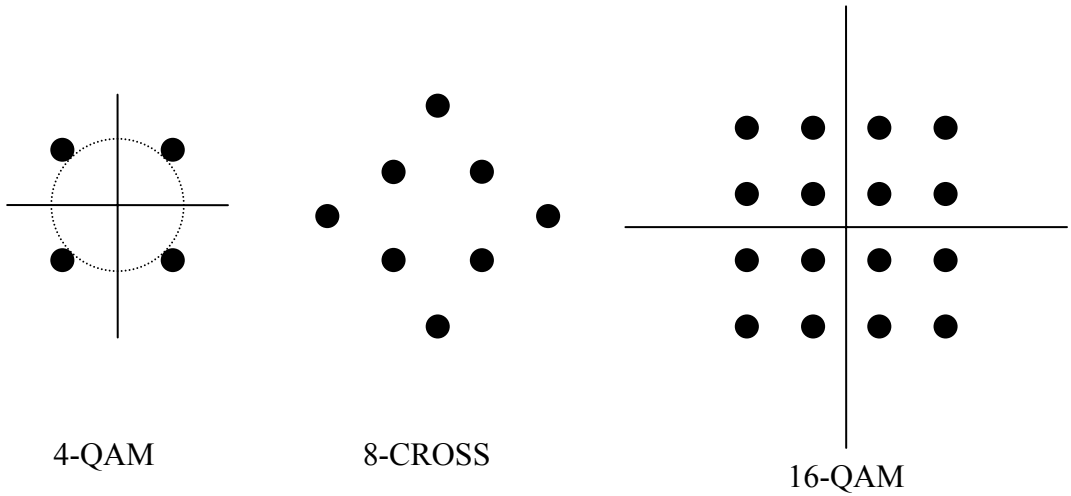


Figure 2. Two-dimensional amplitude modulation signal constellation.

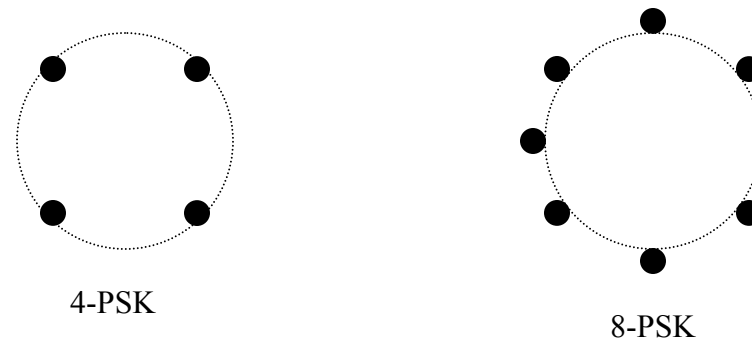


Figure 3. Two-dimensional phase modulation signal constellation.

From Figures 2 and 3 we can see that *4-quadrature amplitude modulation* (4-QAM) and 4-PSK are equivalent. The difference is that 4-QAM, just like any QAM signal, is generated by applying amplitude modulation. On the other hand, 4-PSK, like any PSK signal, is generated by applying phase modulation. PSK signals have the same amplitude regardless of the symbol transmitted.

TCM uses signal set expansion in order to avoid increasing the signal bandwidth, and coding gain is achieved without increasing the rate at which symbols are transmitted. An example that is described in [3] makes the TCM method clearer.

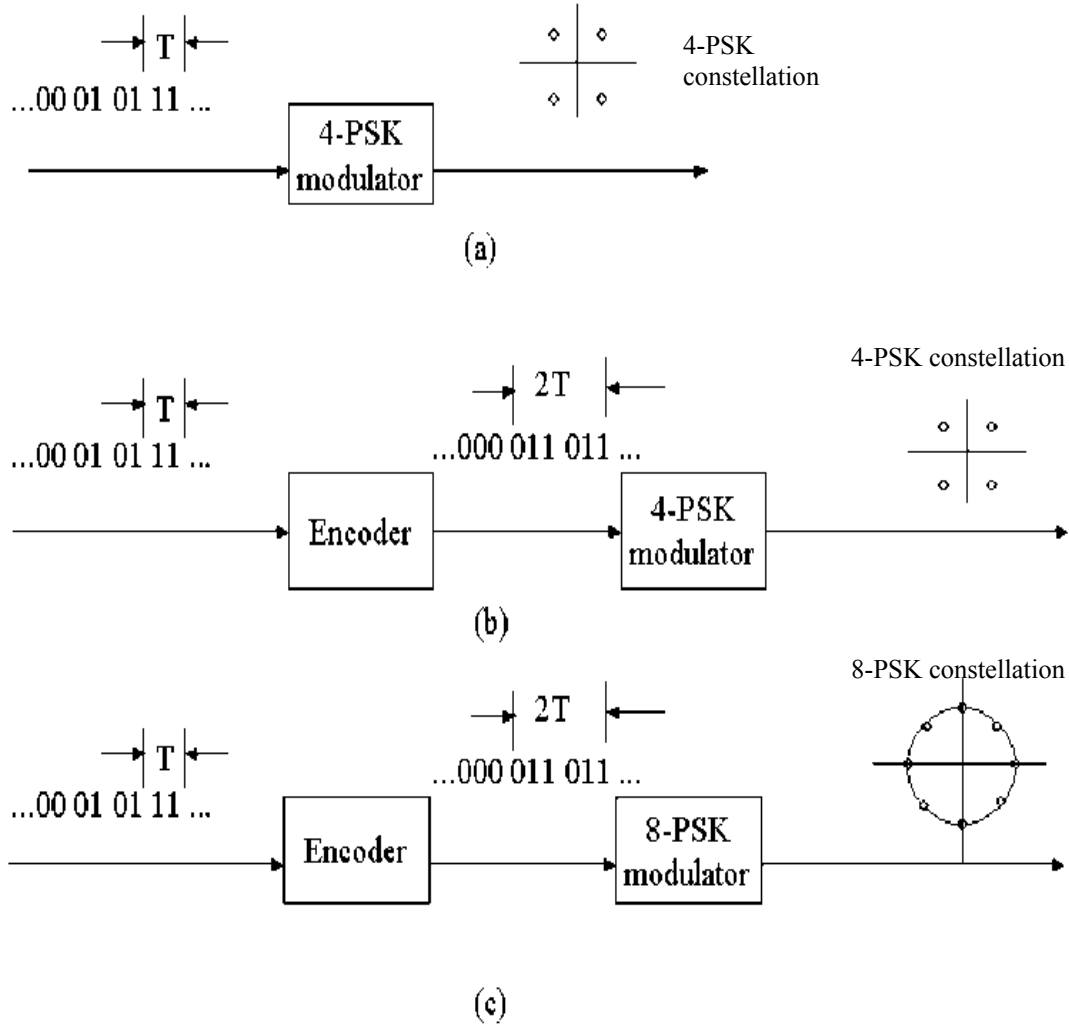


Figure 4. (a) Uncoded transmission transmitting 2 bits every T seconds using 4-PSK modulation. (b) Convolutional encoder transmitting with rate $2/3$ and 4-PSK modulation with bandwidth expansion. (c) Convolutional encoder transmitting with rate $2/3$ and 8-PSK modulation with no bandwidth expansion. From [2].

Figure 4(a) shows a digital scheme that transmits one signal consisting of 2 bits every T seconds using 4-PSK modulation.

Figure 4(b) shows a 2/3 convolutional encoder using 4-PSK modulation. Now the signal represents 4/3 information bits every $2T/3$ seconds in order to have the same information rate as the initial uncoded system in Figure 1(a). The disadvantage of this configuration is that the bandwidth is increased by 50% as compared with the uncoded system.

Figure 4(c) shows a convolutional encoder with code rate 2/3 using 8-PSK modulation. The duration of a symbol is not reduced, and each symbol contains two information bits. In this case there is no bandwidth expansion since 8-PSK and 4-PSK occupy the same bandwidth given the same symbol rate. The disadvantage in this case is the increased complexity of the encoder as compared to the encoder in Figure 4(b).

With TCM, error correction coding and modulation are combined into one step. The redundant bits are created by expanding the modulation signal set with respect to the signal set that is required for uncoded modulation. Error control is provided by signal set expansion without increasing the bandwidth. In this technique, which is called *mapping by set partitioning* [1, 2, 5] the signal set is designed to have maximum free Euclidean distance d_{free} between symbols as compared to maximizing the Hamming distance between sequences. For 2-AM and 4-PSK, Euclidean distance and Hamming distance are equivalent, but this is not true for $M>4$.

2. Set Partitioning

In Figure 5, we see a partitioning of the 8-PSK signal constellation. The signal is partitioned into subsets, increasing the Euclidean distance between symbols in each subset.

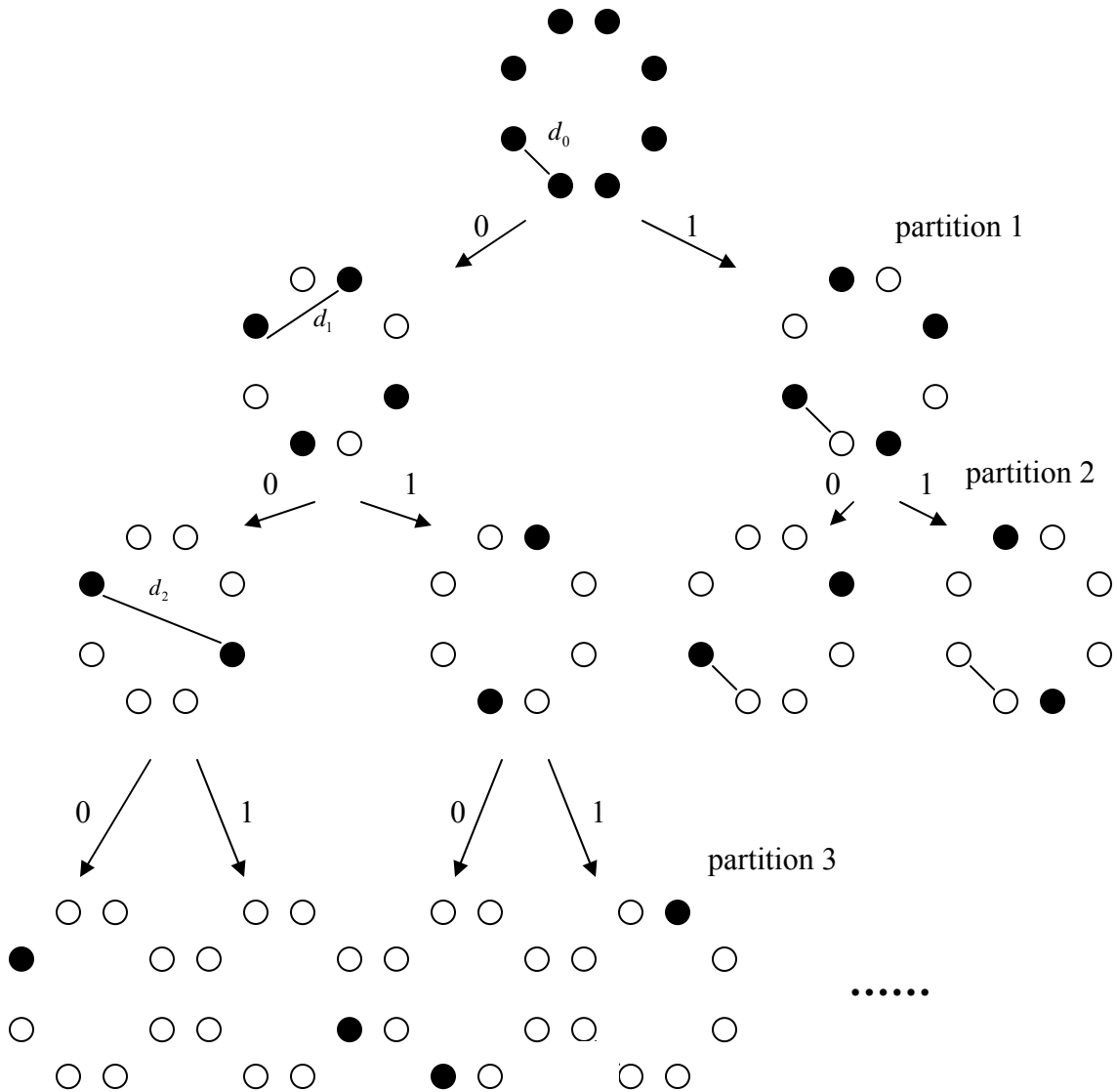


Figure 5. Partitioning of the 8-PSK constellation.

Before partitioning, the minimum distance of 8-PSK is given by d_0 . For Partition 1, the signal constellation is divided into two subsets, where each subset consists of four symbols, and the minimum distance between symbols in each subset has increased to d_1 , as we see in Figure 5.

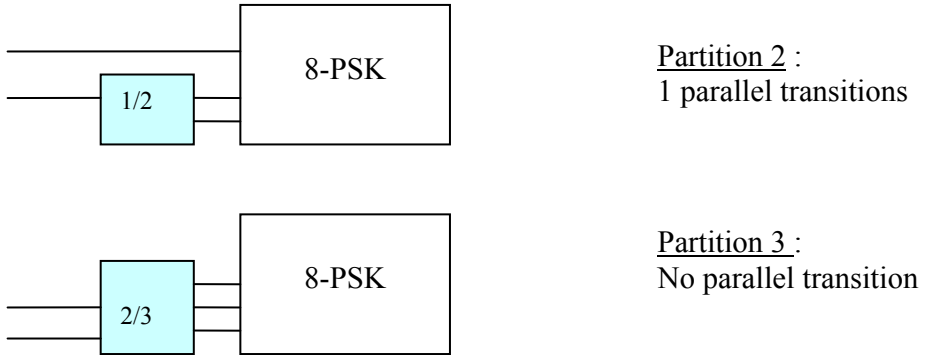


Figure 6. Partition 2 and 3 of 8-PSK with $r = 1/2$ and $r = 2/3$ encoders, respectively.

In Partition 2, the signal constellation is divided into four subsets, where each subset consists of two symbols, and the minimum distance between symbols in each subset has increased to d_2 as we see in Figure 5. As can be seen from Figure 6, we apply one bit to an encoder with code rate $r = 1/2$ and the encoder output selects a symbol set from the second partition level. The remaining one bit is used to select one of the two symbols from that specific set. In this case, the TCM error trellis has one parallel transition, which is shown in Figure 5.

In Figures 7 and 8 we see a TCM encoder and the error trellis diagram for 8-PSK signaling with a single parallel transition, respectively, when two information bits per unit time are transmitted.

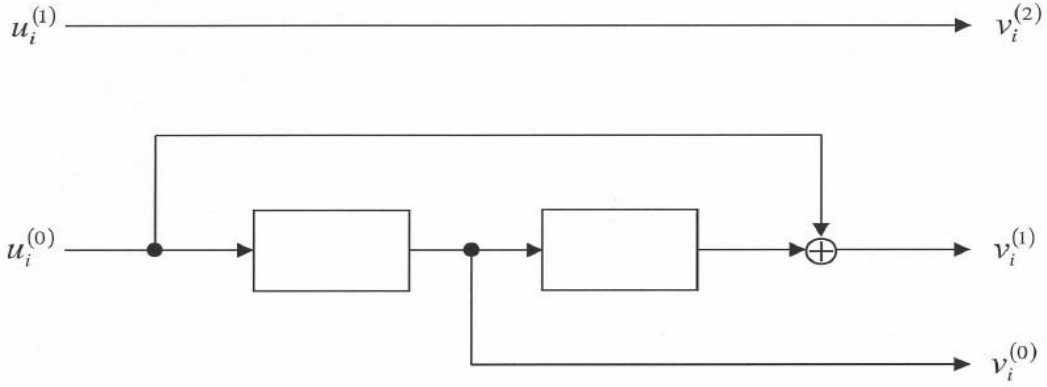


Figure 7. TCM encoder with a single parallel transition/branch for 8-PSK signaling.
From [6].

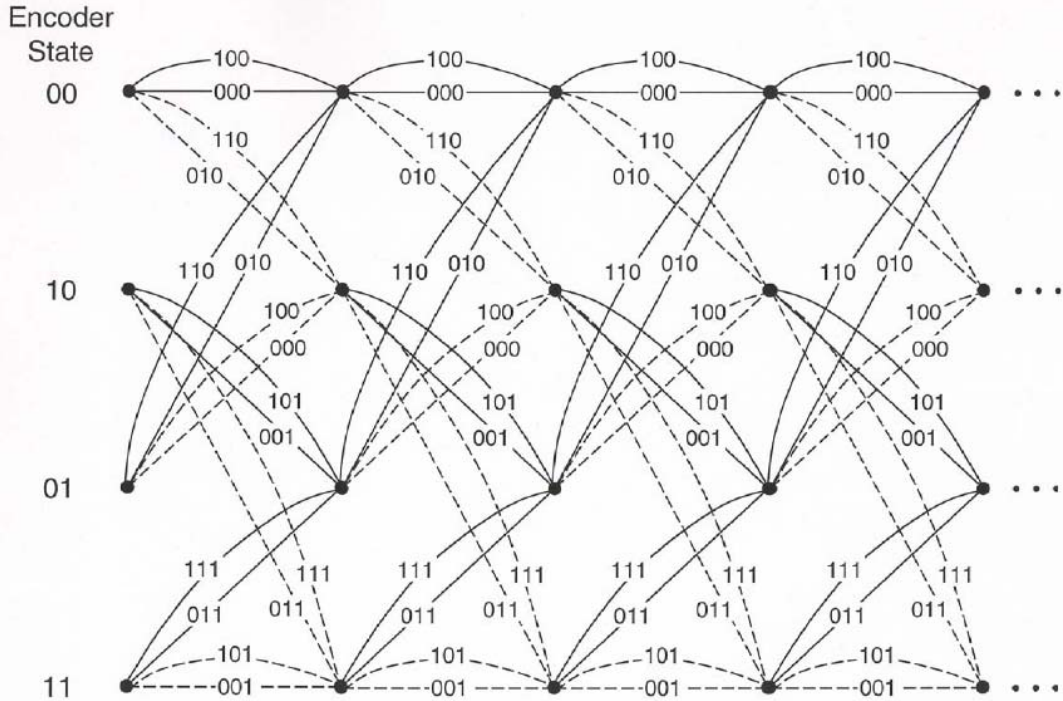


Figure 8. Error trellis diagram for TCM encoder with 8-PSK signaling and parallel transitions. From [6].

In Partition 3, the signal constellation is divided into eight subsets, where each subset consists of one only symbol as we see in Figure 5. If we apply two bits to an encoder with code rate $r = 2/3$, the encoder output selects a symbol set from the third

partition level. As we see from Figure 6, there are no parallel transitions. An example of a TCM encoder with no parallel transition is shown in Figure 9.

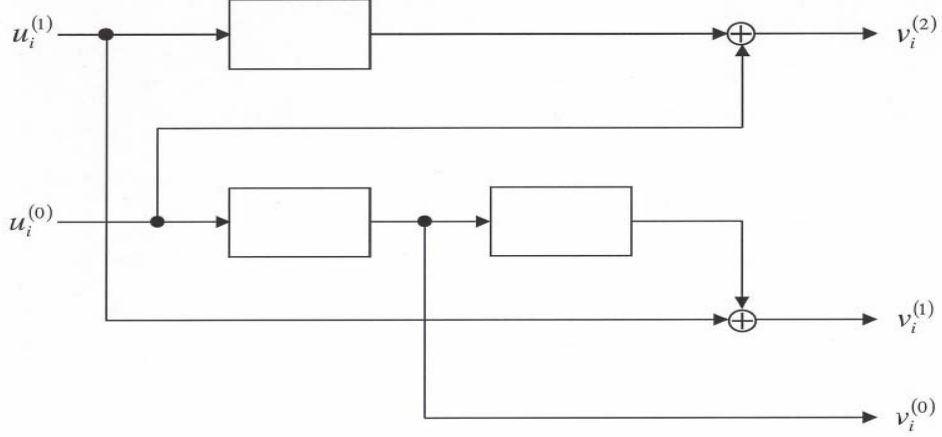


Figure 9. TCM encoder with no parallel transition using 8-PSK signaling. From [6].

B. TCM ENCODER

When we want to transmit m bits per symbol duration T , without coding we can use either 2^m -PSK or 2^m -QAM. In order to achieve forward error correction coding without increasing the bandwidth compared to uncoded modulation and keep the same data rate, we implement TCM using 2^{m+1} -PSK or 2^{m+1} -QAM and partition the signal constellation.

As illustrated in the last section, if we apply one bit to an encoder of code rate $r = 1/2$, the encoder output chooses one of the subsets from the second partition level. Each of the subsets contains 2^{m-1} symbols, and there are $2^{m-1} - 1$ parallel transitions in the TCM trellis. If we apply two bits to an encoder with code rate $r = 2/3$, the output chooses one of the subsets from the third partition level. Each of the subsets contains 2^{m-2} symbols, and there are $2^{m-2} - 1$ parallel transitions in the TCM trellis. Finally, if we apply m bits to an encoder of code rate $r = m/(m+1)$, the output chooses one of the

subsets from the $(m+1)$ partition level. Each of the subsets contains one symbol, and there are no parallel transitions in the TCM trellis. In Figure 10 we see the general structure of Underboeck encoder.

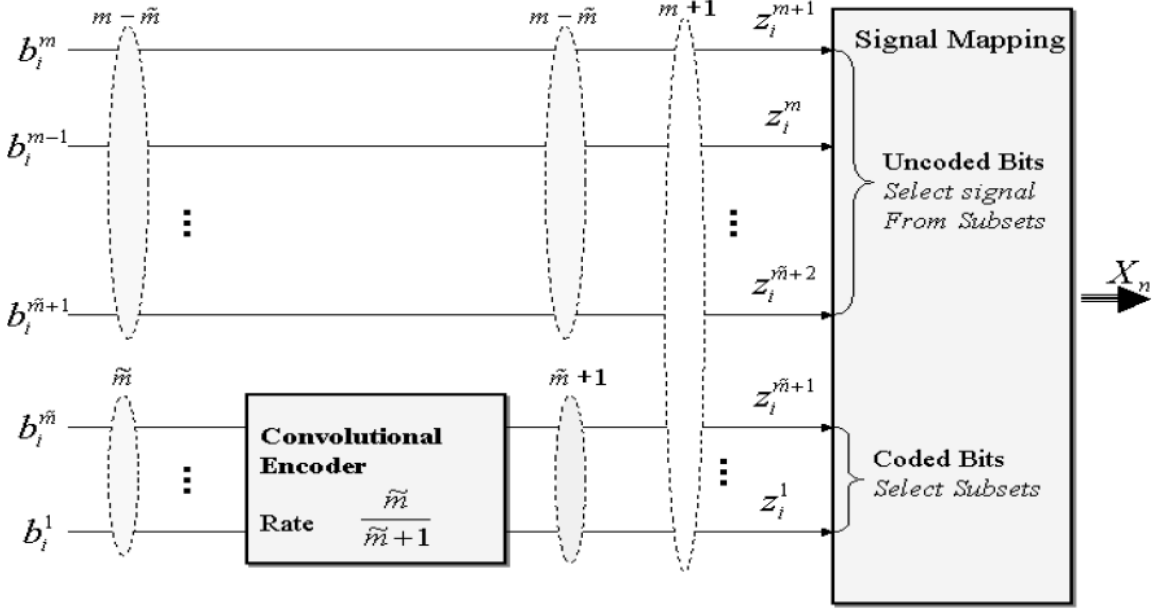


Figure 10. General structure of Underboeck encoder. From [7].

C. TCM PERFORMANCE

Convolutionally encoded systems are linear [8]. For this reason, the encoder output sequences v_1, v_2, \dots, v_n can be obtained as the convolution of the input sequence \mathbf{u} with the appropriate impulse responses.

TCM systems are not in general linear systems. As a result, the probability of bit error depends on the specific code sequence that was transmitted, and it is not possible to use the same approach that is used for conventional convolutional codes. For TCM we must first obtain the *average input-output weight enumerating function* (AIOWEF) $T_{ave}(X, Y)$.

The AIOWEF can be determined by computing the error vector of code sequence v and code sequence v' , which is defined as $e(v, v') = v \oplus v'$ [6]. Although TCM is not generally linear, a convolutional code is a linear code, so without loss of generality, we can choose $v' = 0$, and $e = v$. As a result, the error trellis is identical to the convolutional code trellis with the difference that each branch is labeled with the error vector for that specific transition.

The signal flow graph of the convolutional code shows each branch from one state to another. Each branch is labeled with the product $X^d Y^j Z$, called the branch transmittance, where d is the weight of the encoder output and j is the weight of the information sequence for that specific branch [6]. The exponent of Z corresponds to the length of a branch which is equal to one, since the transition is from one state to the next.

In order to obtain the AIOWEF, we need the *average Euclidean weight enumerator* (AEWE) $\Delta_e^2(X)$, which is the average of the squared-Euclidean distance enumerating functions between all pairs of signal points in the constellation having the same error vector [5]. The *average Euclidean weight enumerator* (AEWE) $\Delta_e^2(X)$ is

given by $\Delta_e^2(X) = \frac{1}{M} \sum_v X^{\Delta_v^2(e)}$, where $\Delta_v^2(e)$ is the squared-Euclidean distance between v and some arbitrary reference v' and M is the number of sequences that have the same error vector.

The AEWE depends on how bits are assigned to constellation symbols, referred to as mapping. For example, consider the mapping shown in Figure 11, referred to as Gray mapping. The procedure is the same for other signal mappings.

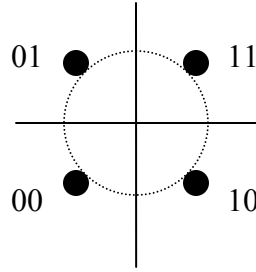


Figure 11. Gray mapping rule for 4-PSK signal constellation.

From Figure 11, for Gray mapping we see that for $\mathbf{e}(00,01)=\mathbf{e}(11,01)=01$. Since $\Delta_e^2(X)=\frac{1}{M} \sum_v X^{\Delta_v^2(e)}$, we have in this case $\Delta_{01}^2(X)=\frac{1}{2} \sum (X^2 + X^2)=\frac{1}{2} X^2 + \frac{1}{2} X^2 = X^2$. Similarly, $\mathbf{e}(00,11)=\mathbf{e}(01,10)=11$ and $\Delta_{11}^2(X)=\frac{1}{2} \sum (X^4 + X^4)=\frac{1}{2} X^4 + \frac{1}{2} X^4 = X^4$. For $\mathbf{e}(00,10)=\mathbf{e}(01,11)=10$ we have $\Delta_{10}^2(X)=\frac{1}{2} \sum (X^2 + X^2)=\frac{1}{2} X^2 + \frac{1}{2} X^2 = X^2$. Finally, for $\mathbf{e}(00,00)=\mathbf{e}(11,11)=00$ we have $\Delta_{00}^2(X)=\frac{1}{2} \sum (X^0 + X^0)=\frac{1}{2} X^0 + \frac{1}{2} X^0 = X^0 = 1$.

These results are summarized in Table 1.

Table 1. Average Euclidean weight enumerator for 4-PSK with Gray mapping.

<u>e</u>	<u>w(e)</u>	<u>$\Delta_e^2(X)$</u>
00	w(00)=0	$\Delta_{00}^2(X) = X^0$
01	w(01)=1	$\Delta_{01}^2(X) = X^2$
10	w(10)=1	$\Delta_{10}^2(X) = X^2$
11	w(11)=2	$\Delta_{11}^2(X) = X^4$

In order to obtain the AIOWEF, we replace X^d in the branch transmittance with the AEWE $\Delta_e^2(X)$.

For the convolutional encoder with code rate $r=1/2$ and constraint length $v=3$, shown in Figure 12, the AIOWEF is obtained by replacing X with X^2 on the signal flow graph, which is shown in Figure 13.

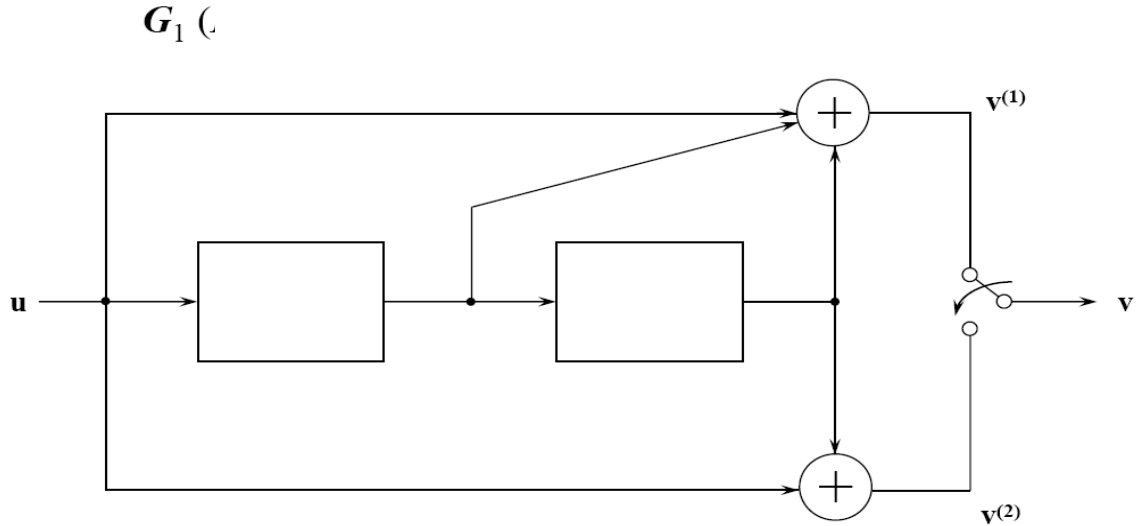


Figure 12. Code rate $r=1/2, v=3$ convolutional encoder. After [6].

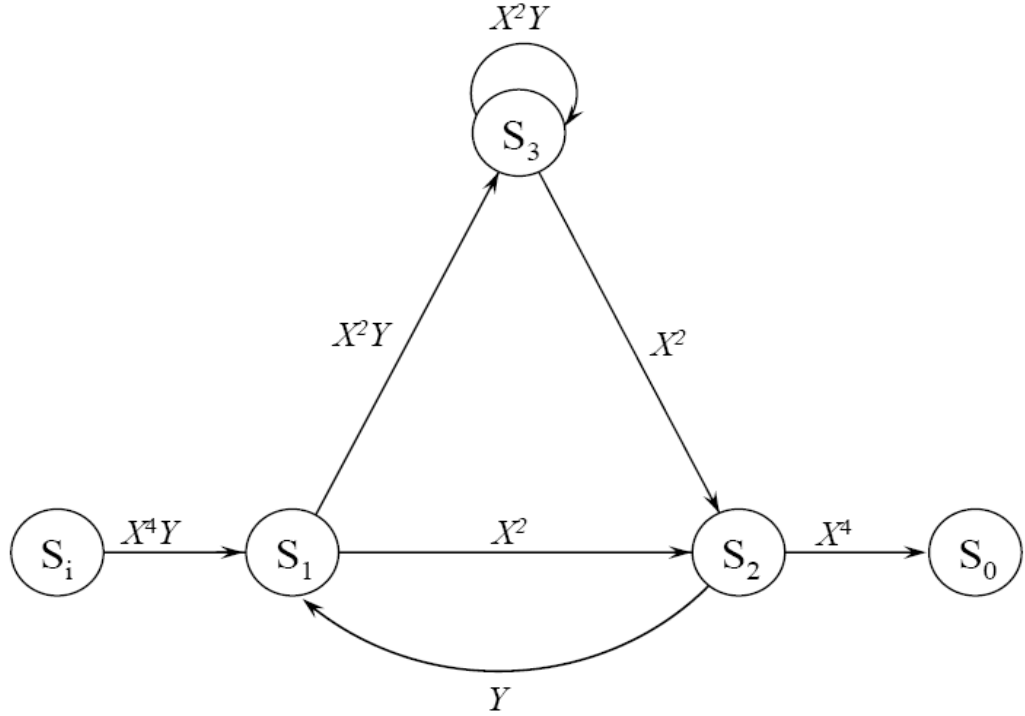


Figure 13. Signal flow graph for $r=1/2$, $v=3$ convolutional encoder with Gray mapped QPSK/TCM. From [6].

We know that the transfer function of the convolutional encoder shown in Figure 12 is given by

$$T(X, Y) = X^5Y(1 - 2XY) \quad (2 - 1)$$

Since $T_{ave}(X, Y) = T(X^2, Y)$ then from (2.1) we have

$$T_{ave}(X, Y) = X^{10}Y[1 - 2X^2Y]^{-1} \quad (2 - 2)$$

We also know that

$$(1 - r)^{-1} = \frac{1}{1 - r} = 1 + r + r^2 + r^3 + r^4 + r^5 + \dots \quad (2 - 3)$$

From (2.2), (2.3) and for $r = 2X^2Y$, we obtain the AIOWEF for the TCM encoder shown in Figure 12 in series form as

$$T_{ave}(X, Y) = X^{10}Y[1 + 2X^2Y + 4X^4Y^2 + 8X^6Y^3 + 16X^8Y^4 + \dots] \quad (2 - 4)$$

From equation (2.4), we see that there is one path with a squared-Euclidean distance of 10, two paths with a squared-Euclidean distance of 12, four paths with a squared-Euclidean distance of 14, eight paths with a squared-Euclidean distance of 16, sixteen paths with a squared-Euclidean distance of 18, and so on.

D. PROBABILITY OF BIT ERROR

The probability of bit error for a TCM system using a convolutional encoder with code rate $r = m/(m+1)$ and 2^m -PSK modulation is given by [6]

$$P_b \approx P_b(\text{parallel}) + \frac{B_{d_{\text{free}}}}{m} Q\left(\sqrt{\frac{E_{sc} d_{\text{free}}^2}{2N_0}}\right) \quad (2 - 5)$$

where $P_b(\text{parallel})$ is the probability of choosing an incorrect parallel path, $B_{d_{\text{free}}}$ is the total number of information bit errors on all non-parallel code sequences that are a distance d_{free} from the correct code sequence, N_0 is the power spectral density of the AWGN, and $E_{sc} = r(m+1)E_b$, where E_b is the average bit energy. As we have seen from the equation (2-5), parallel paths are not desirable because they result in an irreducible error floor. For that reason, in TCM systems it is often preferable to use an encoder with code rate $r = m/(m+1)$ and $2^{(m+1)}$ -PSK modulation. In that case, the probability of bit error is given by

$$P_b \approx \frac{B_{d_{free}}}{m} Q\left(\sqrt{\frac{E_{sc} d_{free}^2}{2N_0}}\right) \quad (2 - 6)$$

where $B_{d_{free}}$ is the total number of information bit errors on all code sequences that are a Euclidean distance d_{free} from the correct code sequence.

In next chapter we will discuss the derivation of equation (2-6) in more detail.

E. SUMMARY

In this chapter we examined the main principles of TCM systems. In the next chapter we will investigate in more detail TCM systems with code rate $r = 1/2$ and QPSK modulation and $r = 2/3$ and 8-PSK modulation and the effect of AWGN as well as the number of memory elements in the convolutional encoders.

THIS PAGE INTENTIONALLY LEFT BLANK

III. PERFORMANCE OF TCM SYSTEMS IN AWGN

A. INTRODUCTION

In Chapter II, we examined the background necessary to understand the basic principles of TCM. One- and two-dimensional signal constellations, transmission of uncoded and coded bits with or without bandwidth expansion, partitioning, trellis diagrams, encoders with and without parallel transmissions, the AEWE, and the AIOWEF of the convolutional code are some of the principles that were discussed.

In this chapter, we apply these principles to TCM systems with code rate $r = 1/2$, QPSK modulation and code rate $r = 2/3$, 8-PSK modulation in AWGN for encoders with $K=1, 2, 3, 4$ memory elements and compare the two systems.

We also examine the effect on the bound on the probability of bit error with forward error correction coding of the number of summation terms that are used to compute P_b .

B. PROBABILITY OF BIT ERROR

The probability of bit error P_b for convolutionally encoded system is upper bounded by [9]:

$$P_b < \frac{1}{k} \sum_{d=d_{free}}^{\infty} B_d P_d \quad (3 - 1)$$

where P_d is the probability that a path of weight d is selected, k is the number of encoded information bits for each block of n code bits, d is the Hamming weight of the path, d_{free} is the minimum Hamming distance, and B_d is the total number of information bit errors that can occur when a path of weight d is selected.

In an analogous manner, for a TCM system with no parallel transitions, P_b is upper bounded by either [6]:

$$P_b < \frac{1}{m} \sum_{i=1}^{\infty} B_{d_i} Q\left(\sqrt{\frac{E_{sc} d_i^2}{2N_0}}\right) \quad (3 - 2)$$

or

$$P_b < \frac{1}{m} Q\left(\sqrt{\frac{E_{sc} d_{free}^2}{2N_0}}\right) \exp\left(\frac{E_{sc} d_{free}^2}{4N_o}\right) \frac{\partial T_{ave}(X, Y)}{\partial Y} \Big|_{X = \exp(-E_{sc}/4N_o), Y=1} \quad (3 - 3)$$

where B_{d_i} is the total number of information bit errors on all paths that are a Euclidean distance d_i^2 from the correct path and $d_i^2 = d_{free}^2$ [6]. When P_b is less than 10^{-2} , the first four nonzero terms are generally sufficient.

We obtain the B_{d_i} 's from the AIOWEF using the same procedure as for convolutional codes:

$$\frac{\partial T_{ave}(X, Y)}{\partial Y} \Big|_{Y=1} = \sum_{i=1}^{\infty} B_{d_i} X^{d_i^2} \quad (3 - 4)$$

The probability of bit error for TCM with no parallel paths is reasonably approximated by the first term of equation (3-2) when $E_b / N_o \gg 1$:

$$P_b \approx \frac{B_{d_{free}}}{m} Q\left(\sqrt{\frac{E_{sc} d_{d_{free}}^2}{2N_0}}\right) \quad (3 - 5)$$

C. PERFORMANCE WITH CODE RATE 1/2 IN AWGN.

For QPSK modulation, we use a rate $\frac{1}{2}$ convolutional code to obtain TCM with parallel transitions. On this section, we consider a simple convolutional encoder with $K=1$ in order to illustrate the basic concept.

Figure 14 is a block diagram of a convolutional encoder with $K = 1$ and code rate $r = 1/2$.

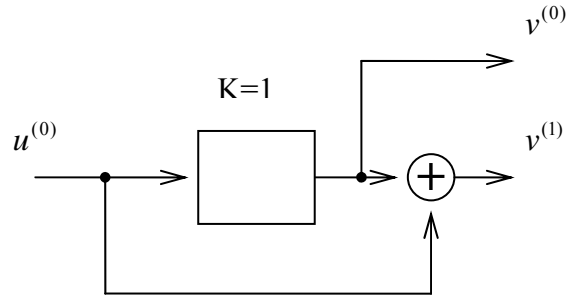


Figure 14. Convolutional encoder with code rate $1/2$ and $K = 1$.

From the state diagram for the encoder shown in Figure 14, shown in Figure 15, we derive the signal flow graph, which is shown in Figure 16.

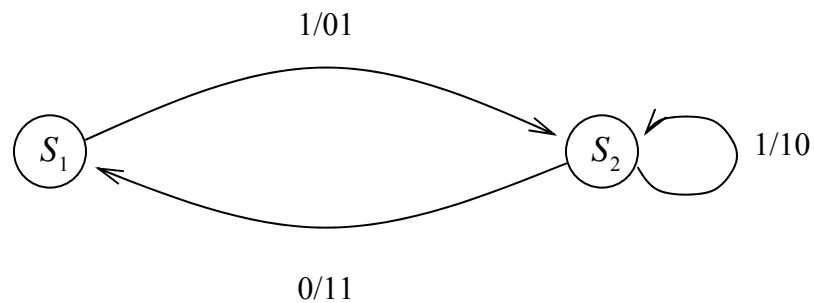


Figure 15. State diagram for the $r = 1/2$, $K=1$ convolutional encoder.

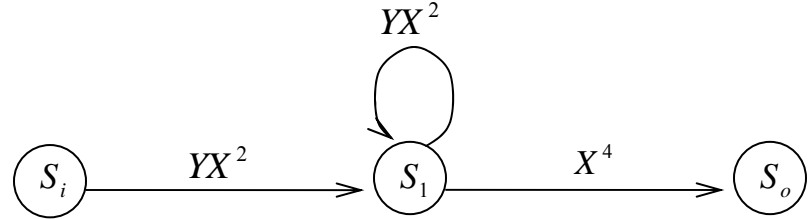


Figure 16. Signal flow graph for the $r = 1/2, K=1$ convolutional encoder with Gray mapping.

In order to find the probability of bit error, we must first to find the *average input-output enumerating transfer function* (AIOWEF) for the convolutional code of the encoder in Figure 14. The AIOWEF is derived from signal flow graph of the convolutional encoder, using Gray mapping, shown in Figure 11 for QPSK.

From the signal flow graph of the encoder in Figure 16, we obtain the state equations:

$$S_0 = X^4 S_1 \quad (3 - 6)$$

$$S_1 = YX^2 S_1 + YX^2 S_i \quad (3 - 7)$$

Combining equations (3-6) and (3-7), we have

$$S_0 = \frac{YX^6}{1 - YX^2} S_i \quad (3 - 8)$$

From equation (3-8) we derive the AIOWEF:

$$T_{ave}(X, Y) = \frac{S_0}{S_i} = \frac{YX^6}{1 - YX^2} = YX^6(1 - YX^2)^{-1} \quad (3 - 9)$$

Taking the derivative of the AIOWEF, we have

$$\frac{\partial T_{ave}(X,Y)}{\partial Y} = X^6 [1 - YX^2(2 - YX^2)]^{-1} \quad (3 - 10)$$

We know that

$$(1-x)^{-1} = 1 + x + x^2 + x^3 + \dots \quad (3 - 11)$$

From equations (3-10) and (3-11) and for $Y=1$, we obtain

$$\left. \frac{\partial T_{ave}(X,Y)}{\partial Y} \right|_{Y=1} = X^6 + 2X^8 + 3X^{10} + 4X^{12} + 5X^{14} + 6X^{16} + \dots \quad (3 - 12)$$

$$\text{Since } \left. \frac{\partial T_{ave}(X,Y)}{\partial Y} \right|_{Y=1} = B_1 X^{d_1^2} + B_2 X^{d_2^2} + B_3 X^{d_3^2} + B_4 X^{d_4^2} + \dots \quad (3 - 13)$$

we can see by comparing (3-12) and (3-13) that

$$B_1 = 1, d_1^2 = 6, B_2 = 2, d_2^2 = 8, B_3 = 3, d_3^2 = 10, \dots \quad (3 - 14)$$

So, the AIOWEF given by equation (3-9) gives the information that there is one path that has a squared-Euclidean distance of six from the reference path, there are two paths that have a squared-Euclidean distance of eight, there are three paths that have a squared-Euclidean distance of ten, four paths with a squared-Euclidean distance of 12, and so on. In this case, we take only the first four terms in order to compute the probability of bit error. This simplification, as we will see later, does not change the results.

Since there are no parallel paths for a TCM system utilizing QPSK modulation with a $r = 1/2$ convolutional code, the probability of bit error be approximated by equation (3-5) with $m=1$ to obtain

$$P_b \approx B_{d_{free}} Q\left(\sqrt{\frac{E_{sc} d_{free}^2}{2N_0}}\right) \quad (3 - 15)$$

Since

$$E_{sc} = r(m+1)E_b \quad (3 - 16)$$

then $E_{sc} = E_b$ in this case.

In light of equation (3-2) and (3-14), we derive the upper bound on the probability of bit error with AWGN as [4, 6]

$$P_b < Q\left(\sqrt{\frac{3E_b}{N_0}}\right) + 2Q\left(\sqrt{\frac{4E_b}{N_0}}\right) + 3Q\left(\sqrt{\frac{5E_b}{N_0}}\right) + 4Q\left(\sqrt{\frac{6E_b}{N_0}}\right) + \\ + 5Q\left(\sqrt{\frac{7E_b}{N_0}}\right) + 6Q\left(\sqrt{\frac{8E_b}{N_0}}\right) + \dots \quad (3 - 17)$$

As mentioned before, we use only the first four terms in order to compute the probability of bit error. This simplification, as we will see later, does not change the results. From equation (3-17), we get

$$P_b \approx Q\left(\sqrt{\frac{3E_b}{N_0}}\right) + 2Q\left(\sqrt{\frac{4E_b}{N_0}}\right) + 3Q\left(\sqrt{\frac{5E_b}{N_0}}\right) + 4Q\left(\sqrt{\frac{6E_b}{N_0}}\right) \quad (3 - 18)$$

Using only the first term when $E_b / N_o \gg 1$, we get

$$P_b \approx Q\left(\sqrt{\frac{3E_b}{N_0}}\right) \quad (3 - 19)$$

In Figure 17, we observe the probability of bit error for a TCM system with QPSK modulation and a $r = 1/2$ encoder with one memory element and gray mapping. Only AWGN was taken into consideration. Figure 17 also compares the results obtained when P_b is computed using six, four, and one summation terms.

As we observe in Figure 17, the probability of bit error is virtually the same for $P_b < 10^{-4}$ regardless of the number of terms used. We also see that the difference between four terms and six terms is very small regardless of P_b . As a result, for a probability of bit error less than 10^{-4} , we need use only the first term since it is the dominant term. For this

encoder, this is not an important simplification, but when there are more memory elements and the complexity of encoder is increased, this simplification will be helpful.

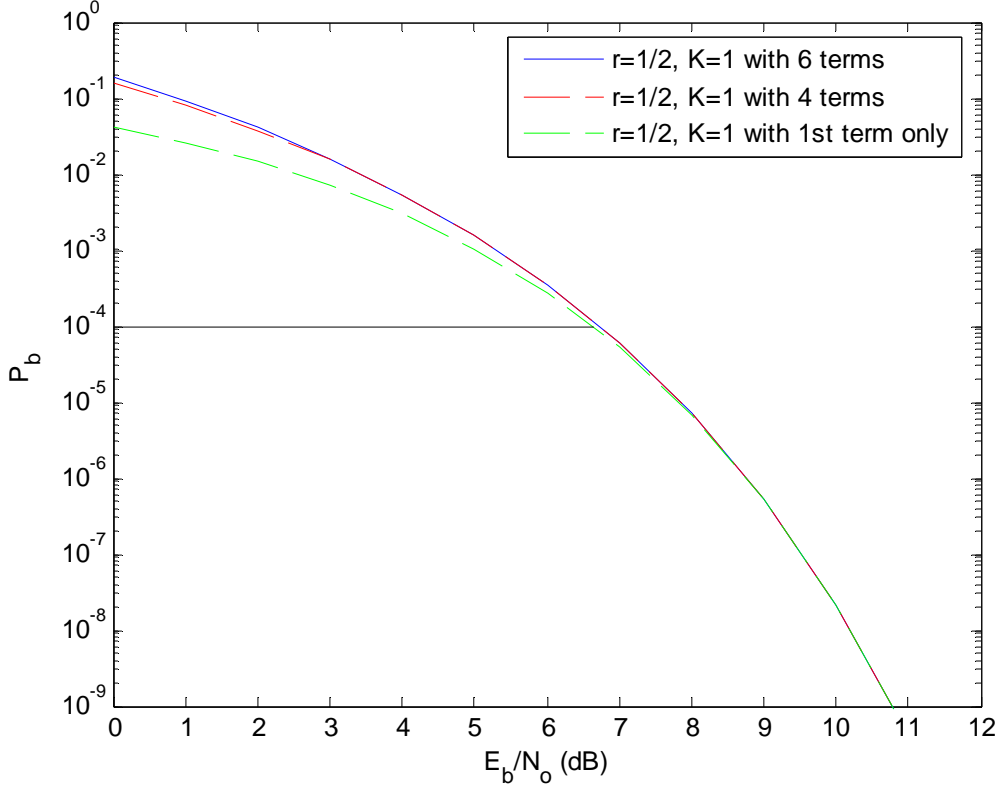


Figure 17. TCM system performance with QPSK modulation and a $r = 1/2$ encoder with $K=1$ and Gray mapping in AWGN.

D. PERFORMANCE OF ENCODER WITH CODE RATE 2/3 IN AWGN

1. Encoder with $r=2/3$ and $K=2$

In this subsection we examine the performance of an encoder with two memory elements $K = 2$ and code rate $r = 2/3$. The modulation we assumed is 8-PSK, and the TCM system using the encoder shown in Figure 18 has no parallel paths. The state diagram is shown in Figure 19 and, instead of using Gray mapping, we use natural mapping. The squared Euclidean distance for naturally mapped 8-PSK is shown in Table 2.

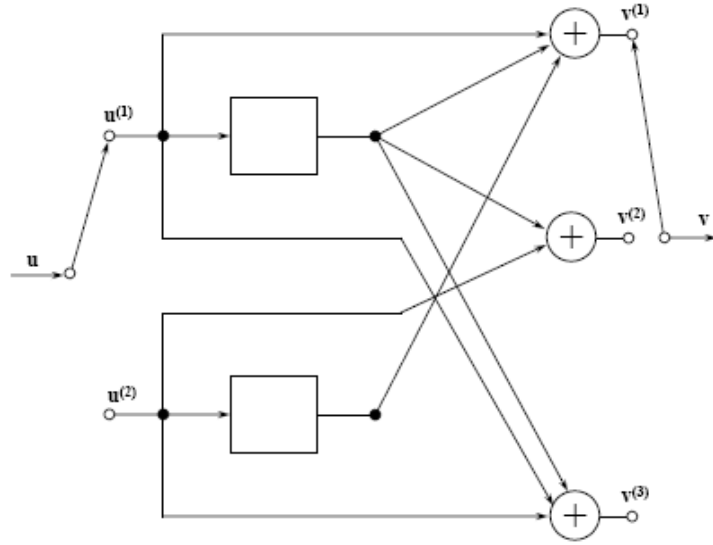


Figure 18. Convolutional encoder with $r = 2/3$ and $K=2$. From [6].

Table 2. Squared-Euclidean distance for naturally mapped 8-PSK.

\underline{e}	$\underline{\Delta_e^2(X)}$
000	X^0
001	$X^{0.586}$
010	X^2
011	$\frac{1}{2}X^{0.586} + \frac{1}{2}X^{3.414}$
100	X^4
101	$X^{3.414}$
110	X^2
111	$\frac{1}{2}X^{0.586} + \frac{1}{2}X^{3.414}$

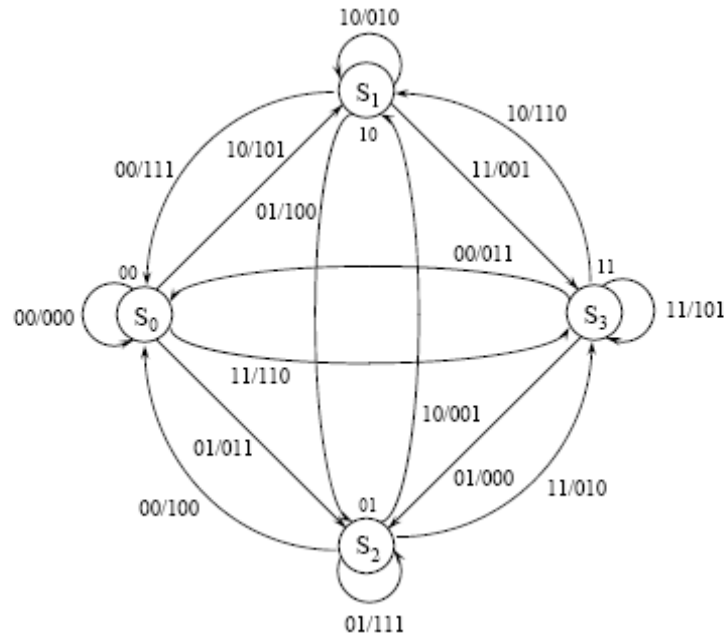


Figure 19. State diagram of the $r = 2/3, K=2$ encoder shown in Figure 18. From [6].

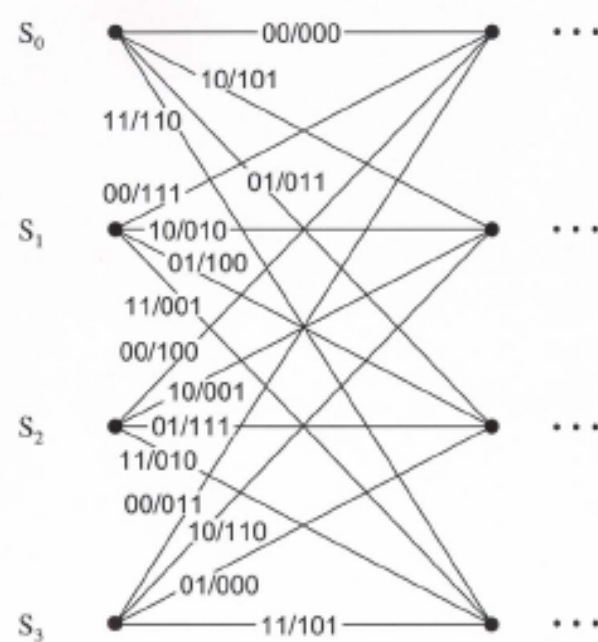


Figure 20. Trellis diagram of the code generated by the rate $r = 2/3, K=2$ encoder shown in Figure 18. From [6].

From the error trellis diagram of the encoder shown in Figure 21, the minimum squared-Euclidean distance corresponds to the path $S_0 - S_2 - S_1 - S_0$ and is $d_{\text{free}}^2 = 1.758$. This path is unique, and its information weight is $B_{d_{\text{free}}} = 1/2$. Continuing, we find the next larger squared-Euclidean distance $d_{\text{free}+1}^2 = 2.344$, which corresponds to the paths $S_0 - S_2 - S_3 - S_0$ and $S_0 - S_2 - S_2 - S_0$. The information weight $B_{d_{\text{free}+1}}$ for these paths is 1 and $3/8$, respectively, so the total information weight $B_{d_{\text{free}+1}} = 11/8$. The next larger squared-Euclidean distance $d_{\text{free}+2}^2 = 2.586$ corresponds to the path $S_0 - S_3 - S_0$, and the information weight is $B_{d_{\text{free}+2}} = 1$. The next larger squared-Euclidean distance corresponds to the two paths $S_0 - S_3 - S_2 - S_1 - S_0$ and $S_0 - S_2 - S_3 - S_0$, with information weight 2 and $3/4$, respectively, and is $d_{\text{free}+3}^2 = 3.172$. The total information weight for $d_{\text{free}+3}^2$ is $B_{d_{\text{free}+3}} = 11/4$.

From equation (3-2) and the results of the previous paragraph, we have

$$\frac{\partial T_{\text{ave}}(X, Y)}{\partial Y} \Big|_{Y=1} = \sum_{i=1}^{\infty} B_{d_i} X^{d_i^2} = \frac{1}{2} X^{d_{\text{free}}^2} + \frac{11}{8} X^{d_{\text{free}+1}^2} + X^{d_{\text{free}+2}^2} + \frac{11}{4} X^{d_{\text{free}+3}^2} + \dots \quad (3 - 20)$$

Since there are no parallel paths in the encoder, from (3-2) and (3-20) the probability of bit error is bounded by

$$P_b < \frac{1}{4} Q\left(\sqrt{1.758 \frac{E_b}{N_0}}\right) + \frac{11}{16} Q\left(\sqrt{2.344 \frac{E_b}{N_0}}\right) + \frac{1}{2} Q\left(\sqrt{2.586 \frac{E_b}{N_0}}\right) + \frac{11}{8} Q\left(\sqrt{3.172 \frac{E_b}{N_0}}\right) \quad (3 - 21)$$

since $m=2$ and $E_{sc} = r(m+1)E_b = 2E_b$. (3 - 22)

The approximate probability of bit error P_b using only the first term is

$$P_b \approx \frac{1}{4} Q\left(\sqrt{1.758 \frac{E_b}{N_0}}\right) \quad (3 - 23)$$

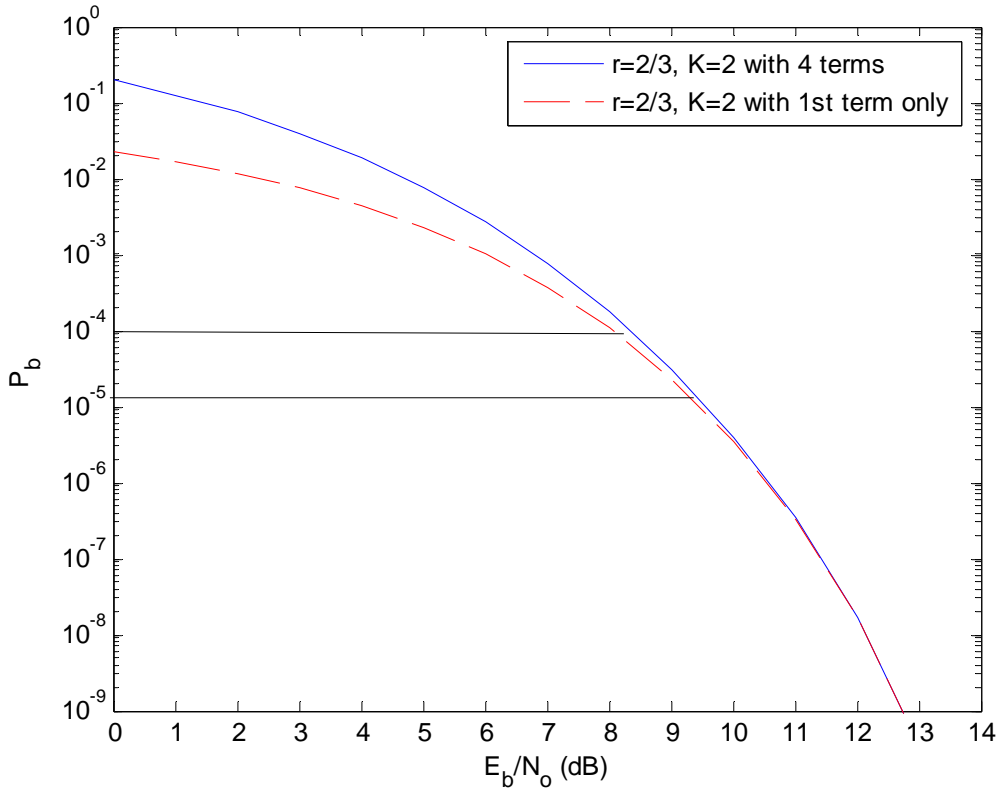


Figure 21. The probability of bit error for TCM with a $r = 2/3$, $K=2$ encoder and 8-PSK.

As we observe in Figure 21, the probability of bit error with respect to E_b / N_o for TCM with the $r = 2/3$, $K=2$ encoder and 8-PSK is the same for $P_b < 10^{-5}$ regardless of the number of summation terms used. In this case, the difference between one term and four terms is almost negligible for $10^{-5} < P_b < 10^{-4}$. As a result, for a probability of bit error less than 10^{-4} , only the first term is needed since it is the dominant term.

2. Encoder with $r=2/3$ and $K=3$

In this section we examine the performance of an encoder with $K=3$ and code rate $r = 2/3$. The modulation is again 8-PSK, and the resulting TCM system trellis has no parallel paths. The encoder is shown in Figure 22 and Figure 23 is the trellis diagram of the encoder. Once again, natural mapping, shown in Table 2, is used.

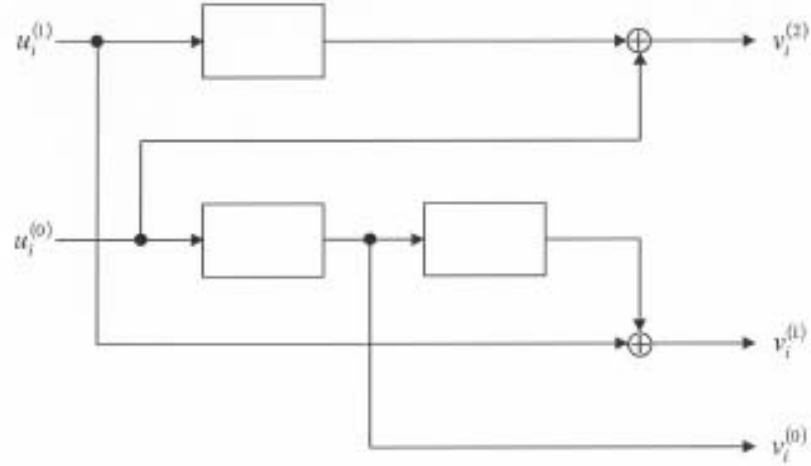


Figure 22. Convolutional encoder with $r = 2/3$ and $K=3$. From [6].

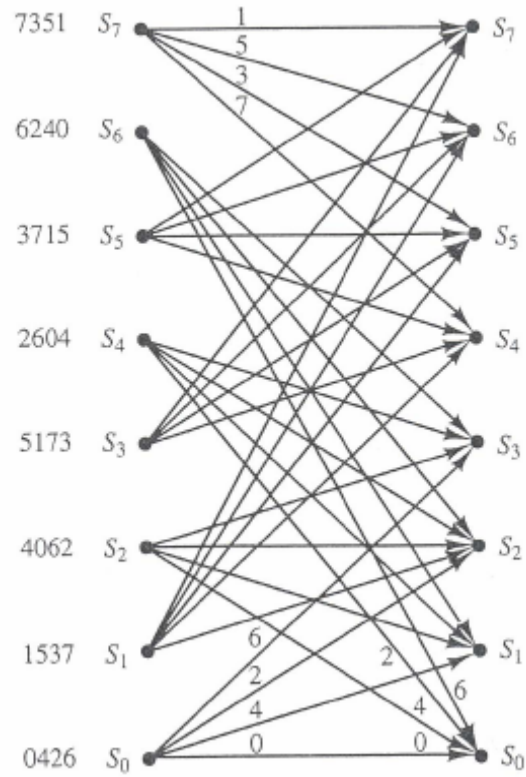


Figure 23. Trellis diagram of the code generated by the $r = 2/3$, $K=3$ encoder shown in Figure 22. From [6].

From trellis diagram shown in Figure 23, the minimum squared-Euclidean distance corresponds to the paths $S_0 - S_1 - S_2 - S_4 - S_0$, $S_0 - S_3 - S_6 - S_0$, and $S_0 - S_1 - S_2 - S_6 - S_0$, and $d_{free}^2 = 4.586$. The information weight of each of them is 2, 3/2, and 3/2, respectively, and the total information weight is $B_{d_{free}} = 5$. Continuing with the same procedure, the next larger squared-Euclidean distance is $d_{free+1}^2 = 5.172$ and corresponds to the paths $S_0 - S_3 - S_5 - S_4 - S_0$, $S_0 - S_3 - S_5 - S_6 - S_0$, $S_0 - S_3 - S_6 - S_3 - S_6 - S_0$, $S_0 - S_3 - S_7 - S_4 - S_0$, and $S_0 - S_1 - S_2 - S_7 - S_4 - S_0$. The information weight $B_{d_{free+1}}$ for these paths is 3/2, 4, 3/2, 1, and 1, respectively, which makes the total information weight $B_{d_{free+1}} = 9$. The next largest squared-Euclidean distance is $d_{free+2}^2 = 5.758$ and corresponds to the paths $S_0 - S_3 - S_7 - S_5 - S_4 - S_0$ and $S_0 - S_1 - S_2 - S_7 - S_5 - S_4 - S_0$ with information weight equal to 5/6 for each of them. This results in $B_{d_{free+2}} = 5/3$.

From equation (3-4) and the results of the previous paragraph, we have

$$\frac{\partial T_{ave}(X, Y)}{\partial Y} \Big|_{Y=1} = \sum_{i=1}^{\infty} B_{d_i} X^{d_i^2} = 5X^{d_{free}^2} + 9X^{d_{free+1}^2} + \frac{5}{3}X^{d_{free+2}^2} + \dots \quad (3 - 24)$$

As was previously explained and shown in Figures 17 and 21 for encoders with $r=1/2$, $K=1$ and $r=2/3$, $K=2$, the first term in the series is generally the dominant term. In this case, for the encoder with $r=2/3$ and $K=3$, we compute probability of bit error bound using only the first term.

From (3-2) and using only the first term, we get

$$P_b \approx \frac{5}{2} Q\left(\sqrt{4.586 \frac{E_b}{N_0}}\right) \quad (3 - 25)$$

since $E_{sc} = 2E_b$ and $m=2$.

From equation (3-25), the approximate probability of bit error for a TCM system with 8-PSK modulation and a $r = 2/3$ encoder with three memory elements and natural mapping is shown in Figure 24. Comparing Figure 24 with Figure 21, we see a significant improvement when K increases from two to three.

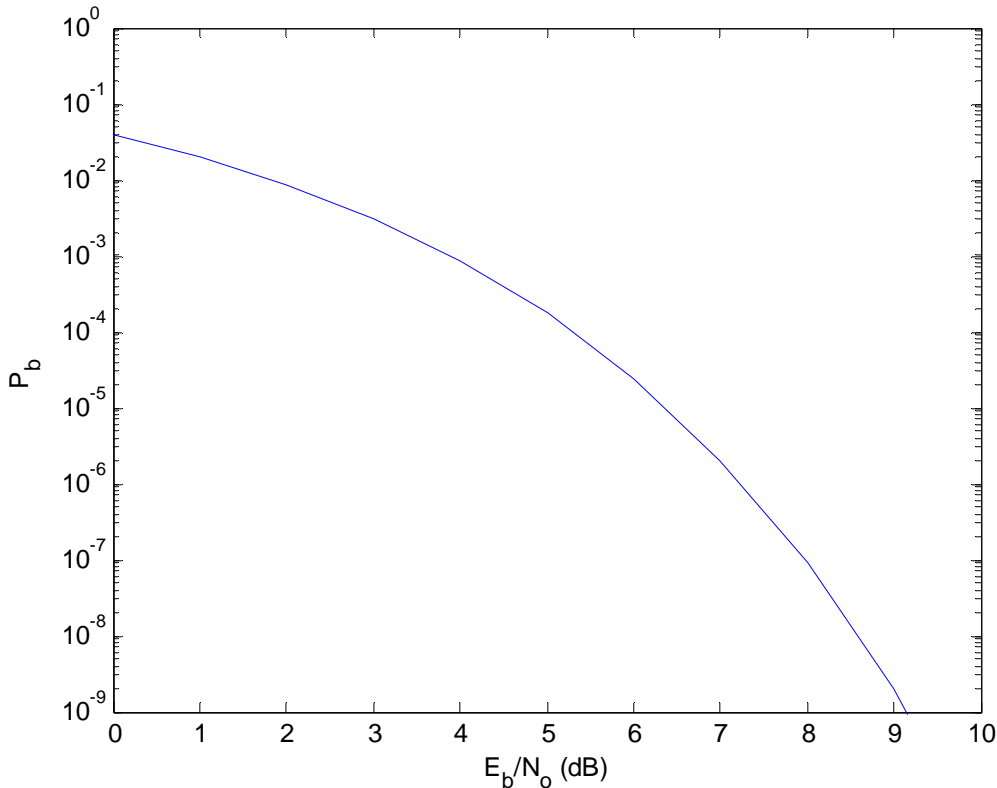


Figure 24. TCM system performance with 8-PSK modulation and a $r=2/3$ encoder with $K=3$ and natural mapping in AWGN .

3. Encoder with $r=2/3$ and $K=4$

In this section we examine the performance of an encoder with $K=4$ memory elements and code rate $r = 2/3$. Once again, the modulation used is 8-PSK with natural mapping. The encoder is shown in Figure 25, and the resulting TCM system trellis has no parallel paths. Figure 26 is a diagram of the encoder trellis.

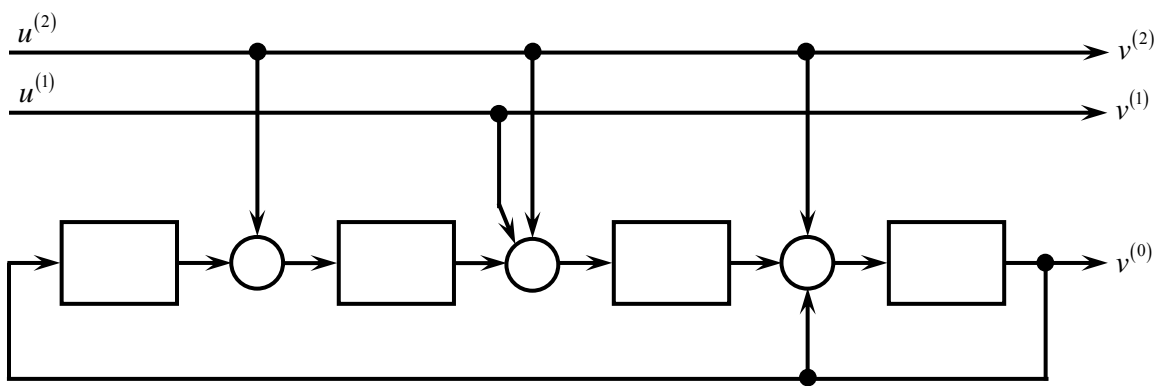


Figure 25. Encoder with code rate $r = 2/3$ and $K=4$.

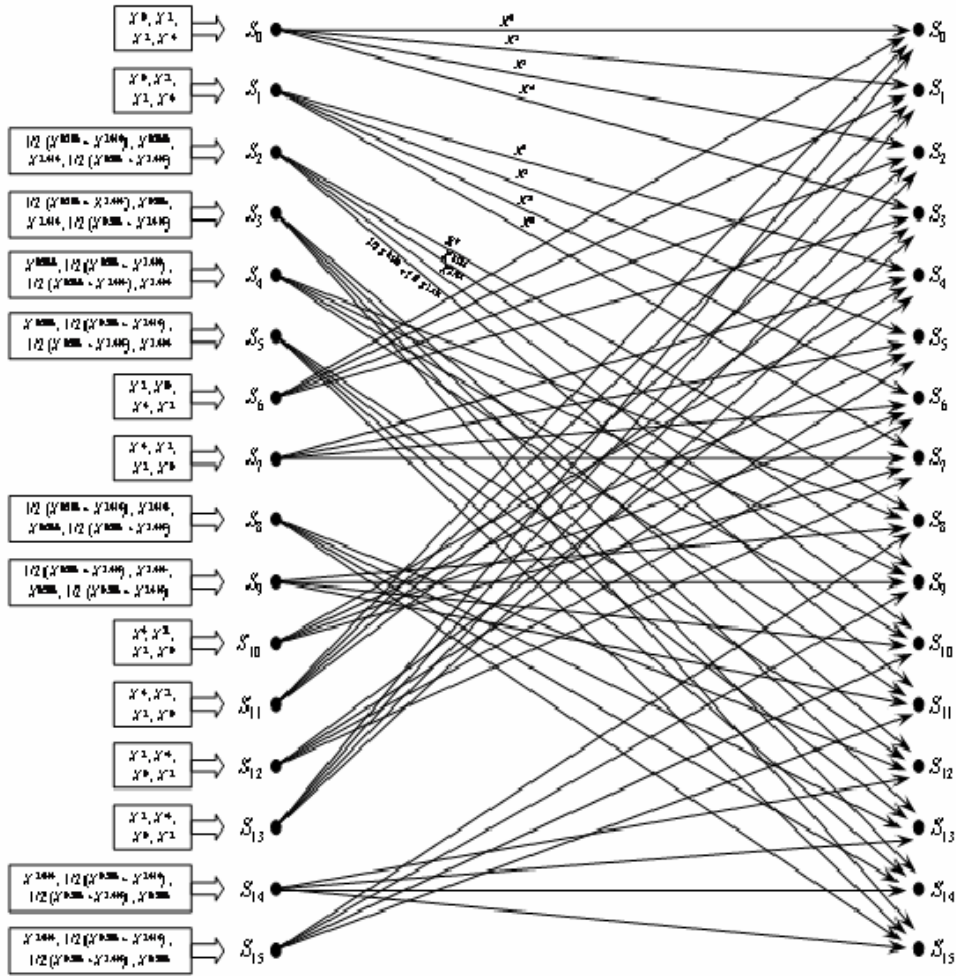


Figure 26. Trellis diagram of Encoder with code rate $r = 2/3$ and four memory elements.

From trellis diagram in Figure 26, the minimum squared-Euclidean distance corresponds to the paths $S_0 - S_2 - S_8 - S_{12} - S_6 - S_0$, $S_0 - S_1 - S_4 - S_{10} - S_7 - S_5 - S_{12} - S_6 - S_0$, $S_0 - S_1 - S_4 - S_{10} - S_7 - S_5 - S_{13} - S_0$, and $S_0 - S_1 - S_4 - S_8 - S_{12} - S_6 - S_0$, and $d_{free}^2 = 5.172$. The information weight of each path is $1/4, 1/2, 1/4$, and $1/2$, respectively, and the total information weight is $B_{d_{free}} = 3/2$.

Following the same steps as previously, we obtain the approximate probability of bit error for the $r=2/3$, $K=4$ TCM system as

$$P_b \approx \frac{3}{4} Q\left(\sqrt{5.172 \frac{E_b}{N_0}}\right) \quad (3 - 26)$$

From equation (3-26), the approximate probability of bit error for a TCM system with 8-PSK modulation and a $r = 2/3$ encoder with four memory elements and natural mapping is shown in Figure 27.

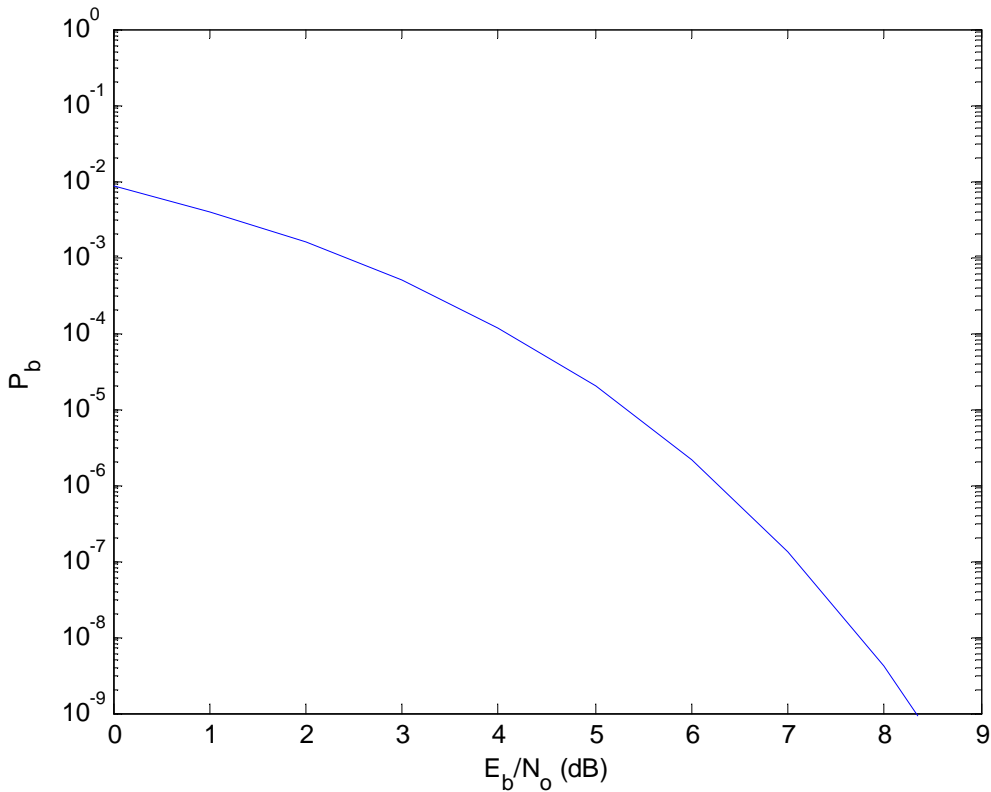


Figure 27. TCM system performance with 8-PSK modulation and a $r = 2/3$ encoder with $K=4$ and natural mapping in AWGN.

E. COMPARISON BETWEEN TCM SYSTEMS WITH DIFFERENT CODE RATES AND AN EQUAL NUMBER OF MEMORY ELEMENTS IN AWGN

1. Comparison between Different TCM Systems with $K=2$ in AWGN

In this subsection, the performance between TCM with QPSK, $r=1/2$ encoding and 8-PSK, $r=2/3$ encoding, but the same number of encoder memory elements $K=2$, is compared. The encoders are shown in Figures 14 and 18, respectively.

As we see from Figure 28, for $P_b = 10^{-5}$ the QPSK, $r=1/2$ system requires $E_b / N_o = 5.6$ dB, and the 8-PSK, $r=2/3$ system requires $E_b / N_o = 9.7$ dB, which yields a difference of 2.1 dB. We also notice that for decreasing P_b , the difference in E_b / N_o between the two systems increases, and the 8-PSK, $r=2/3$ system requires a much higher E_b / N_o than the QPSK, $r=1/2$ system in order to achieve the same probability of bit error. It is obvious that when $K=2$, the QPSK, $r=1/2$ system has better performance than the 8-PSK, $r=2/3$ system.

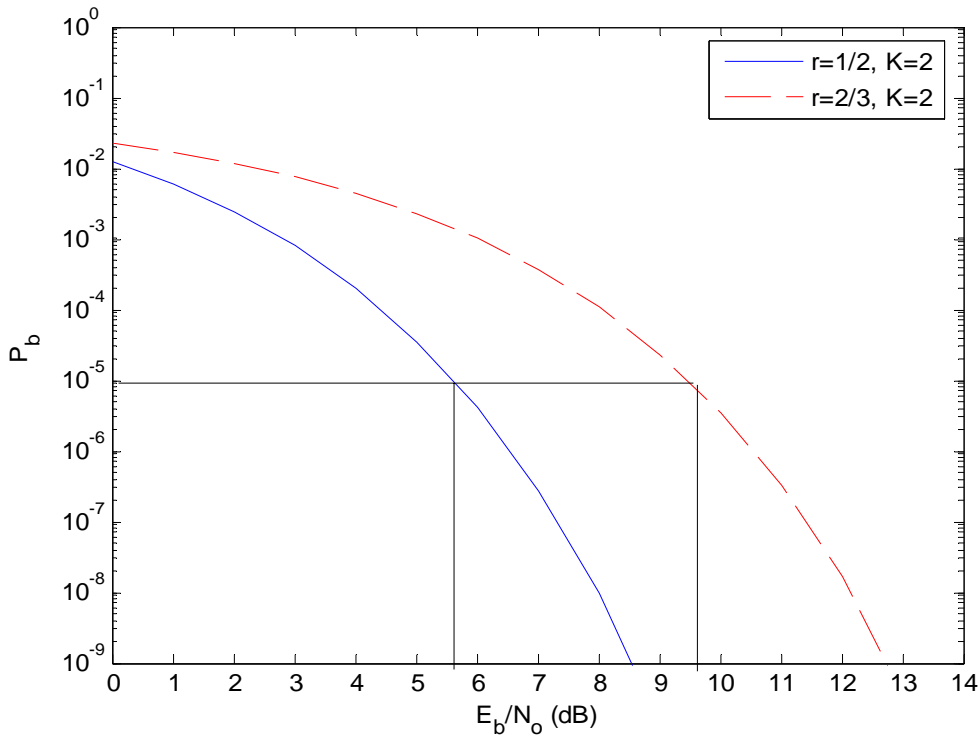


Figure 28. Comparison between TCM with $r=1/2$ and $r=2/3$ encoders for $K=2$.

2. Comparison between Different TCM Systems with $K=3$ in AWGN

In this subsection, the performance between TCM with QPSK, $r=1/2$ encoding and 8-PSK, $r=2/3$ encoding is compared when $K=3$.

As we see from Figure 29, for $P_b = 10^{-5}$ the QPSK, $r=1/2$ system requires $E_b / N_o = 5.1$ dB, and the system with 8-PSK, $r=2/3$ requires $E_b / N_o = 6.3$ dB, which yields a difference of 1.2 dB. It is obvious that with $K=3$, the QPSK, $r=1/2$ system has better performance than the 8-PSK, $r=2/3$ system, but the difference is much less than when $K=2$.

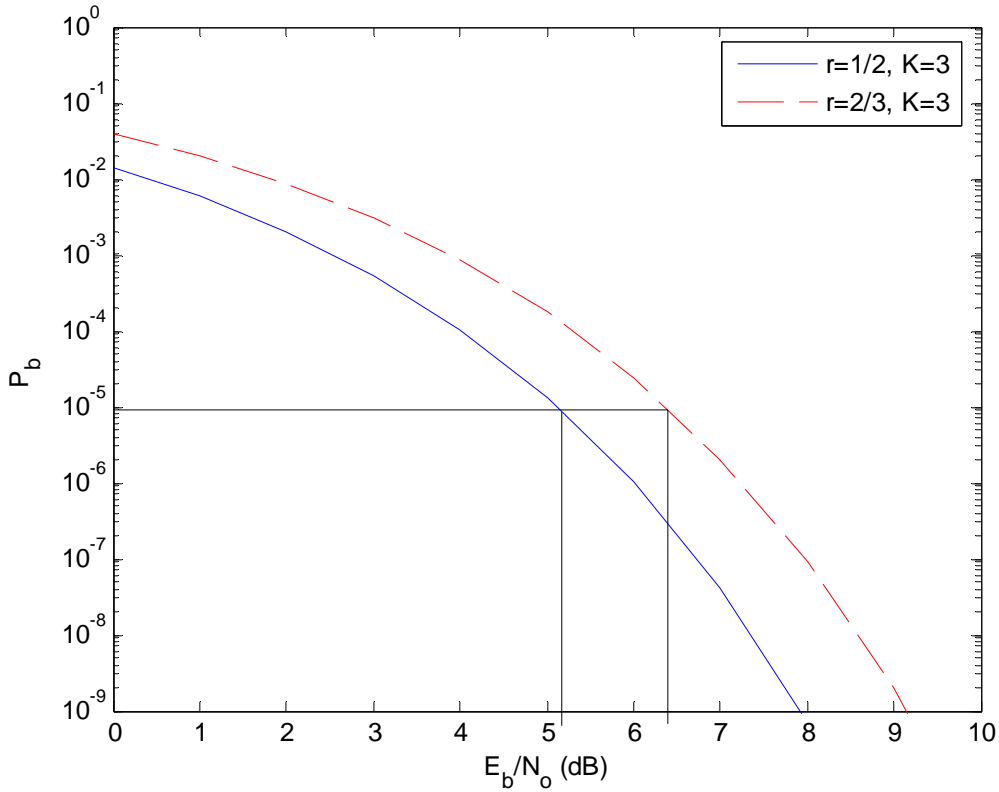


Figure 29. Comparison between TCM with $r=1/2$ and $r=2/3$ encoders for $K=3$.

3. Comparison between Different TCM Systems with $K=4$ in AWGN

In this subsection, the performance between TCM with QPSK, $r=1/2$ encoding and 8-PSK, $r=2/3$ encoding is compared when $K=4$.

As we see from Figure 30, for a probability of bit error greater than 10^{-3} , the 8-PSK, $r=2/3$ system has better performance than the QPSK, $r=1/2$ system. When the probability of bit error is less than 10^{-3} , the performance of the QPSK, $r=1/2$ system is better. For $P_b = 10^{-5}$, the QPSK, $r=1/2$ system requires $E_b / N_o = 4.7$ dB, and the system with 8-PSK, $r=2/3$ requires $E_b / N_o = 5.3$ dB, which yields a difference of 0.6 dB. For $P_b = 10^{-9}$, these values are 7.4 dB and 8.3 dB respectively, and the difference is 0.9 dB, which means that for smaller P_b , the performance of the QPSK, $r=1/2$ system is better relative to the 8-PSK, $r=2/3$ system. These results were expected because using a higher code rate yields higher data rates at the cost of a loss in performance.

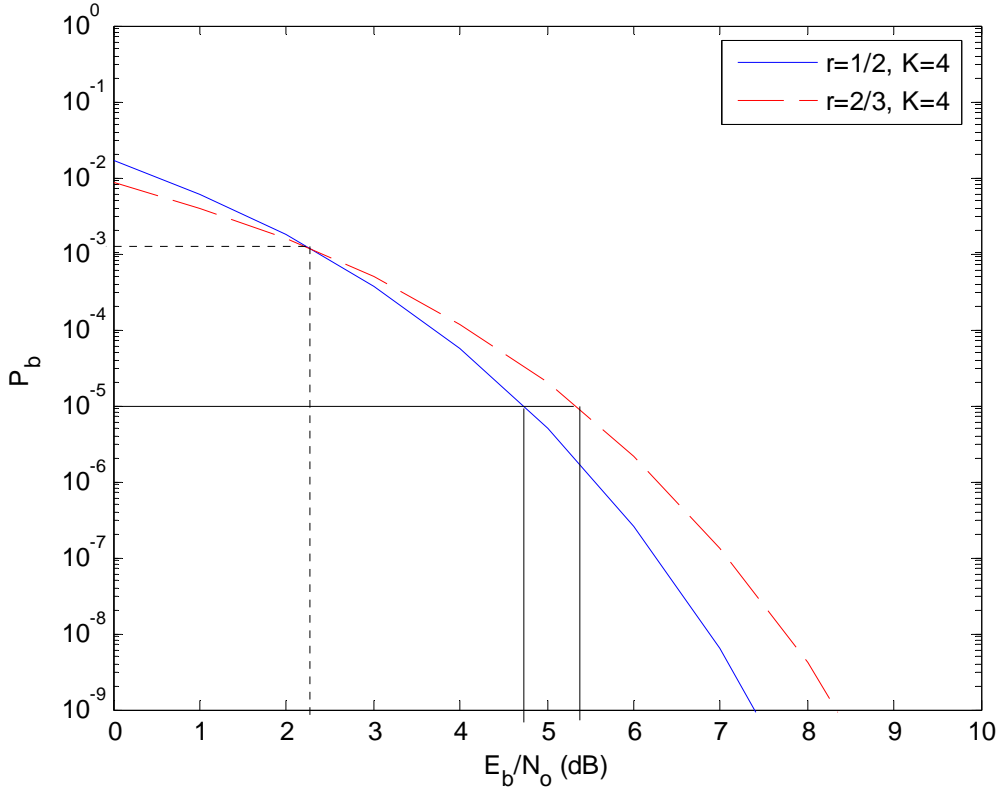


Figure 30. Comparison between TCM with $r=1/2$ and $r=2/3$ encoders for $K=4$.

F. COMPARISON BETWEEN TCM SYSTEMS WITH DIFFERENT CODE RATES AND NUMBERS OF MEMORY ELEMENTS IN AWGN

1. Comparison between TCM Systems with $r=1/2, K=1$ and $r=2/3, K=2$

In this subsection, we compare the performance between two TCM systems when the number of memory elements increases linearly with code rate. As we see in Figure 31, the TCM system with QPSK, $r=1/2$ and $K=1$ has better performance than the TCM system with 8-PSK, $r=2/3$ and $K=2$. For $P_b = 10^{-5}$, the QPSK, $r=1/2$ system requires $E_b / N_o = 7.9$ dB, while the TCM system with 8-PSK, $r=2/3$ requires $E_b / N_o = 9.6$ dB, which yields a difference of 1.7 dB. For $P_b = 10^{-9}$, E_b / N_o is 10.8 dB and 12.7 dB, respectively, and the difference is 1.9 dB. Once again, the overall performance of 8-PSK, $r=2/3$ is poorer than QPSK, $r=1/2$.

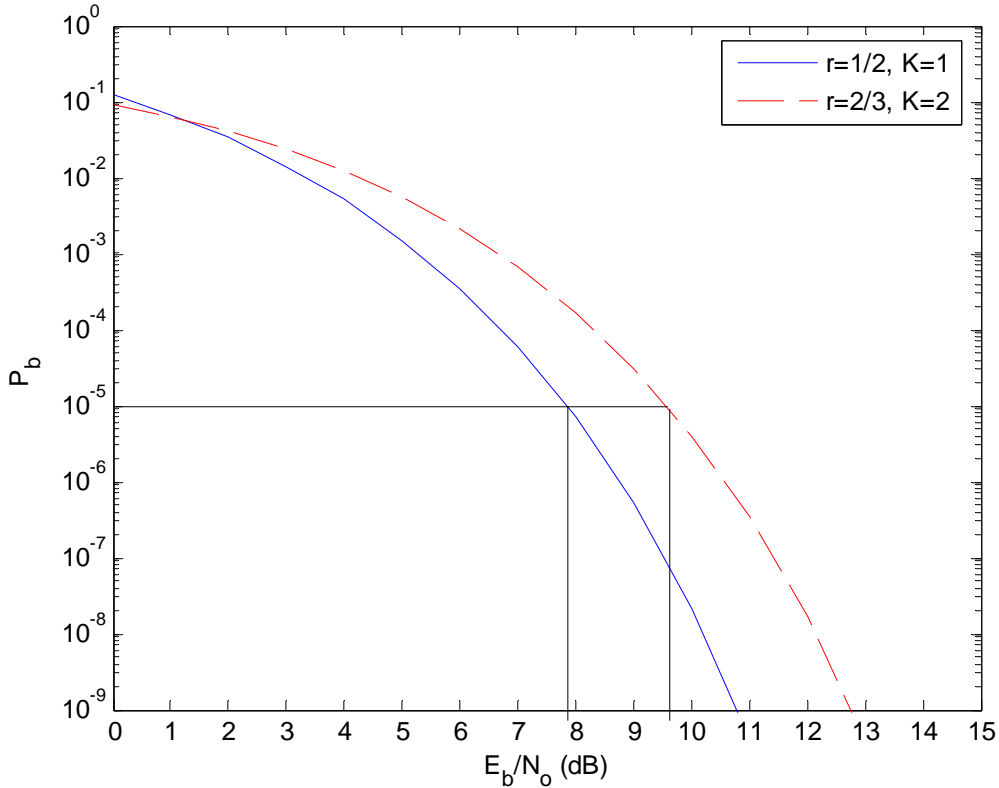


Figure 31. Comparison between TCM with QPSK, $r=1/2, K=1$ and 8-PSK, $r=2/3, K=2$.

2. Comparison between TCM Systems with QPSK, $r=1/2$, $K=2$ and 8-PSK, $r=2/3$, $K=4$

In this subsection, we compare the performance between the QPSK, $r=1/2$, $K=2$ and 8-PSK, $r=2/3$, $K=4$ TCM systems. As we see in Figure 32, the performance of these two systems is the same for a probability of bit error of 10^{-5} . For $P_b < 10^{-5}$, the performance of the QPSK, $r=1/2$ system is better than that of the 8-PSK, $r=2/3$ system. On the other hand, when $P_b < 10^{-5}$, the 8-PSK, $r=2/3$ system is better, and for $P_b = 10^{-9}$, the required E_b / N_o improves by a little bit less than a half of dB as compared with the QPSK, $r=1/2$ system.

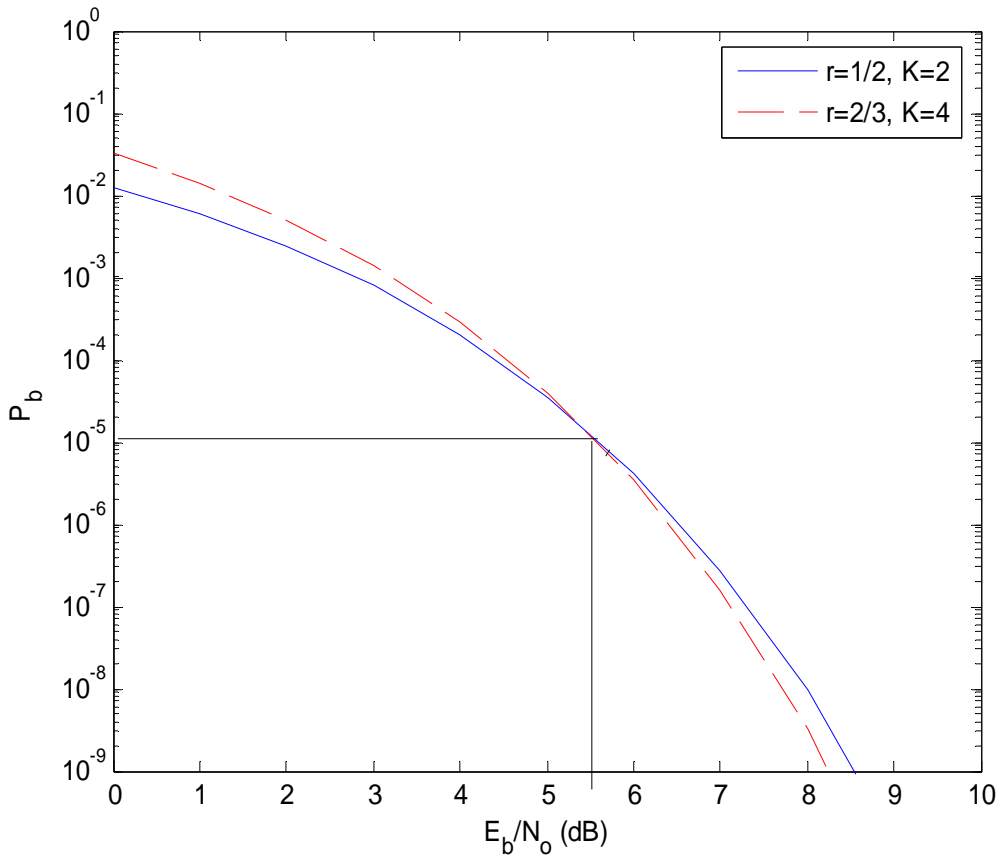


Figure 32. Comparison between TCM with QPSK, $r=1/2$, $K=2$ and 8-PSK, $r=2/3$, $K=4$.

3. Comparison between TCM Systems with QPSK, $r=1/2$, $K=2$ and $r=2/3$, $K=8$

In this subsection, we compare the performance between the QPSK, $r=1/2$, $K=2$ and 8-PSK, $r=2/3$, $K=8$ TCM systems. As we see in Figure 33, this time the overall performance of the 8-PSK, $r=2/3$ system is better than QPSK, $r=1/2$ system. For $P_b = 10^{-5}$, the 8-PSK, $r=2/3$ system requires 1.6 dB less E_b / N_o as compared with the QPSK, $r=1/2$ system. It is obvious that increasing the number of memory elements in the 8-PSK, $r=2/3$ system improves performance at the expense of decoding complexity.

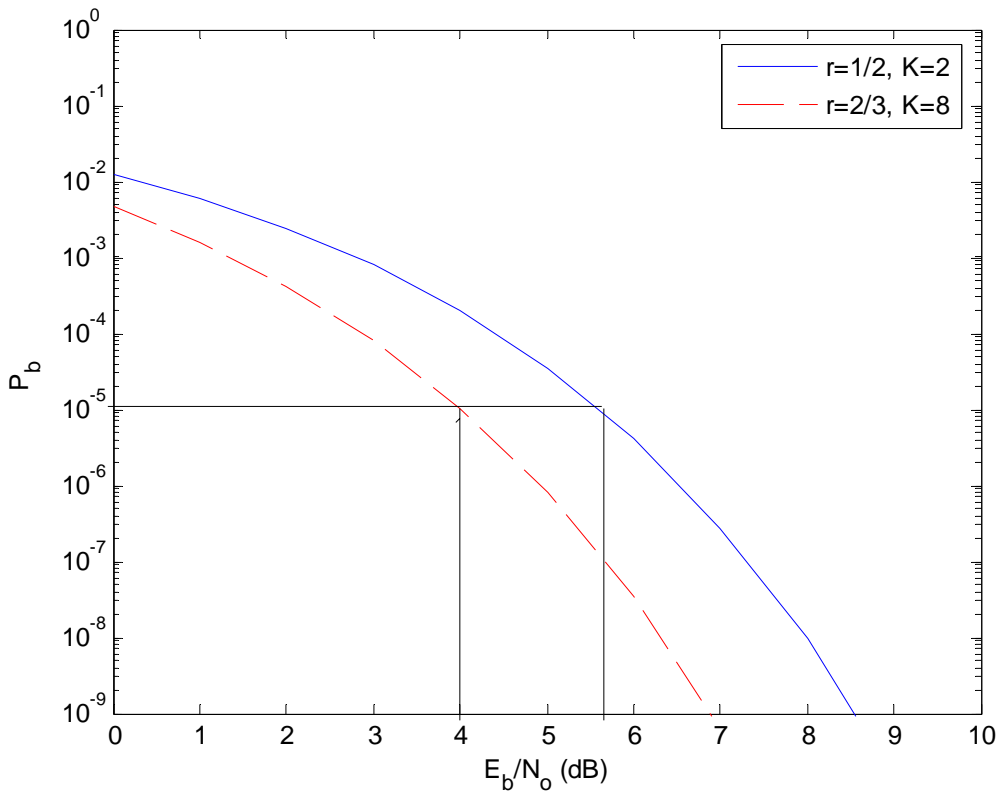


Figure 33. Comparison between TCM with QPSK, $r=1/2$, $K=2$ and 8-PSK, $r=2/3$, $K=8$.

G. SUMMARY

In this chapter, the performance of TCM in AWGN with $r=1/2$ encoding and QPSK modulation and $r=2/3$ encoding with 8-PSK modulation was examined for $K=1, 2, 3$, and 4 . In order to compute the probability of bit error, only the first term in the upper bound, which is the dominant term for $P_b < 10^{-5}$, was used. This does not significantly affect the precision of the results.

A comparison between TCM systems with the same number of memory elements K was made. The QPSK, $r=1/2$ system always has better performance than the 8-PSK, $r=2/3$ system.

The two TCM systems were also compared when the number of memory elements in the 8-PSK, $r=2/3$ system was larger than for the QPSK, $r=1/2$ system. It was found that the QPSK, $r=1/2, K=1$ system has better performance than the 8-PSK, $r=2/3, K=2$ system, no matter what E_b / N_o is. When we increase the number of memory elements in both encoders by a factor of two, we get an improvement, but for $P_b > 10^{-5}$, the QPSK, $r=1/2$ system still has better performance. For P_b smaller than 10^{-5} , the 8-PSK, $r=2/3$ system has a slightly better performance, on the order of one-half dB. Finally, when the 8-PSK, $r=2/3$ system has four times as many memory elements as the QPSK, $r=1/2$ system, the 8-PSK, $r=2/3$ system achieves a better performance, on the order of 1.6 dB for a probability of bit error of 10^{-5} . In this case we get both a higher data rate and better performance, but the complexity of the decoder increases significantly.

In the next chapter, the performance of the TCM systems examined in this chapter are examined when both AWGN and pulse-noise interference are present.

IV. PERFORMANCE OF TCM SYSTEMS WITH PULSE NOISE INTERFERENCE

A. INTRODUCTION

In the previous chapter, the performance of TCM systems in AWGN was examined. A comparison between two different systems having same number of memory elements as well as one TCM system having more memory elements was made.

In this chapter the same two TCM systems are examined when, in addition to AWGN, pulse noise interference (PNI) is also present. We assume that the average interference power remains constant regardless of the time that the PNI is on. That implies that the instantaneous interference power increases as the fraction of the time the interference is on decreases.

B. PERFORMANCE BOUNDS ON TCM WITH PNI

The probability of bit error is upper bounded by

$$P_b < \frac{1}{m} \sum_{j=1}^{\infty} \frac{1}{A_{d_j}} \sum_{l=l_{\min}}^{\infty} \sum_{k=1}^{\infty} B_{d_j, l_k} P'_{d_j, l_k} \quad (4 - 1)$$

where A_{d_j} is the total number of error paths that are a squared-Euclidean distance of d_j^2 from the all-zero error path regardless of length, B_{d_j, l_k} is the total number of information bit ones on the k^{th} error path consisting of l branches that are a squared-Euclidean distance of d_j^2 from the all-zero path, and P'_{d_j, l_k} is the probability of selecting the k^{th} error path of length l that is a squared-Euclidean distance of d_j^2 from the all-zero error path.

The conditional probability P'_{d_j, l_k} is given by [6]:

$$P'_{d_j, l_k} = \sum_{i=0}^{l_k} \binom{l_k}{i} \rho^i (1-\rho)^{l_k-i} P'_{d_j, l_k}(i) \quad (4 - 2)$$

where ρ is the fraction of time the PNI is on, $\rho=1$ implies continuous interference, i of the l_k are the branches are affected by PNI and AWGN, and the remaining $(l_k - i)$ branches are affected only by AWGN.

C. PERFORMANCE OF TCM WITH QPSK AND RATE 1/2 ENCODING WITH PNI

Figure 14 shows a block diagram of an encoder with $K=1$ and code rate $r=1/2$. The state diagram and the signal flow graph of the encoder is shown in Figures 15 and 16, respectively.

As we mentioned at the beginning of Chapter III, for TCM with QPSK and $r=1/2$ encoding, each transmitted symbol contains one data bit, and $m=1$. Hence, from equation (3-16), $E_{sc} = E_b$.

In light of equation (3-9) and (3-14), we see there is one path that has a squared-Euclidean distance of six, there are two paths that have a squared-Euclidean distance of eight, there are three paths that have a squared-Euclidean distance of ten, four paths with a squared-Euclidean distance of 12, and so on. In this case, we use only the first term in order to approximate the probability of bit error. This simplification does not significantly affect the results. From the signal flow graph in Figure 16, we see that the path $S_0 - S_1 - S_0$ has $d_{free}^2 = 6$. Since $l_1=3$, there are three different probabilities that the signal is affected by PNI. In the first occasion, the interference affects no branch of the path, in the second it affects one of the two branches of the path, $S_0 - S_1$ or $S_1 - S_0$, and finally, it can affect both of them. Generally, the formula for the probability of selecting a specific sequence is

$$P'_{d_j, l_k}(i) = Q\left(\sqrt{\frac{E_b}{2}\left(\frac{a}{N_0} + \frac{b}{N_T}\right)}\right) \quad (4 - 3)$$

where we define

$$P_{d_j, l_k}(i) = \frac{B_{d_j, l_k}}{m} P'_{d_j, l_k}(i) \quad (4 - 4)$$

and $N_T = N_o + N_i / \rho$, a and b are the sum of the squared-Euclidean distances of the branches affected by AWGN only and by both AWGN and PNI, respectively, given that N_o is the power spectral density (PSD) of the AWGN and N_i is the PSD of the interference.

In light of equation (4-3) and (4-4), when PNI affects all branches, the probability of selecting this specific sequence is

$$P_{d_{free}, l_1}(2) = Q\left(\sqrt{\frac{E_b}{2}\left(\frac{2+4}{N_T}\right)}\right) = Q\left(\sqrt{\frac{3E_b}{N_T}}\right) \quad (4 - 5)$$

When the interference affects zero branches, the probability of selecting this specific sequence is

$$P_{d_{free}, l_1}(0) = Q\left(\sqrt{\frac{E_b}{2}\left(\frac{2+4}{N_0}\right)}\right) = Q\left(\sqrt{\frac{3E_b}{N_0}}\right) \quad (4 - 6)$$

When the interference affects only one branch the probability of selecting this specific sequence is

$$P_{d_{free}, l_1}(1) = \frac{1}{2}Q\left(\sqrt{\frac{E_b}{2}\left(\frac{2}{N_0} + \frac{4}{N_T}\right)}\right) + \frac{1}{2}Q\left(\sqrt{\frac{E_b}{2}\left(\frac{4}{N_0} + \frac{2}{N_T}\right)}\right) \quad (4 - 7)$$

In light of (4-1), (4-2), (4-5), (4-6), and (4-7) we have

$$P_b \approx (1-\rho)^2 Q\left(\sqrt{\frac{3E_b}{N_o}}\right) + \rho(1-\rho)[Q\left(\sqrt{\frac{E_b}{N_T} + \frac{2E_b}{N_0}}\right) + Q\left(\sqrt{\frac{2E_b}{N_T} + \frac{E_b}{N_0}}\right)] + \rho^2 Q\left(\sqrt{\frac{3E_b}{N_T}}\right) \quad (4 - 8)$$

since $A_{d_{free}} = 1$ and $B_{d_{free}, 3_1} = 1$.

In Figure 34, we see the performance of the QPSK, $r=1/2$, $K=1$ TCM system with PNI. In this and all other figures in this thesis examining the effects of PNI, E_b / N_0 is chosen so that $P_b = 10^{-8}$ when $E_b / N_i >> 1$. The fraction of the time ρ that the

interference is on is varied from $\rho=1$ to $\rho=0.01$. Taking as a reference $P_b=10^{-5}$ and $P_b=10^{-6}$, we compare the required E_b/N_i for different ρ .

As we see in Figure 34, the maximum degradation due to PNI occurs for $\rho=0.01$ and is 7.6 dB for $P_b=10^{-5}$. For $P_b=10^{-6}$, the degradation increases to 10.7 dB.

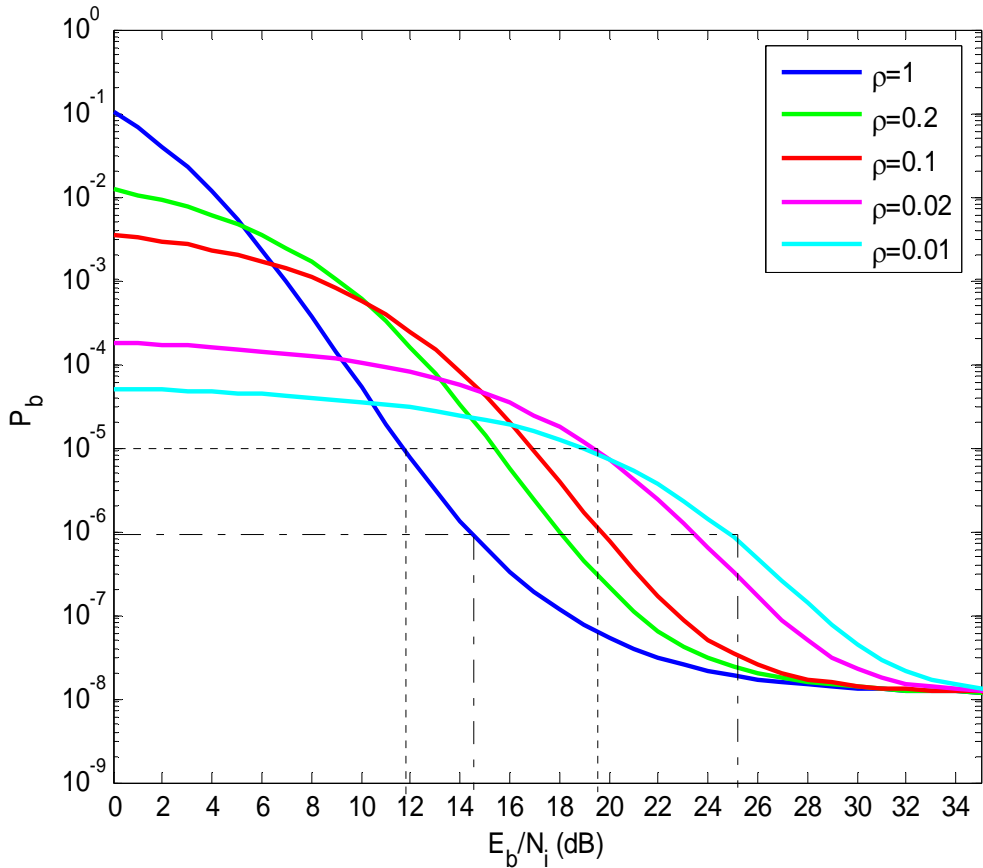


Figure 34. Performance of QPSK, $r=1/2$ TCM system with $K=1$ and PNI with $E_b/N_o = 10.2$ dB.

D. PERFORMANCE OF TCM WITH 8-PSK AND RATE 2/3 ENCODING WITH PNI

In this section, we consider the same 8-PSK, $r=2/3$ TCM system that was examined in Chapter III.

1. Encoder with $K=2$

The encoder, the state diagram and the error trellis diagram are shown in Figures 18, 19, and 20, respectively. From the error trellis diagram, the minimum squared-Euclidean distance corresponds to the path $S_0 - S_2 - S_1 - S_0$, and $d_{free}^2 = 1.758$. This path is unique, and its information weight is $B_{d_{free},3_1} = 1/2$. The PNI can affect $i=0$, $i=1$, $i=2$, or $i=3$ branches of this path. When $i=0$, there is no PNI on any branch. When $i=1$, the PNI can occur on any one of the three branches, $S_0 - S_2$, or $S_2 - S_1$, or, $S_1 - S_0$. When $i=2$, PNI can occur on $\binom{3}{2}$ combinations of three branches, and for $i=3$ all branches are affected by PNI.

From (4-2), (4-4) and (4-5), we have for the path $S_0 - S_2 - S_1 - S_0$

$$\begin{aligned}
 P_{d_{free},3_1} &= \binom{3}{0} (1-\rho)^3 P_{d_{free},3_1}(0) + && \text{when } i=0 \\
 &+ \binom{3}{1} \rho (1-\rho)^2 P_{d_{free},3_1}(1) + && \text{when } i=1 \\
 &+ \binom{3}{2} \rho^2 (1-\rho)^1 P_{d_{free},3_1}(2) + && \text{when } i=2 \\
 &+ \binom{3}{3} \rho^3 P_{d_{free},3_1}(3) && \text{when } i=3
 \end{aligned} \tag{4 - 9}$$

where

$$P_{d_{free},3_1}(0) = \frac{1}{4} Q\left(\sqrt{E_b \left(\frac{0.586}{N_0} + \frac{0.586}{N_0} + \frac{0.586}{N_0} \right)}\right) = \frac{1}{4} Q\left(\sqrt{\frac{1.758 E_b}{N_0}}\right) \tag{4 - 10}$$

$$P_{d_{free},3_1}(1) = \frac{1}{4} Q\left(\sqrt{E_b\left(\frac{0.586}{N_T} + \frac{0.586}{N_0} + \frac{0.586}{N_0}\right)}\right) = \frac{1}{4} Q\left(\sqrt{E_b\left(\frac{0.586}{N_T} + \frac{1.172}{N_0}\right)}\right) \quad (4 - 11)$$

$$P_{d_{free},3_1}(2) = \frac{1}{4} Q\left(\sqrt{E_b\left(\frac{0.586}{N_T} + \frac{0.586}{N_T} + \frac{0.586}{N_0}\right)}\right) = \frac{1}{4} Q\left(\sqrt{E_b\left(\frac{1.172}{N_T} + \frac{0.586}{N_0}\right)}\right) \quad (4 - 12)$$

$$P_{d_{free},3_1}(3) = \frac{1}{4} Q\left(\sqrt{E_b\left(\frac{0.586}{N_T} + \frac{0.586}{N_T} + \frac{0.586}{N_T}\right)}\right) = \frac{1}{4} Q\left(\sqrt{\frac{1.758 E_b}{N_T}}\right) \quad (4 - 13)$$

The next larger squared-Euclidean distance $d_{free+1}^2 = 2.344$, which corresponds to the paths $S_0 - S_2 - S_1 - S_3 - S_0$ and $S_0 - S_2 - S_2 - S_1 - S_0$. The information weight $B_{d_{free+1},4_1}$, $B_{d_{free+1},4_2}$ for these paths is 1 and 3/8, respectively, so the total information weight is $B_{d_{free+1},4} = 11/8$. The PNI can affect $i=0$, $i=1$, $i=2$, $i=3$, or $i=4$ branches of this path.

From (4-2), (4-4) and (4-5), for the path $S_0 - S_2 - S_1 - S_3 - S_0$, we have

$$\begin{aligned} P_{d_{free},4_1} &= \binom{4}{0} (1-\rho)^4 P_{d_{free},4_1}(0) + \binom{4}{1} \rho (1-\rho)^3 P_{d_{free},4_1}(1) + \binom{4}{2} \rho^2 (1-\rho)^2 P_{d_{free},4_1}(2) + \\ &\quad + \binom{4}{3} \rho^3 (1-\rho)^1 P_{d_{free},4_1}(3) + \binom{4}{4} \rho^4 P_{d_{free},4_1}(4) \end{aligned} \quad (4 - 14)$$

where

$$P_{d_{free},4_1}(0) = \frac{11}{16} Q\left(\sqrt{E_b\left(\frac{0.586}{N_0} + \frac{0.586}{N_0} + \frac{0.586}{N_0} + \frac{0.586}{N_0}\right)}\right) \quad (4 - 15)$$

$$P_{d_{free},4_1}(1) = \frac{11}{16} Q\left(\sqrt{E_b \left(\frac{0.586}{N_T} + \frac{1.758}{N_0} \right)}\right) \quad (4 - 16)$$

$$P_{d_{free},4_1}(2) = \frac{11}{16} Q\left(\sqrt{E_b \left(\frac{1.172}{N_T} + \frac{1.172}{N_0} \right)}\right) \quad (4 - 17)$$

$$P_{d_{free},4_1}(3) = \frac{11}{16} Q\left(\sqrt{E_b \left(\frac{1.758}{N_T} + \frac{0.586}{N_0} \right)}\right) \quad (4 - 18)$$

$$P_{d_{free},4_1}(4) = \frac{11}{16} Q\left(\sqrt{\frac{2.344 E_b}{N_T}}\right) \quad (4 - 19)$$

For the path $S_0 - S_2 - S_2 - S_1 - S_0$, we have

$$\begin{aligned} P_{d_{free},4_2} &= \binom{4}{0} (1-\rho)^4 P_{d_{free},4_2}(0) + \binom{4}{1} \rho (1-\rho)^3 P_{d_{free},4_2}(1) + \binom{4}{2} \rho^2 (1-\rho)^2 P_{d_{free},4_2}(2) + \\ &\quad + \binom{4}{3} \rho^3 (1-\rho)^1 P_{d_{free},4_2}(3) + \binom{4}{4} \rho^4 P_{d_{free},4_2}(4) \end{aligned} \quad (4 - 20)$$

where

$$P_{d_{free},4_2}(0) = \frac{11}{16} Q\left(\sqrt{E_b \left(\frac{0.586}{N_0} + \frac{0.586}{N_0} + \frac{0.586}{N_0} + \frac{0.586}{N_0} \right)}\right) \quad (4 - 21)$$

$$P_{d_{free},4_2}(1) = \frac{11}{16} Q\left(\sqrt{E_b \left(\frac{0.586}{N_T} + \frac{1.758}{N_0} \right)}\right) \quad (4 - 22)$$

$$P_{d_{free},4_2}(2) = \frac{11}{16} Q\left(\sqrt{E_b \left(\frac{1.172}{N_T} + \frac{1.172}{N_0} \right)}\right) \quad (4 - 23)$$

$$P_{d_{free},4_2}(3) = \frac{11}{16} Q\left(\sqrt{E_b \left(\frac{1.758}{N_T} + \frac{0.586}{N_0} \right)}\right) \quad (4 - 24)$$

$$P_{d_{free},4_2}(4) = \frac{11}{16} Q\left(\sqrt{\frac{2.344 E_b}{N_T}}\right) \quad (4 - 25)$$

The next largest squared-Euclidean distance $d_{free+2}^2 = 2.586$ corresponds to the path $S_0 - S_3 - S_0$, and the information weight is $B_{d_{free+2},2} = 1$. The PNI can affect $i=0$, $i=1$, or $i=2$ branches of this path.

From (4-2), (4-4) and (4-5) for the path $S_0 - S_3 - S_0$, we have

$$P_{d_{free},2_1} = \binom{2}{0} (1-\rho)^2 P_{d_{free},2_1}(0) + \binom{2}{1} \rho (1-\rho) P_{d_{free},2_1}(1) + \binom{2}{2} \rho^2 P_{d_{free},2_1}(2) \quad (4 - 26)$$

where

$$P_{d_{free},2_1}(0) = \frac{1}{2} Q\left(\sqrt{\frac{2.586 E_b}{N_0}}\right) \quad (4 - 27)$$

$$P_{d_{free},2_1}(1) = \frac{1}{4} Q\left(\sqrt{E_b \left(\frac{2}{N_T} + \frac{0.586}{N_0} \right)}\right) + \frac{1}{4} Q\left(\sqrt{E_b \left(\frac{0.586}{N_T} + \frac{2}{N_0} \right)}\right) \quad (4 - 28)$$

$$P_{d_{free},2_1}(2) = \frac{1}{2} Q\left(\sqrt{E_b \left(\frac{2.586}{N_T} \right)}\right) \quad (4 - 29)$$

From (4-1), the bound on P_b is

$$P_b \approx P_{d_{free},3_1} + P_{d_{free},4_1} + P_{d_{free},4_2} + P_{d_{free},2_1} \quad (4 - 30)$$

As we see from Figure 35, PNI degrades system performance. Taking as a reference point $P_b = 10^{-5}$ and $E_b / N_o = 12.2$ dB, $E_b / N_i = 11.5$ dB is required for $\rho = 1$ and $E_b / N_i = 18.6$ dB for $\rho = 0.02$. Hence, the maximum degradation due to PNI at $P_b = 10^{-5}$ occurs for $\rho = 0.02$ and is 7.1 dB. For $P_b = 10^{-6}$, $E_b / N_i = 13.46$ dB and $E_b / N_i = 24.1$ dB are required for $\rho = 1$ and $\rho = 0.01$, respectively, which increases the degradation to 10.6 dB.

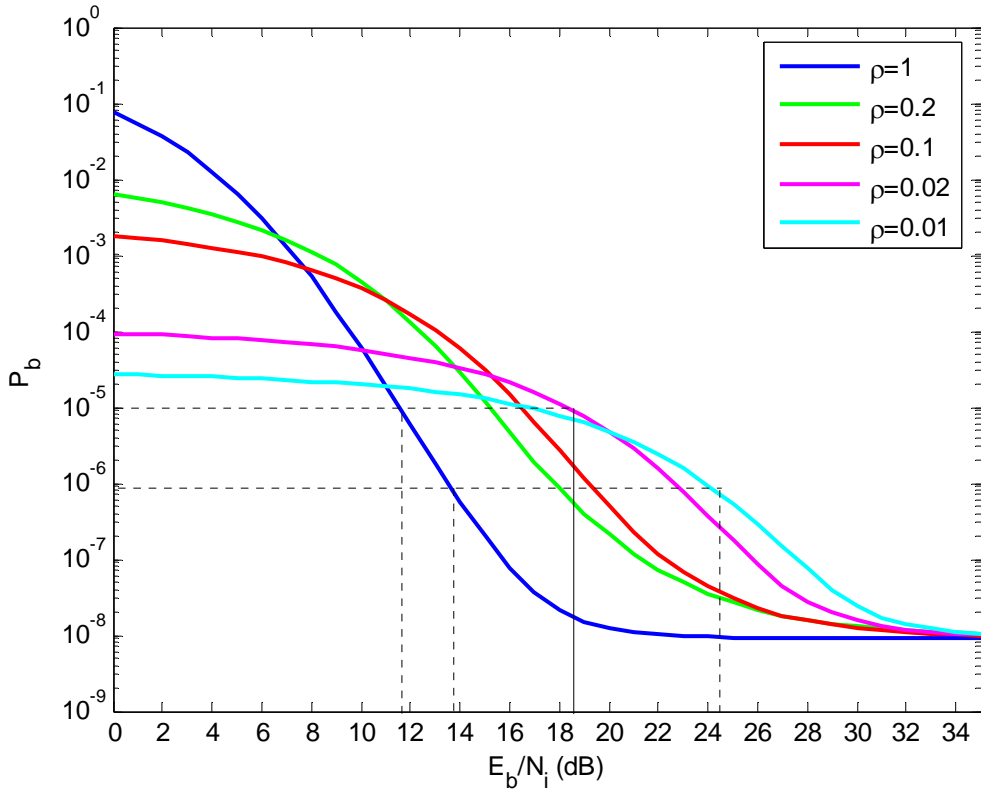


Figure 35. Performance of 8-PSK, $r=2/3$ TCM with $K=2$ and PNI with $E_b / N_o = 12.2$ dB.

2. Encoder with $K=3$

The encoder and the error trellis diagram are shown in Figures 22 and 23, respectively. From the error trellis diagram, the minimum squared-Euclidean distance corresponds to the paths $S_0 - S_1 - S_2 - S_4 - S_0$, $S_0 - S_3 - S_6 - S_0$, and

$S_0 - S_1 - S_2 - S_6 - S_0$ and $d_{free}^2 = 4.586$. The information weight of each path is 2, 3/2, and 3/2, respectively, and the total information weight is $B_{d_{free}} = 5$.

For the first path $S_0 - S_1 - S_2 - S_4 - S_0$, the interference can occur for $i=0, i=1, i=2, i=3$, or $i=4$ branches of the path. From (4-2), (4-4) and (4-5) we have

$$P_{d_{free},4_1} = \binom{4}{0}(1-\rho)^4 P_{d_{free},4_1}(0) + \binom{4}{1}\rho(1-\rho)^3 P_{d_{free},4_1}(1) + \binom{4}{2}\rho^2(1-\rho)^2 P_{d_{free},4_1}(2) + \\ + \binom{4}{3}\rho^3(1-\rho) P_{d_{free},4_1}(3) + \binom{4}{4}\rho^4 P_{d_{free},4_1}(4) \quad (4 - 31)$$

where

$$P_{d_{free},4_1}(0) = Q\left(\sqrt{E_b\left(\frac{2}{N_0} + \frac{0}{N_0} + \frac{0.586}{N_0} + \frac{2}{N_0}\right)}\right) = Q\left(\sqrt{\frac{4.586 E_b}{N_0}}\right) \quad (4 - 32)$$

$$P_{d_{free},4_1}(1) = \frac{1}{4}Q\left(\sqrt{E_b\left(\frac{2}{N_T} + 0 + \frac{0.586}{N_0} + \frac{2}{N_0}\right)}\right) + \frac{1}{4}Q\left(\sqrt{E_b\left(\frac{2}{N_0} + 0 + \frac{0.586}{N_0} + \frac{2}{N_0}\right)}\right) + \\ + \frac{1}{4}Q\left(\sqrt{E_b\left(\frac{2}{N_0} + 0 + \frac{0.586}{N_T} + \frac{2}{N_0}\right)}\right) + \frac{1}{4}Q\left(\sqrt{E_b\left(\frac{2}{N_0} + 0 + \frac{0.586}{N_0} + \frac{2}{N_T}\right)}\right) \quad (4 - 33)$$

$$\begin{aligned}
P_{d_{free},4_1}(2) = & \frac{1}{6} Q\left(\sqrt{E_b\left(\frac{2}{N_T} + 0 + \frac{0.586}{N_0} + \frac{2}{N_0}\right)}\right) + \frac{1}{6} Q\left(\sqrt{E_b\left(\frac{2}{N_T} + 0 + \frac{0.586}{N_T} + \frac{2}{N_0}\right)}\right) + \\
& + \frac{1}{6} Q\left(\sqrt{E_b\left(\frac{2}{N_T} + 0 + \frac{0.586}{N_0} + \frac{2}{N_T}\right)}\right) + \frac{1}{6} Q\left(\sqrt{E_b\left(\frac{2}{N_0} + 0 + \frac{0.586}{N_T} + \frac{2}{N_0}\right)}\right) + \\
& + \frac{1}{6} Q\left(\sqrt{E_b\left(\frac{2}{N_0} + 0 + \frac{0.586}{N_0} + \frac{2}{N_T}\right)}\right) + \frac{1}{6} Q\left(\sqrt{E_b\left(\frac{2}{N_0} + 0 + \frac{0.586}{N_T} + \frac{2}{N_T}\right)}\right) \\
P_{d_{free},4_1}(2) = & \frac{1}{3} Q\left(\sqrt{E_b\left(\frac{2}{N_T} + \frac{2.586}{N_0}\right)}\right) + \frac{1}{3} Q\left(\sqrt{E_b\left(\frac{2.586}{N_T} + \frac{2}{N_0}\right)}\right) + \frac{1}{6} Q\left(\sqrt{E_b\left(\frac{4}{N_T} + \frac{0.586}{N_0}\right)}\right) + \\
& + \frac{1}{6} Q\left(\sqrt{E_b\left(\frac{0.586}{N_T} + \frac{4}{N_0}\right)}\right) \tag{4 - 34}
\end{aligned}$$

$$\begin{aligned}
P_{d_{free},4_1}(3) = & \frac{1}{4} Q\left(\sqrt{E_b\left(\frac{2}{N_T} + 0 + \frac{0.586}{N_T} + \frac{2}{N_0}\right)}\right) + \frac{1}{4} Q\left(\sqrt{E_b\left(\frac{2}{N_T} + 0 + \frac{0.586}{N_0} + \frac{2}{N_T}\right)}\right) + \\
& + \frac{1}{4} Q\left(\sqrt{E_b\left(\frac{2}{N_T} + 0 + \frac{0.586}{N_T} + \frac{2}{N_T}\right)}\right) + \frac{1}{4} Q\left(\sqrt{E_b\left(\frac{2}{N_0} + 0 + \frac{0.586}{N_T} + \frac{2}{N_T}\right)}\right) \\
P_{d_{free},4_1}(3) = & \frac{1}{2} Q\left(\sqrt{E_b\left(\frac{2.586}{N_T} + \frac{2}{N_0}\right)}\right) + \frac{1}{4} Q\left(\sqrt{E_b\left(\frac{4}{N_T} + \frac{0.586}{N_0}\right)}\right) + \frac{1}{4} Q\left(\sqrt{E_b\left(\frac{4.586}{N_T}\right)}\right) \tag{4 - 35}
\end{aligned}$$

$$P_{d_{free},4_1}(4) = Q\left(\sqrt{\frac{4.586 E_b}{N_T}}\right) \tag{4 - 36}$$

For the second path, $S_0 - S_3 - S_6 - S_0$, the interference can occur for $i=0, i=1, i=2$, or $i=3$ branches of the path. From (4-2), (4-4) and (4-5), we have

$$P_{d_{free},3_1} = \binom{3}{0}(1-\rho)^3 P_{d_{free},3_1}(0) + \binom{3}{1}\rho(1-\rho)^2 P_{d_{free},3_1}(1) + \binom{3}{2}\rho^2(1-\rho) P_{d_{free},3_1}(2) + \binom{3}{3}\rho^3 P_{d_{free},3_1}(3) \quad (4 - 37)$$

where

$$P_{d_{free},3_1}(0) = \frac{3}{4}Q\left(\sqrt{E_b\left(\frac{2}{N_0} + \frac{0.586}{N_0} + \frac{2}{N_0}\right)}\right) = \frac{3}{4}Q\left(\sqrt{\frac{4.586E_b}{N_0}}\right) \quad (4 - 38)$$

$$P_{d_{free},3_1}(1) = \frac{3}{4}\left(\frac{1}{3}Q\left(\sqrt{E_b\left(\frac{2}{N_T} + \frac{0.586}{N_0} + \frac{2}{N_0}\right)}\right) + \frac{1}{3}Q\left(\sqrt{E_b\left(\frac{2}{N_0} + \frac{0.586}{N_T} + \frac{2}{N_0}\right)}\right) + \frac{1}{3}Q\left(\sqrt{E_b\left(\frac{2}{N_0} + \frac{0.586}{N_0} + \frac{2}{N_T}\right)}\right)\right) \\ P_{d_{free},3_1}(1) = \frac{1}{2}Q\left(\sqrt{E_b\left(\frac{2}{N_T} + \frac{2.586}{N_0}\right)}\right) + \frac{1}{4}Q\left(\sqrt{E_b\left(\frac{0.586}{N_T} + \frac{4}{N_0}\right)}\right) \quad (4 - 39)$$

$$P_{d_{free},3_1}(2) = \frac{1}{4}\left(\frac{1}{3}Q\left(\sqrt{E_b\left(\frac{2}{N_T} + \frac{0.586}{N_T} + \frac{2}{N_0}\right)}\right) + \frac{1}{3}Q\left(\sqrt{E_b\left(\frac{2}{N_T} + \frac{0.586}{N_0} + \frac{2}{N_T}\right)}\right) + \frac{1}{3}Q\left(\sqrt{E_b\left(\frac{2}{N_0} + \frac{0.586}{N_T} + \frac{2}{N_T}\right)}\right)\right) =$$

$$P_{d_{free},3_1}(2) = \frac{1}{2}Q\left(\sqrt{E_b\left(\frac{2.586}{N_T} + \frac{2}{N_0}\right)}\right) + \frac{1}{4}Q\left(\sqrt{E_b\left(\frac{4}{N_T} + \frac{0.586}{N_0}\right)}\right) \quad (4 - 40)$$

$$P_{d_{free},3_1}(3) = \frac{3}{4}Q\left(\sqrt{\frac{4.586E_b}{N_T}}\right) \quad (4 - 41)$$

For the third path, $S_0 - S_1 - S_2 - S_6 - S_0$, the interference can occur for $i=0, i=1, i=2, i=3$, or $i=4$ branches of the path. From (4-2), (4-4) and (4-5), we have

$$\begin{aligned}
P_{d_{free},4_2} = & \binom{4}{0}(1-\rho)^4 P_{d_{free},4_2}(0) + \binom{4}{1}\rho(1-\rho)^3 P_{d_{free},4_2}(1) + \binom{4}{2}\rho^2(1-\rho)^2 P_{d_{free},4_2}(2) + \\
& + \binom{4}{3}\rho^3(1-\rho) P_{d_{free},4_2}(3) + \binom{4}{4}\rho^4 P_{d_{free},4_2}(4)
\end{aligned} \tag{4 - 42}$$

where

$$P_{d_{free},4_2}(0) = \frac{3}{4}Q\left(\sqrt{E_b\left(\frac{2}{N_0} + \frac{0}{N_0} + \frac{0.586}{N_0} + \frac{2}{N_0}\right)}\right) = \frac{3}{4}Q\left(\sqrt{\frac{4.586E_b}{N_0}}\right) \tag{4 - 43}$$

$$P_{d_{free},4_2}(1) = \frac{3}{16}Q\left(\sqrt{E_b\left(\frac{2}{N_T} + 0 + \frac{0.586}{N_0} + \frac{2}{N_0}\right)}\right) + \frac{3}{16}Q\left(\sqrt{E_b\left(\frac{2}{N_0} + 0 + \frac{0.586}{N_0} + \frac{2}{N_0}\right)}\right) +$$

$$+ \frac{3}{16}Q\left(\sqrt{E_b\left(\frac{2}{N_0} + 0 + \frac{0.586}{N_T} + \frac{2}{N_0}\right)}\right) + \frac{3}{16}Q\left(\sqrt{E_b\left(\frac{2}{N_0} + 0 + \frac{0.586}{N_0} + \frac{2}{N_T}\right)}\right) \tag{4 - 44}$$

$$P_{d_{free},4_2}(2) = \frac{1}{8}Q\left(\sqrt{E_b\left(\frac{2}{N_T} + 0 + \frac{0.586}{N_0} + \frac{2}{N_0}\right)}\right) + \frac{1}{8}Q\left(\sqrt{E_b\left(\frac{2}{N_T} + 0 + \frac{0.586}{N_T} + \frac{2}{N_0}\right)}\right) +$$

$$+ \frac{1}{8}Q\left(\sqrt{E_b\left(\frac{2}{N_T} + 0 + \frac{0.586}{N_0} + \frac{2}{N_T}\right)}\right) + \frac{1}{8}Q\left(\sqrt{E_b\left(\frac{2}{N_0} + 0 + \frac{0.586}{N_T} + \frac{2}{N_0}\right)}\right) +$$

$$+ \frac{1}{8}Q\left(\sqrt{E_b\left(\frac{2}{N_0} + 0 + \frac{0.586}{N_0} + \frac{2}{N_T}\right)}\right) + \frac{1}{8}Q\left(\sqrt{E_b\left(\frac{2}{N_0} + 0 + \frac{0.586}{N_T} + \frac{2}{N_T}\right)}\right)$$

$$P_{d_{free},4_2}(2) = \frac{1}{4}Q\left(\sqrt{E_b\left(\frac{2}{N_T} + \frac{2.586}{N_0}\right)}\right) + \frac{1}{4}Q\left(\sqrt{E_b\left(\frac{2.586}{N_T} + \frac{2}{N_0}\right)}\right) + \frac{1}{8}Q\left(\sqrt{E_b\left(\frac{4}{N_T} + \frac{0.586}{N_0}\right)}\right) +$$

$$+ \frac{1}{8} Q\left(\sqrt{E_b \left(\frac{0.586}{N_T} + \frac{4}{N_0} \right)} \right) \quad (4 - 45)$$

$$\begin{aligned} P_{d_{free},4_2}(3) &= \frac{3}{16} Q\left(\sqrt{E_b \left(\frac{2}{N_T} + 0 + \frac{0.586}{N_T} + \frac{2}{N_0} \right)} \right) + \frac{3}{16} Q\left(\sqrt{E_b \left(\frac{2}{N_T} + 0 + \frac{0.586}{N_0} + \frac{2}{N_T} \right)} \right) + \\ &+ \frac{3}{16} Q\left(\sqrt{E_b \left(\frac{2}{N_T} + 0 + \frac{0.586}{N_T} + \frac{2}{N_T} \right)} \right) + \frac{3}{16} Q\left(\sqrt{E_b \left(\frac{2}{N_0} + 0 + \frac{0.586}{N_T} + \frac{2}{N_T} \right)} \right) \\ P_{d_{free},4_2}(3) &= \frac{3}{8} Q\left(\sqrt{E_b \left(\frac{2.586}{N_T} + \frac{2}{N_0} \right)} \right) + \frac{3}{16} Q\left(\sqrt{E_b \left(\frac{4}{N_T} + \frac{0.586}{N_0} \right)} \right) + \\ &+ \frac{3}{16} Q\left(\sqrt{E_b \left(\frac{4.586}{N_T} \right)} \right) \end{aligned} \quad (4 - 46)$$

$$P_{d_{free},4_2}(4) = \frac{3}{4} Q\left(\sqrt{\frac{4.586 E_b}{N_T}} \right) \quad (4 - 47)$$

Finally, from (4-1), (4-4) and (4-5) the total P_b is

$$P_b \approx P_{d_{free},3_1} + P_{d_{free},4_1} + P_{d_{free},4_2} \quad (4 - 48)$$

As we see from Figure 36, once again system performance is degraded by PNI, but much less than when $K=2$. Taking as a reference point $P_b = 10^{-5}$, $E_b / N_i = 10.2$ dB is required for $\rho = 1$ and $E_b / N_i = 14.3$ dB is required for $\rho = 0.1$, where $E_b / N_0 = 8.6$ dB. Hence, the maximum degradation due to PNI at $P_b = 10^{-5}$ occurs for $\rho = 0.1$ and is 4.1 dB. For $P_b = 10^{-6}$, $E_b / N_i = 12.9$ dB and $E_b / N_i = 19.6$ dB are required for $\rho = 1$ and $\rho = 0.01$, respectively, which increases the degradation to 6.7 dB. It is noteworthy that, in order to attain $P_b = 10^{-6}$, we require $E_b / N_i < 19.6$ dB, but $P_b = 10^{-5}$ is attained for all E_b / N_i when $\rho = 0.01$ and $E_b / N_0 = 8.6$ dB.

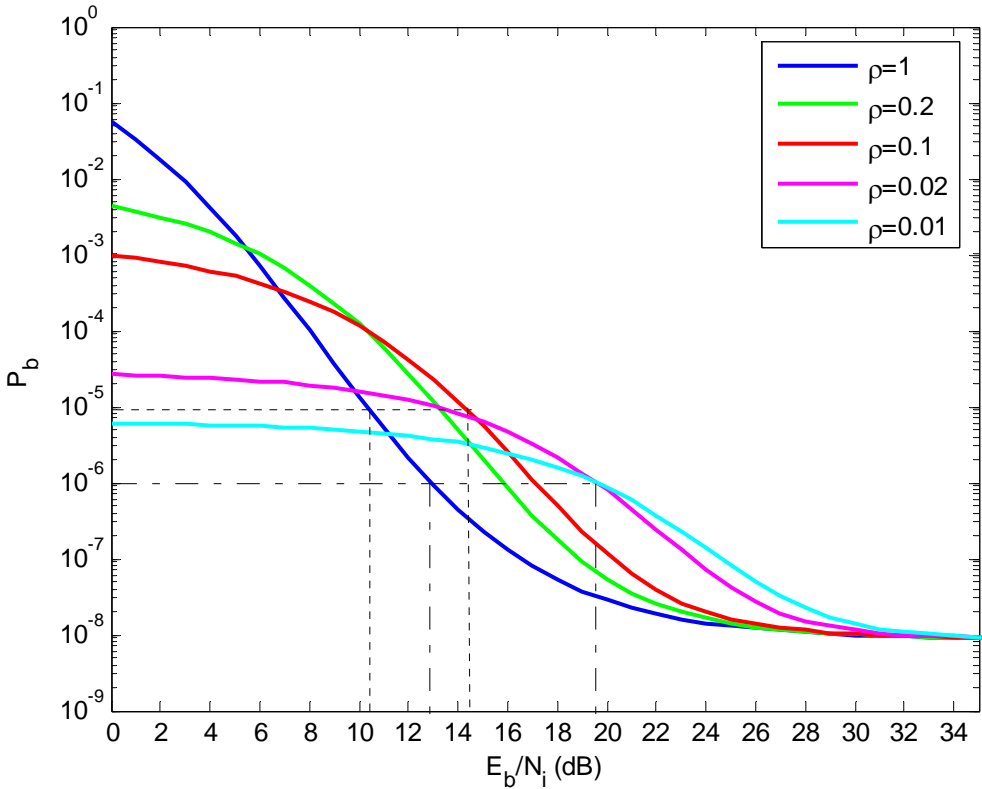


Figure 36. Performance of 8-PSK, $r=2/3$, TCM with $K=3$ and PNI with $E_b / N_o = 8.6$ dB.

3. Encoder with $K=4$

The encoder and the error trellis diagram are shown in Figures 25 and 26, respectively.

From the error trellis diagram, the minimum squared-Euclidean distance corresponds to the paths $S_0 - S_2 - S_8 - S_{12} - S_6 - S_0$, $S_0 - S_1 - S_4 - S_{10} - S_7 - S_5 - S_{12} - S_6 - S_0$, $S_0 - S_1 - S_4 - S_{10} - S_7 - S_5 - S_{13} - S_0$, and $S_0 - S_1 - S_4 - S_8 - S_{12} - S_6 - S_0$, and $d_{free}^2 = 5.172$. The information weight of each path is 1/4, 1/2, 1/4, and 1/2, respectively, and the total information weight is $B_{d_{free}} = 3/2$.

For the first path, $S_0 - S_2 - S_8 - S_{12} - S_6 - S_0$, the interference can occur for $i=0$, $i=1$, $i=2$, $i=3$, $i=4$, or $i=5$ branches of the path. Hence, from (4-2), (4-4) and (4-5), we have

$$\begin{aligned}
P_{d_{free},5_1} = & \binom{5}{0}(1-\rho)^5 P_{d_{free},5_1}(0) + \binom{5}{1}\rho(1-\rho)^4 P_{d_{free},5_1}(1) + \binom{5}{2}\rho^2(1-\rho)^3 P_{d_{free},5_1}(2) + \\
& + \binom{5}{3}\rho^3(1-\rho)^2 P_{d_{free},5_1}(3) + \binom{5}{4}\rho^4(1-\rho) P_{d_{free},5_1}(4) + \binom{5}{5}\rho^5 P_{d_{free},5_1}(5) \quad (4 - 49)
\end{aligned}$$

where

$$P_{d_{free},5_1}(0) = \frac{1}{8}Q\left(\sqrt{\frac{5.172E_b}{N_0}}\right) \quad (4 - 50)$$

$$\begin{aligned}
P_{d_{free},5_1}(1) = & \frac{1}{20}Q\left(\sqrt{E_b\left(\frac{2}{N_T} + \frac{3.172}{N_0}\right)}\right) + \frac{1}{20}Q\left(\sqrt{E_b\left(\frac{0.586}{N_T} + \frac{4.586}{N_0}\right)}\right) + \\
& + \frac{1}{40}Q\left(\sqrt{E_b\left(\frac{5.172}{N_0}\right)}\right) \quad (4 - 51)
\end{aligned}$$

$$\begin{aligned}
P_{d_{free},5_1}(2) = & \frac{3}{80}Q\left(\sqrt{E_b\left(\frac{2.586}{N_T} + \frac{2.586}{N_0}\right)}\right) + \frac{2}{80}Q\left(\sqrt{E_b\left(\frac{2}{N_T} + \frac{3.172}{N_0}\right)}\right) + \\
& + \frac{2}{80}Q\left(\sqrt{E_b\left(\frac{0.586}{N_T} + \frac{4.586}{N_0}\right)}\right) + \frac{1}{80}Q\left(\sqrt{E_b\left(\frac{4}{N_T} + \frac{1.172}{N_0}\right)}\right) + \\
& + \frac{1}{80}Q\left(\sqrt{E_b\left(\frac{1.172}{N_T} + \frac{4}{N_0}\right)}\right) + \frac{1}{80}Q\left(\sqrt{E_b\left(\frac{4.586}{N_T} + \frac{0.586}{N_0}\right)}\right) \quad (4 - 52)
\end{aligned}$$

$$P_{d_{free},5_1}(3) = \frac{3}{80}Q\left(\sqrt{E_b\left(\frac{2.586}{N_T} + \frac{2.586}{N_0}\right)}\right) + \frac{2}{80}Q\left(\sqrt{E_b\left(\frac{3.172}{N_T} + \frac{2}{N_0}\right)}\right) +$$

$$\begin{aligned}
& + \frac{2}{80} Q \left(\sqrt{E_b \left(\frac{4.586}{N_T} + \frac{0.586}{N_0} \right)} \right) + \frac{1}{80} Q \left(\sqrt{E_b \left(\frac{1.172}{N_T} + \frac{4}{N_0} \right)} \right) + \\
& + \frac{1}{80} Q \left(\sqrt{E_b \left(\frac{4}{N_T} + \frac{1.172}{N_0} \right)} \right) + \frac{1}{80} Q \left(\sqrt{E_b \left(\frac{0.586}{N_T} + \frac{4.586}{N_0} \right)} \right)
\end{aligned} \tag{4 - 53}$$

$$\begin{aligned}
P_{d_{free},5_1}(4) &= \frac{1}{20} Q \left(\sqrt{E_b \left(\frac{3.172}{N_T} + \frac{2}{N_0} \right)} \right) + \frac{1}{20} Q \left(\sqrt{E_b \left(\frac{4.586}{N_T} + \frac{0.586}{N_0} \right)} \right) + \\
& + \frac{1}{40} Q \left(\sqrt{E_b \left(\frac{5.172}{N_T} \right)} \right)
\end{aligned} \tag{4 - 54}$$

$$P_{d_{free},5_1}(5) = \frac{1}{8} Q \left(\sqrt{\frac{5.172 E_b}{N_T}} \right) \tag{4 - 55}$$

For the second path, $S_0 - S_1 - S_4 - S_{10} - S_7 - S_5 - S_{12} - S_6 - S_0$, the interference can occur for $i=0, i=1, i=2, i=3, i=4, i=5, i=6, i=7$, or $i=8$ branches of the path.

Hence, from (4-2), (4-4) and (4-5), we have

$$\begin{aligned}
P_{d_{free},8_1} &= \binom{8}{0} (1-\rho)^8 P_{d_{free},8_1}(0) + \binom{8}{1} \rho (1-\rho)^7 P_{d_{free},8_1}(1) + \binom{8}{2} \rho^2 (1-\rho)^6 P_{d_{free},8_1}(2) + \\
& + \binom{8}{3} \rho^3 (1-\rho)^5 P_{d_{free},8_1}(3) + \binom{8}{4} \rho^4 (1-\rho)^4 P_{d_{free},8_1}(4) + \binom{8}{5} \rho^5 (1-\rho)^3 P_{d_{free},8_1}(5) +
\end{aligned}$$

$$+ \binom{8}{6} \rho^6 (1-\rho)^2 P_{d_{free}, 8_1}(6) + \binom{8}{7} \rho^7 (1-\rho) P_{d_{free}, 8_1}(7) + \binom{8}{8} \rho^8 P_{d_{free}, 8_1}(8) \quad (4 - 56)$$

where

$$P_{d_{free}, 8_1}(0) = \frac{1}{4} Q\left(\sqrt{\frac{5.172 E_b}{N_0}}\right) \quad (4 - 57)$$

$$\begin{aligned} P_{d_{free}, 8_1}(1) &= \frac{1}{16} Q\left(\sqrt{E_b\left(\frac{2}{N_T} + \frac{3.172}{N_0}\right)}\right) + \frac{1}{16} Q\left(\sqrt{E_b\left(\frac{0.586}{N_T} + \frac{4.586}{N_0}\right)}\right) + \\ &+ \frac{1}{8} Q\left(\sqrt{E_b\left(\frac{5.172}{N_0}\right)}\right) \end{aligned} \quad (4 - 58)$$

$$\begin{aligned} P_{d_{free}, 8_1}(2) &= \frac{1}{14} Q\left(\sqrt{E_b\left(\frac{2}{N_T} + \frac{3.172}{N_0}\right)}\right) + \frac{1}{28} Q\left(\sqrt{E_b\left(\frac{2.586}{N_T} + \frac{2.586}{N_0}\right)}\right) + \\ &+ \frac{1}{112} Q\left(\sqrt{E_b\left(\frac{4}{N_T} + \frac{1.172}{N_0}\right)}\right) + \frac{1}{14} Q\left(\sqrt{E_b\left(\frac{0.586}{N_T} + \frac{4.586}{N_0}\right)}\right) + \\ &+ \frac{3}{56} Q\left(\sqrt{E_b\left(\frac{5.172}{N_0}\right)}\right) + \frac{1}{112} Q\left(\sqrt{E_b\left(\frac{1.172}{N_T} + \frac{4}{N_0}\right)}\right) \end{aligned} \quad (4 - 59)$$

$$\begin{aligned} P_{d_{free}, 8_1}(3) &= \frac{2}{25} Q\left(\sqrt{E_b\left(\frac{2.586}{N_T} + \frac{2.586}{N_0}\right)}\right) + \frac{3}{50} Q\left(\sqrt{E_b\left(\frac{2}{N_T} + \frac{3.172}{N_0}\right)}\right) + \\ &+ \frac{1}{50} Q\left(\sqrt{E_b\left(\frac{4}{N_T} + \frac{1.172}{N_0}\right)}\right) + \frac{13}{200} Q\left(\sqrt{E_b\left(\frac{0.586}{N_T} + \frac{4.586}{N_0}\right)}\right) + \end{aligned}$$

$$\begin{aligned}
& + \frac{1}{50} Q \left(\sqrt{E_b \left(\frac{1.172}{N_T} + \frac{4}{N_0} \right)} \right) + \frac{1}{50} Q \left(\sqrt{E_b \left(\frac{5.172}{N_T} \right)} \right) + \\
& + \frac{1}{200} Q \left(\sqrt{E_b \left(\frac{3.172}{N_T} + \frac{2}{N_0} \right)} \right) + \frac{1}{100} Q \left(\sqrt{E_b \left(\frac{4.586}{N_T} + \frac{0.586}{N_0} \right)} \right)
\end{aligned} \quad (4 - 60)$$

$$\begin{aligned}
P_{d_{free}, 8_1}(4) = & \frac{3}{35} Q \left(\sqrt{E_b \left(\frac{2.586}{N_T} + \frac{2.586}{N_0} \right)} \right) + \frac{1}{35} Q \left(\sqrt{E_b \left(\frac{0.586}{N_T} + \frac{4.586}{N_0} \right)} \right) + \\
& + \frac{3}{140} Q \left(\sqrt{E_b \left(\frac{1.172}{N_T} + \frac{4}{N_0} \right)} \right) + \frac{1}{35} Q \left(\sqrt{E_b \left(\frac{3.172}{N_T} + \frac{2}{N_0} \right)} \right) + \\
& + \frac{1}{35} Q \left(\sqrt{E_b \left(\frac{4.586}{N_T} + \frac{0.586}{N_0} \right)} \right) + \frac{1}{35} Q \left(\sqrt{E_b \left(\frac{2}{N_T} + \frac{3.172}{N_0} \right)} \right) + \\
& + \frac{3}{140} Q \left(\sqrt{E_b \left(\frac{4}{N_T} + \frac{1.172}{N_0} \right)} \right) + Q \left(\sqrt{E_b \left(\frac{5.172}{N_0} \right)} \right) + \\
& + Q \left(\sqrt{E_b \left(\frac{5.172}{N_T} \right)} \right)
\end{aligned} \quad (4 - 61)$$

$$\begin{aligned}
P_{d_{free}, 8_1}(5) = & \frac{2}{25} Q \left(\sqrt{E_b \left(\frac{2.586}{N_T} + \frac{2.586}{N_0} \right)} \right) + \frac{3}{50} Q \left(\sqrt{E_b \left(\frac{3.172}{N_T} + \frac{2}{N_0} \right)} \right) + \\
& + \frac{1}{50} Q \left(\sqrt{E_b \left(\frac{1.172}{N_T} + \frac{4}{N_0} \right)} \right) + \frac{13}{200} Q \left(\sqrt{E_b \left(\frac{4.586}{N_T} + \frac{0.586}{N_0} \right)} \right) +
\end{aligned}$$

$$\begin{aligned}
& + \frac{1}{50} Q \left(\sqrt{E_b \left(\frac{4}{N_T} + \frac{1.172}{N_0} \right)} \right) + \frac{1}{50} Q \left(\sqrt{E_b \left(\frac{5.172}{N_0} \right)} \right) + \\
& + \frac{1}{200} Q \left(\sqrt{E_b \left(\frac{2}{N_T} + \frac{3.172}{N_0} \right)} \right) + \frac{1}{100} Q \left(\sqrt{E_b \left(\frac{0.586}{N_T} + \frac{4.586}{N_0} \right)} \right)
\end{aligned} \quad (4 - 62)$$

$$\begin{aligned}
P_{d_{free}, 8_1}(6) = & \frac{1}{14} Q \left(\sqrt{E_b \left(\frac{3.172}{N_T} + \frac{2}{N_0} \right)} \right) + \frac{1}{28} Q \left(\sqrt{E_b \left(\frac{2.586}{N_T} + \frac{2.586}{N_0} \right)} \right) + \\
& + \frac{1}{112} Q \left(\sqrt{E_b \left(\frac{1.172}{N_T} + \frac{4}{N_0} \right)} \right) + \frac{1}{14} Q \left(\sqrt{E_b \left(\frac{4.586}{N_T} + \frac{0.586}{N_0} \right)} \right) + \\
& + \frac{3}{56} Q \left(\sqrt{E_b \left(\frac{5.172}{N_T} \right)} \right) + \frac{1}{112} Q \left(\sqrt{E_b \left(\frac{4}{N_T} + \frac{1.172}{N_0} \right)} \right)
\end{aligned} \quad (4 - 63)$$

$$\begin{aligned}
P_{d_{free}, 8_1}(7) = & \frac{1}{16} Q \left(\sqrt{E_b \left(\frac{3.172}{N_T} + \frac{2}{N_0} \right)} \right) + \frac{1}{16} Q \left(\sqrt{E_b \left(\frac{4.586}{N_T} + \frac{0.586}{N_0} \right)} \right) + \\
& + \frac{1}{8} Q \left(\sqrt{E_b \left(\frac{5.172}{N_T} \right)} \right)
\end{aligned} \quad (4 - 64)$$

$$P_{d_{free}, 8_1}(8) = \frac{1}{4} Q \left(\sqrt{\frac{5.172 E_b}{N_T}} \right) \quad (4 - 65)$$

For the third path, $S_0 - S_1 - S_4 - S_{10} - S_7 - S_5 - S_{13} - S_0$, the interference can occur for $i=0, i=1, i=2, i=3, i=4, i=5, i=6$, or $i=7$ branches of the path.

Hence, from (4-2), (4-4) and (4-5), we have

$$\begin{aligned}
P_{d_{free},7_1} = & \binom{7}{0}(1-\rho)^7 P_{d_{free},7_1}(0) + \binom{7}{1}\rho(1-\rho)^6 P_{d_{free},7_1}(1) + \binom{7}{2}\rho^2(1-\rho)^5 P_{d_{free},7_1}(2) + \\
& + \binom{7}{3}\rho^3(1-\rho)^4 P_{d_{free},7_1}(3) + \binom{7}{4}\rho^4(1-\rho)^3 P_{d_{free},7_1}(4) + \binom{7}{5}\rho^5(1-\rho)^2 P_{d_{free},7_1}(5) + \\
& + \binom{7}{6}\rho^6(1-\rho) P_{d_{free},7_1}(6) + \binom{7}{7}\rho^7 P_{d_{free},7_1}(7)
\end{aligned} \tag{4 - 66}$$

where

$$P_{d_{free},7_1}(0) = \frac{1}{8}Q\left(\sqrt{\frac{5.172E_b}{N_0}}\right) \tag{4 - 67}$$

$$\begin{aligned}
P_{d_{free},7_1}(1) = & \frac{1}{28}Q\left(\sqrt{E_b\left(\frac{2}{N_T} + \frac{3.172}{N_0}\right)}\right) + \frac{1}{28}Q\left(\sqrt{E_b\left(\frac{0.586}{N_T} + \frac{4.586}{N_0}\right)}\right) + \\
& + \frac{3}{56}Q\left(\sqrt{E_b\left(\frac{5.172}{N_0}\right)}\right)
\end{aligned} \tag{4 - 68}$$

$$\begin{aligned}
P_{d_{free},7_1}(2) = & \frac{3}{84}Q\left(\sqrt{E_b\left(\frac{2}{N_T} + \frac{3.172}{N_0}\right)}\right) + \frac{1}{22}Q\left(\sqrt{E_b\left(\frac{2.586}{N_T} + \frac{2.586}{N_0}\right)}\right) + \\
& + \frac{1}{168}Q\left(\sqrt{E_b\left(\frac{4}{N_T} + \frac{1.172}{N_0}\right)}\right) + \frac{3}{84}Q\left(\sqrt{E_b\left(\frac{0.586}{N_T} + \frac{4.586}{N_0}\right)}\right) +
\end{aligned}$$

$$+ \frac{3}{168} Q\left(\sqrt{E_b\left(\frac{5.172}{N_0}\right)}\right) + \frac{1}{168} Q\left(\sqrt{E_b\left(\frac{1.172}{N_T} + \frac{4}{N_0}\right)}\right) \quad (4 - 69)$$

$$\begin{aligned} P_{d_{free}, 7_1}(3) = & \frac{3}{70} Q\left(\sqrt{E_b\left(\frac{2.586}{N_T} + \frac{2.586}{N_0}\right)}\right) + \frac{3}{140} Q\left(\sqrt{E_b\left(\frac{2}{N_T} + \frac{3.172}{N_0}\right)}\right) + \\ & + \frac{3}{280} Q\left(\sqrt{E_b\left(\frac{1.172}{N_T} + \frac{4}{N_0}\right)}\right) + \frac{3}{140} Q\left(\sqrt{E_b\left(\frac{0.586}{N_T} + \frac{4.586}{N_0}\right)}\right) + \\ & + \frac{3}{280} Q\left(\sqrt{E_b\left(\frac{4}{N_T} + \frac{1.172}{N_0}\right)}\right) + \frac{1}{280} Q\left(\sqrt{E_b\left(\frac{5.172}{N_0}\right)}\right) + \\ & + \frac{1}{140} Q\left(\sqrt{E_b\left(\frac{3.172}{N_T} + \frac{2}{N_0}\right)}\right) + \frac{1}{140} Q\left(\sqrt{E_b\left(\frac{4.586}{N_T} + \frac{0.586}{N_0}\right)}\right) \quad (4 - 70) \end{aligned}$$

$$\begin{aligned} P_{d_{free}, 7_1}(4) = & \frac{3}{70} Q\left(\sqrt{E_b\left(\frac{2.586}{N_T} + \frac{2.586}{N_0}\right)}\right) + \frac{3}{140} Q\left(\sqrt{E_b\left(\frac{3.172}{N_T} + \frac{2}{N_0}\right)}\right) + \\ & + \frac{3}{280} Q\left(\sqrt{E_b\left(\frac{4}{N_T} + \frac{1.172}{N_0}\right)}\right) + \frac{3}{140} Q\left(\sqrt{E_b\left(\frac{4.586}{N_T} + \frac{0.586}{N_0}\right)}\right) + \\ & + \frac{3}{280} Q\left(\sqrt{E_b\left(\frac{1.172}{N_T} + \frac{4}{N_0}\right)}\right) + \frac{1}{280} Q\left(\sqrt{E_b\left(\frac{5.172}{N_T}\right)}\right) + \\ & + \frac{1}{140} Q\left(\sqrt{E_b\left(\frac{2}{N_T} + \frac{3.172}{N_0}\right)}\right) + \frac{1}{140} Q\left(\sqrt{E_b\left(\frac{0.586}{N_T} + \frac{4.586}{N_0}\right)}\right) \quad (4 - 71) \end{aligned}$$

$$P_{d_{free}, 7_1}(5) = \frac{3}{84} Q\left(\sqrt{E_b\left(\frac{3.172}{N_T} + \frac{2}{N_0}\right)}\right) + \frac{1}{22} Q\left(\sqrt{E_b\left(\frac{2.586}{N_T} + \frac{2.586}{N_0}\right)}\right) +$$

$$\begin{aligned}
& + \frac{1}{168} Q \left(\sqrt{E_b \left(\frac{1.172}{N_T} + \frac{4}{N_0} \right)} \right) + \frac{3}{84} Q \left(\sqrt{E_b \left(\frac{4.586}{N_T} + \frac{0.586}{N_0} \right)} \right) + \\
& + \frac{3}{168} Q \left(\sqrt{E_b \left(\frac{5.172}{N_T} \right)} \right) + \frac{1}{168} Q \left(\sqrt{E_b \left(\frac{4}{N_T} + \frac{1.172}{N_0} \right)} \right)
\end{aligned} \tag{4 - 72}$$

$$\begin{aligned}
P_{d_{free},7_1}(6) &= \frac{1}{28} Q \left(\sqrt{E_b \left(\frac{3.172}{N_T} + \frac{2}{N_0} \right)} \right) + \frac{1}{28} Q \left(\sqrt{E_b \left(\frac{4.586}{N_T} + \frac{0.586}{N_0} \right)} \right) + \\
& + \frac{3}{56} Q \left(\sqrt{E_b \left(\frac{5.172}{N_T} \right)} \right)
\end{aligned} \tag{4 - 73}$$

$$P_{d_{free},7_1}(7) = \frac{1}{8} Q \left(\sqrt{\frac{5.172 E_b}{N_T}} \right) \tag{4 - 74}$$

For the fourth path, $S_0 - S_1 - S_4 - S_8 - S_{12} - S_6 - S_0$, the interference can occur for $i=0, i=1, i=2, i=3, i=4, i=5$, or $i=6$ branches of the path.

Hence, from (4-2), (4-4) and (4-5), we have

$$\begin{aligned}
P_{d_{free},6_1} &= \binom{6}{0} (1-\rho)^6 P_{d_{free},6_1}(0) + \binom{6}{1} \rho (1-\rho)^5 P_{d_{free},6_1}(1) + \binom{6}{2} \rho^2 (1-\rho)^4 P_{d_{free},6_1}(2) + \\
& + \binom{6}{3} \rho^3 (1-\rho)^3 P_{d_{free},6_1}(3) + \binom{6}{4} \rho^4 (1-\rho)^2 P_{d_{free},6_1}(4) + \binom{6}{5} \rho^5 (1-\rho) P_{d_{free},6_1}(5) + \\
& + \binom{6}{6} \rho^6 P_{d_{free},6_1}(6)
\end{aligned} \tag{4 - 75}$$

where

$$P_{d_{free},6_1}(0) = \frac{1}{4}Q\left(\sqrt{\frac{5.172E_b}{N_0}}\right) \quad (4 - 76)$$

$$\begin{aligned} P_{d_{free},6_1}(1) &= \frac{1}{12}Q\left(\sqrt{E_b\left(\frac{2}{N_T} + \frac{3.172}{N_0}\right)}\right) + \frac{1}{12}Q\left(\sqrt{E_b\left(\frac{0.586}{N_T} + \frac{4.586}{N_0}\right)}\right) + \\ &\quad + \frac{1}{12}Q\left(\sqrt{E_b\left(\frac{5.172}{N_0}\right)}\right) \end{aligned} \quad (4 - 77)$$

$$\begin{aligned} P_{d_{free},6_1}(2) &= \frac{1}{15}Q\left(\sqrt{E_b\left(\frac{2}{N_T} + \frac{3.172}{N_0}\right)}\right) + \frac{1}{15}Q\left(\sqrt{E_b\left(\frac{2.586}{N_T} + \frac{2.586}{N_0}\right)}\right) + \\ &\quad + \frac{1}{60}Q\left(\sqrt{E_b\left(\frac{4}{N_T} + \frac{1.172}{N_0}\right)}\right) + \frac{1}{15}Q\left(\sqrt{E_b\left(\frac{0.586}{N_T} + \frac{4.586}{N_0}\right)}\right) + \\ &\quad + \frac{1}{60}Q\left(\sqrt{E_b\left(\frac{5.172}{N_0}\right)}\right) + \frac{1}{60}Q\left(\sqrt{E_b\left(\frac{1.172}{N_T} + \frac{4}{N_0}\right)}\right) \end{aligned} \quad (4 - 78)$$

$$\begin{aligned} P_{d_{free},6_1}(3) &= \frac{1}{10}Q\left(\sqrt{E_b\left(\frac{2.586}{N_T} + \frac{2.586}{N_0}\right)}\right) + \frac{1}{40}Q\left(\sqrt{E_b\left(\frac{2}{N_T} + \frac{3.172}{N_0}\right)}\right) + \\ &\quad + \frac{1}{40}Q\left(\sqrt{E_b\left(\frac{4.586}{N_T} + \frac{0.586}{N_0}\right)}\right) + \frac{1}{40}Q\left(\sqrt{E_b\left(\frac{4}{N_T} + \frac{1.172}{N_0}\right)}\right) + \\ &\quad + \frac{1}{40}Q\left(\sqrt{E_b\left(\frac{0.586}{N_T} + \frac{4.586}{N_0}\right)}\right) + \frac{1}{40}Q\left(\sqrt{E_b\left(\frac{3.172}{N_T} + \frac{2}{N_T}\right)}\right) + \\ &\quad + \frac{1}{40}Q\left(\sqrt{E_b\left(\frac{1.172}{N_T} + \frac{4}{N_0}\right)}\right) \end{aligned} \quad (4 - 79)$$

$$\begin{aligned}
P_{d_{free},6_1}(4) = & \frac{1}{15}Q\left(\sqrt{E_b\left(\frac{3.172}{N_T} + \frac{2}{N_0}\right)}\right) + \frac{1}{15}Q\left(\sqrt{E_b\left(\frac{2.586}{N_T} + \frac{2.586}{N_0}\right)}\right) + \\
& + \frac{1}{60}Q\left(\sqrt{E_b\left(\frac{1.172}{N_T} + \frac{4}{N_0}\right)}\right) + \frac{1}{15}Q\left(\sqrt{E_b\left(\frac{4.586}{N_T} + \frac{0.586}{N_0}\right)}\right) + \\
& + \frac{1}{60}Q\left(\sqrt{E_b\left(\frac{5.172}{N_T}\right)}\right) + \frac{1}{60}Q\left(\sqrt{E_b\left(\frac{4}{N_T} + \frac{1.172}{N_0}\right)}\right)
\end{aligned} \tag{4 - 80}$$

$$\begin{aligned}
P_{d_{free},6_1}(5) = & \frac{1}{12}Q\left(\sqrt{E_b\left(\frac{3.172}{N_T} + \frac{2}{N_0}\right)}\right) + \frac{1}{12}Q\left(\sqrt{E_b\left(\frac{4.586}{N_T} + \frac{0.586}{N_0}\right)}\right) + \\
& + \frac{1}{12}Q\left(\sqrt{E_b\left(\frac{5.172}{N_T}\right)}\right)
\end{aligned} \tag{4 - 81}$$

$$P_{d_{free},6_1}(6) = \frac{1}{4}Q\left(\sqrt{\frac{5.172E_b}{N_T}}\right) \tag{4 - 82}$$

Finally, from (4-1), (4-4) and (4-5), the total P_b is

$$P_b \approx P_{d_{free},5_1} + P_{d_{free},6_1} + P_{d_{free},7_1} + P_{d_{free},8_1} \tag{4 - 83}$$

As we see from Figure 37, and taking as a reference point $P_b = 10^{-5}$ and $E_b / N_0 = 7.8$ dB, $E_b / N_i = 9.0$ dB is required for $\rho = 1$ and $E_b / N_i = 11.7$ dB for $\rho = 0.1$. The maximum degradation due to PNI, which occurs for $\rho = 0.1$, is 2.7 dB. For $P_b = 10^{-6}$ and the same signal-to-noise ratio, $E_b / N_i = 9.0$ dB and $E_b / N_i = 15.6$ dB are

required for $\rho = 0.01$ and $\rho = 0.02$, respectively, which increases the degradation to 6.6 dB. We easily conclude that, while PNI degrades performance, the degradation is much less than for smaller value of K .

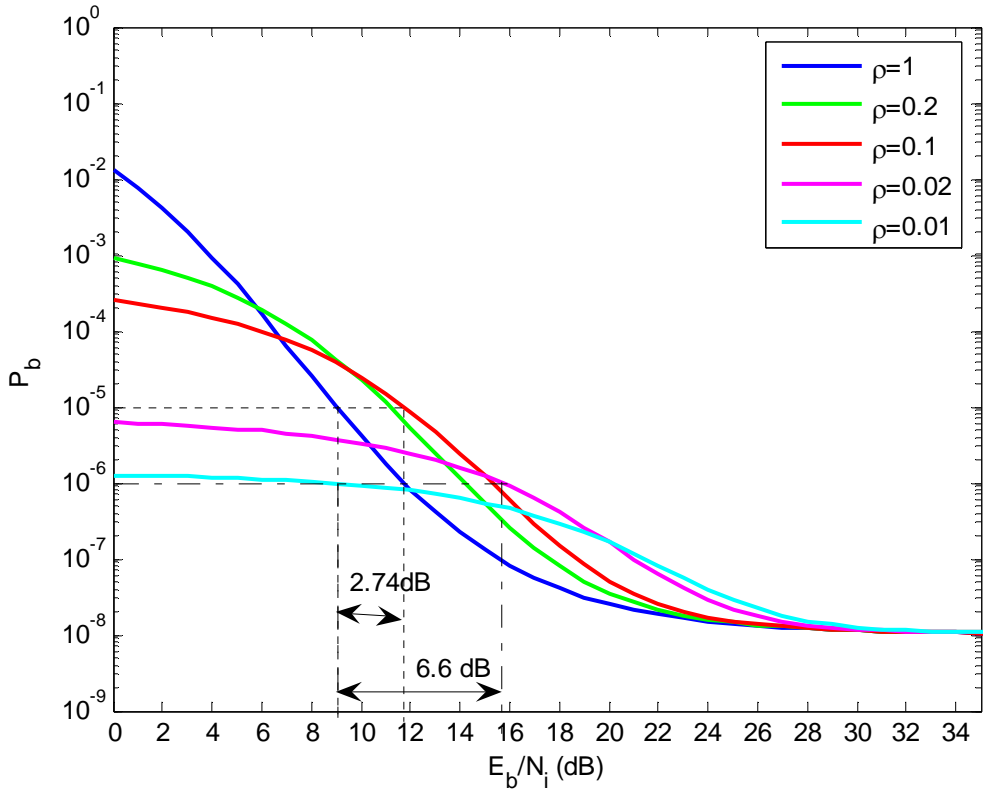


Figure 37. Performance of 8-PSK, $r=2/3$, TCM with $K=4$ and PNI with $E_b / N_o = 7.8$ dB.

The results for 8-PSK, $r=2/3$, TCM with $K=2$, 3, and 4 are summarized in Tables 3 and 4, where the E_b / N_o was selected for $P_b = 10^{-8}$ when $E_b / N_i \gg 1$.

Table 3. Performance of 8-PSK, $r=2/3$ TCM with $K=2, 3, 4$ for $P_b = 10^{-5}$ in PNI.

Encoder	E_b / N_o	ρ	E_b / N_i	Remarks
$r=2/3, K=2$	12.2 dB	$\rho = 1$	11.5 dB	Degradation of the system by 7.1 dB.
$r=2/3, K=2$	12.2 dB	$\rho = 0.02$	18.6 dB	
$r=2/3, K=3$	8.6 dB	$\rho = 1$	12.2 dB	Degradation of the system by 4.1 dB.
$r=2/3, K=3$	8.6 dB	$\rho = 0.1$	14.3 dB	
$r=2/3, K=4$	7.8 dB	$\rho = 1$	9.0 dB	Degradation of the system by 2.7 dB.
$r=2/3, K=4$	7.8 dB	$\rho = 0.1$	11.7 dB	

Table 4. Performance of 8-PSK, $r=2/3$, TCM with $K=2, 3, 4$ for $P_b = 10^{-6}$ in PNI.

Encoder	E_b / N_o	ρ	E_b / N_i	Remarks
$r=2/3, K=2$	12.2 dB	$\rho = 1$	13.2 dB	Degradation of the system by 10.6 dB.
$r=2/3, K=2$	12.2 dB	$\rho = 0.01$	24.1 dB	
$r=2/3, K=3$	8.6 dB	$\rho = 1$	12.9 dB	Degradation of the system by 6.7 dB.
$r=2/3, K=3$	8.6 dB	$\rho = 0.01$	19.6 dB	
$r=2/3, K=4$	7.8 dB	$\rho = 1$	9.0 dB	Degradation of the system by 6.6 dB.
$r=2/3, K=4$	7.8 dB	$\rho = 0.02$	15.6 dB	

E. COMPARISON BETWEEN QPSK AND 8-PSK TCM SYSTEMS

1. Comparison between QPSK, $r=1/2$ and 8-PSK, $r=2/3$ TCM with $K=2$

As can bee seen from Figure 38, for $\rho=1$, taking as a reference $P_b = 10^{-5}$, the QPSK, $r=1/2$, $K=2$ system has better performance than the 8-PSK, $r=2/3$, $K=2$ system by 1.8dB. At $P_b = 10^{-7}$, the two systems have the same performance, and for $P_b < 10^{-7}$, the 8-PSK, $r=2/3$ system is superior. Figure 39 shows that for $P_b = 10^{-5}$ and $\rho=0.2$, the QPSK, $r=1/2$, $K=3$ system has better performance than the 8-PSK, $r=2/3$, $K=3$ system by 2.8 dB, and Figure 40 shows that for $\rho=0.01$, the QPSK, $r=1/2$ system has $P_b < 10^{-5}$ for all E_b / N_i . As can be seen, when $\rho < 1$, the lower data rate system always outperforms the higher data rate system in terms of the E_b / N_i and E_b / N_o required to achieve a specific P_b .

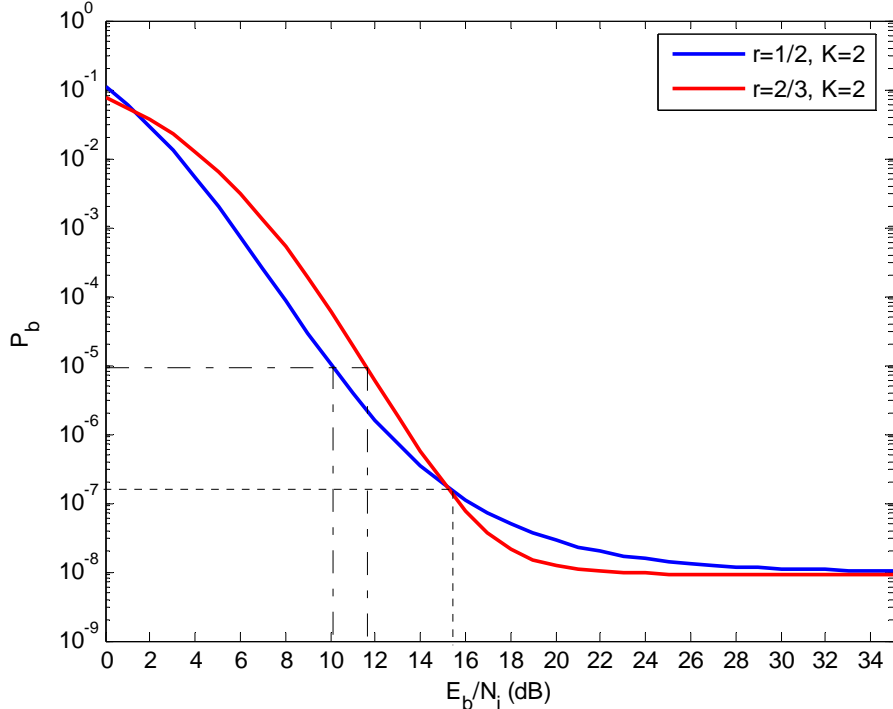


Figure 38. Comparison between QPSK, $r=1/2$ and 8-PSK, $r=2/3$ TCM with $K=2$ in PNI for $\rho=1$ with $E_b / N_o = 8$ dB and $E_b / N_o = 12.2$ dB, respectively.

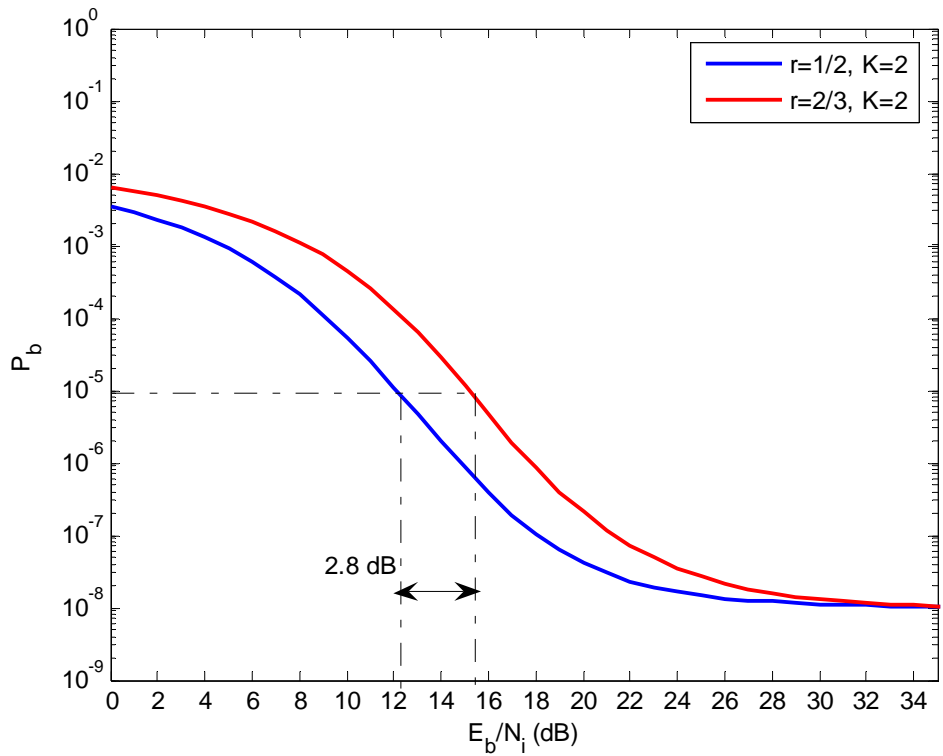


Figure 39. Comparison between QPSK, $r=1/2$ and 8-PSK, $r=2/3$ TCM with $K=2$ in PNI for $\rho=0.2$ with $E_b/N_o=8$ dB and $E_b/N_o=12.2$ dB, respectively.

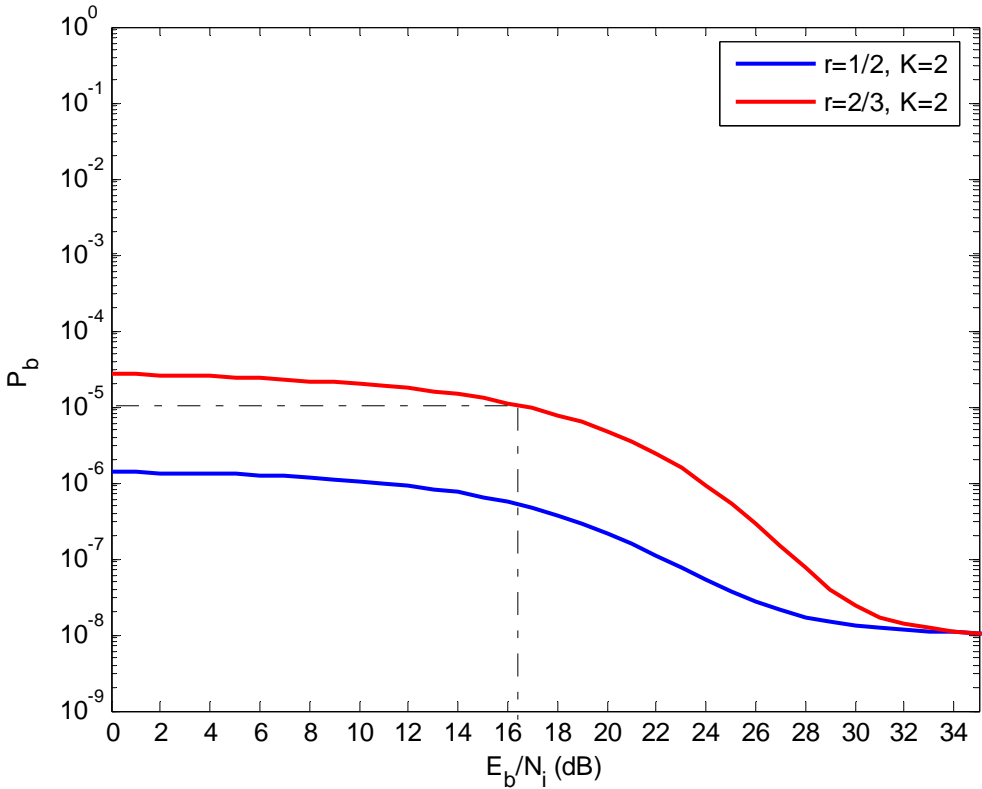


Figure 40. Comparison between QPSK, $r=1/2$ and 8-PSK, $r=2/3$ TCM with $K=2$ in PNI for $\rho=0.01$ with $E_b/N_o=8$ dB and $E_b/N_o=12.2$ dB, respectively.

2. Comparison between QPSK, $r=1/2$ and 8-PSK, $r=2/3$, TCM with $K=3$.

As can be seen from Figures 41 and 42, for $\rho=1$ and $\rho=0.2$, respectively, and for $P_b=10^{-5}$, the QPSK, $r=1/2$, $K=3$ system has better performance than the 8-PSK, $r=2/3$, $K=3$ system by 1.1 dB and 1.6 dB for $\rho=1$ and $\rho=0.2$, respectively. Figure 43 shows that for $\rho=0.01$ the 8-PSK, $r=2/3$ system has better performance, and $P_b < 10^{-5}$ no matter what E_b/N_i is.

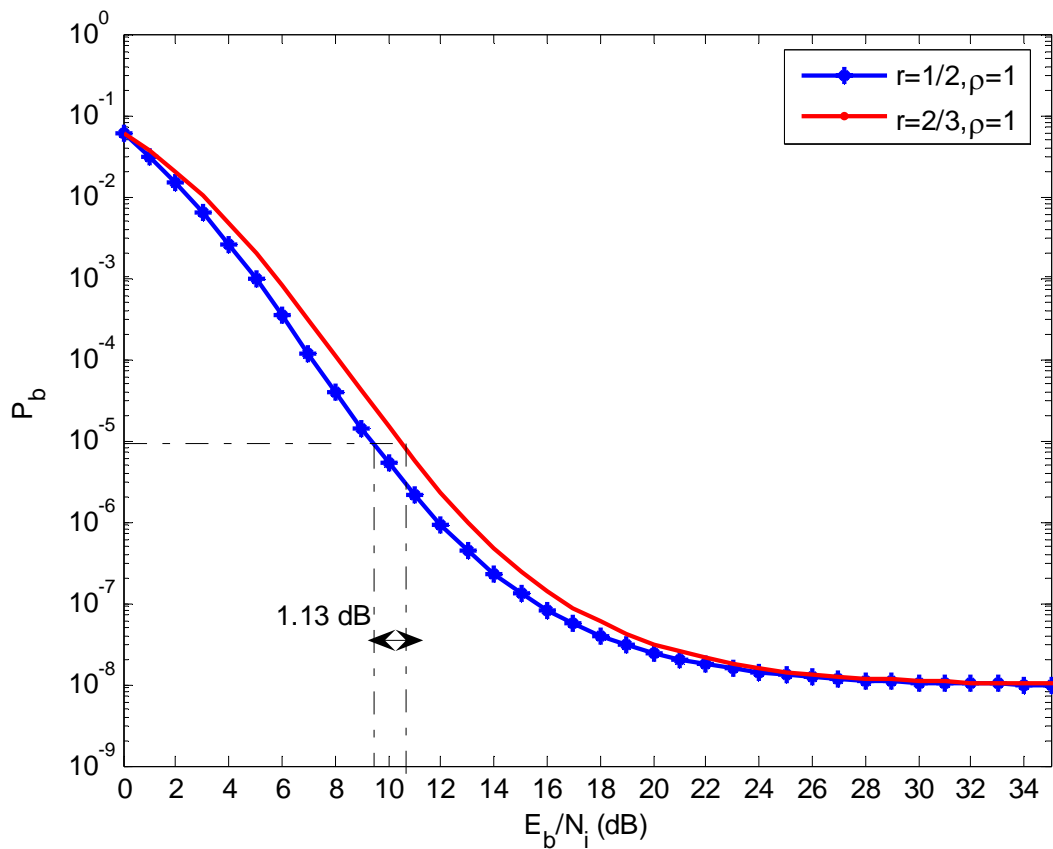


Figure 41. Comparison between QPSK, $r=1/2$ and 8-PSK, $r=2/3$ TCM with $K=3$ for $\rho=1$ in PNI with $E_b / N_o = 7.4$ dB and $E_b / N_o = 8.6$ dB, respectively.

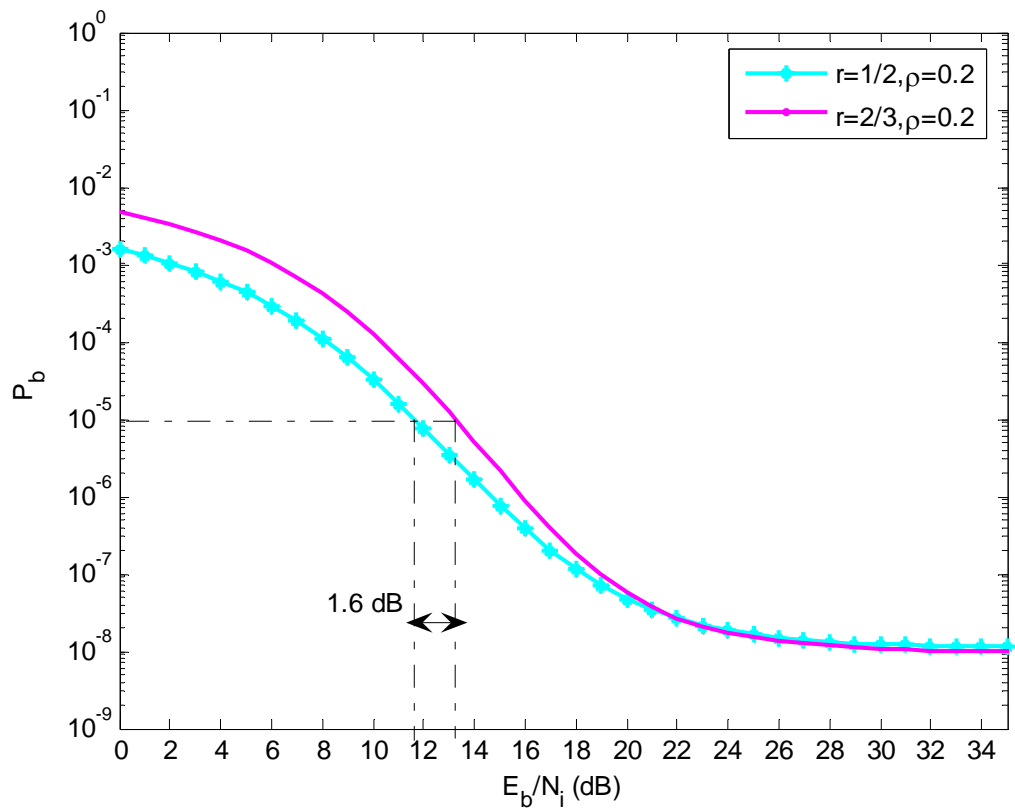


Figure 42. Comparison between QPSK, $r=1/2$ and 8-PSK, $r=2/3$ TCM with $K=3$ for $\rho=0.2$ in PNI with $E_b/N_o=7.4$ dB and $E_b/N_o=8.6$ dB, respectively.

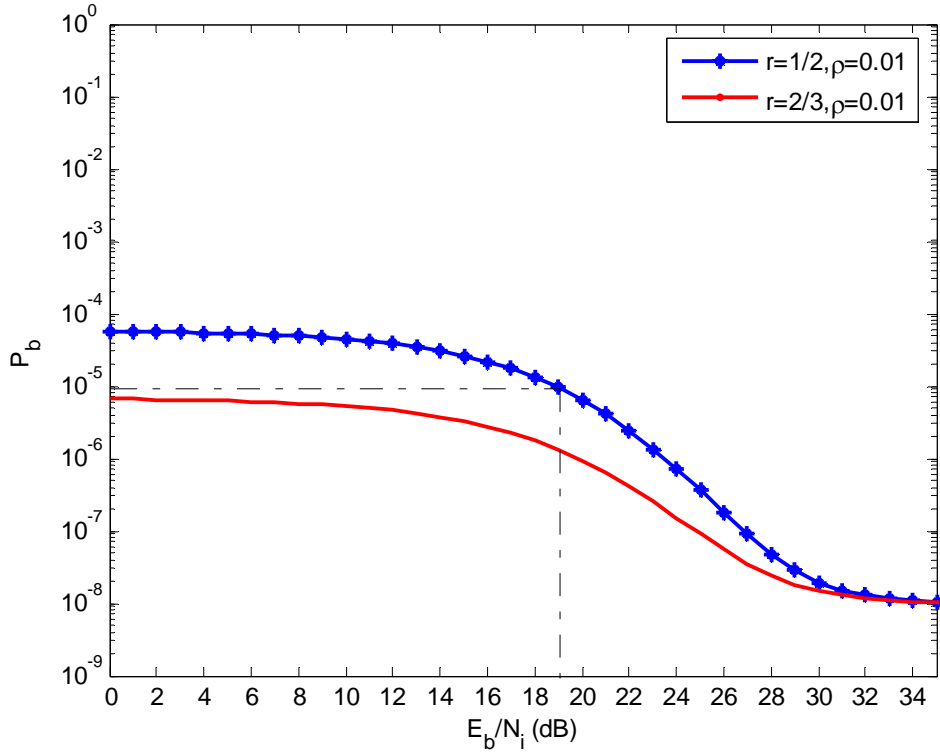


Figure 43. Comparison between QPSK, $r=1/2$ and 8-PSK, $r=2/3$ TCM with $K=3$ for $\rho=0.01$ in PNI with $E_b/N_o=7.4$ dB and $E_b/N_o=8.6$ dB, respectively.

3. Comparison between QPSK, $r=1/2$ and 8-PSK, $r=2/3$ TCM with $K=4$

As can be seen from Figures 44 and 45, for $\rho=1$ and $\rho=0.2$, respectively, and for $P_b=10^{-5}$, the 8-PSK, $r=2/3$ system has better performance than the QPSK, $r=1/2$ system by 0.9 dB and 0.1 dB for $\rho=1$ and $\rho=0.2$, respectively. Figure 46 shows that for $\rho=0.01$ the QPSK, $r=1/2$ system is better than the 8-PSK, $r=2/3$ system, but $P_b < 10^{-5}$ for both systems for all E_b/N_i .

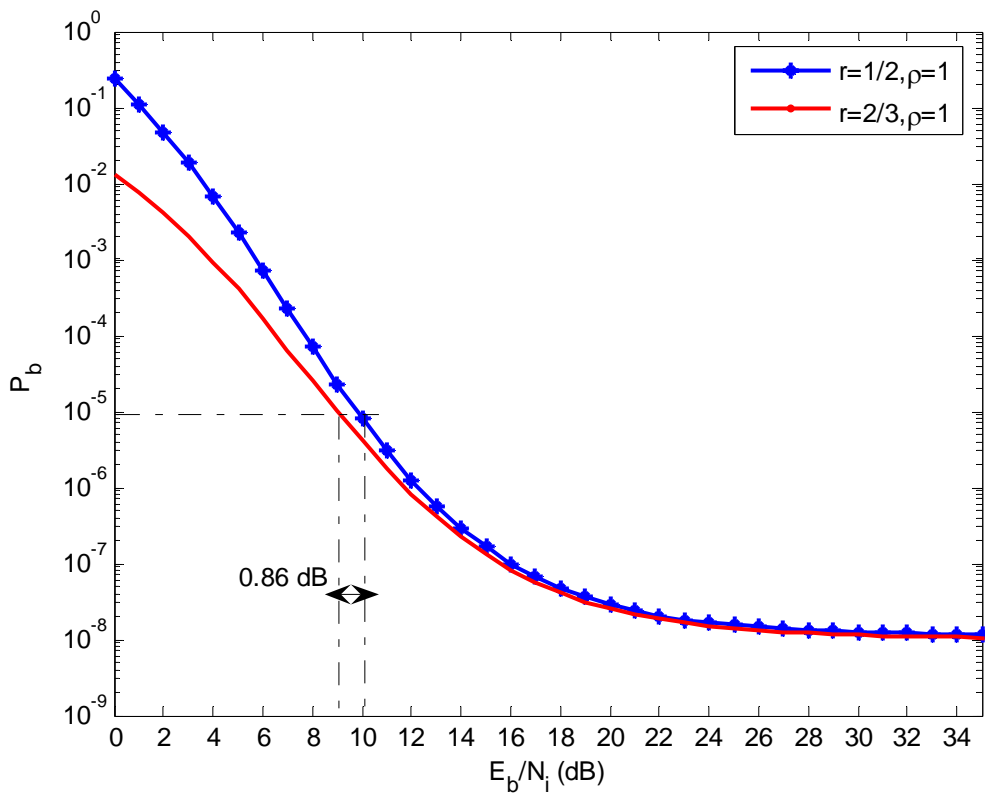


Figure 44. Comparison between QPSK, $r=1/2$ and 8-PSK, $r=2/3$ TCM with $K=4$ for $\rho=1$ in PNI with $E_b / N_o = 7.1$ dB and $E_b / N_o = 7.8$ dB, respectively.

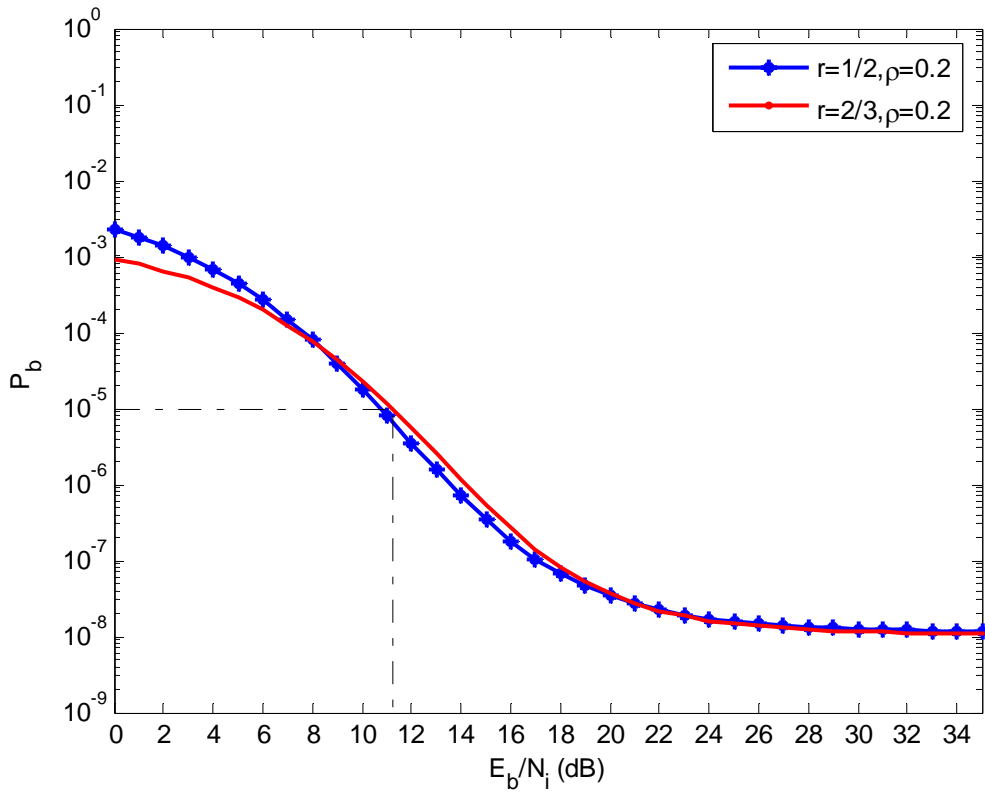


Figure 45. Comparison between QPSK, $r=1/2$ and 8-PSK, $r=2/3$ TCM with $K=4$ for $\rho=0.2$ in PNI with $E_b / N_o = 7.1$ dB and $E_b / N_o = 7.8$ dB, respectively.

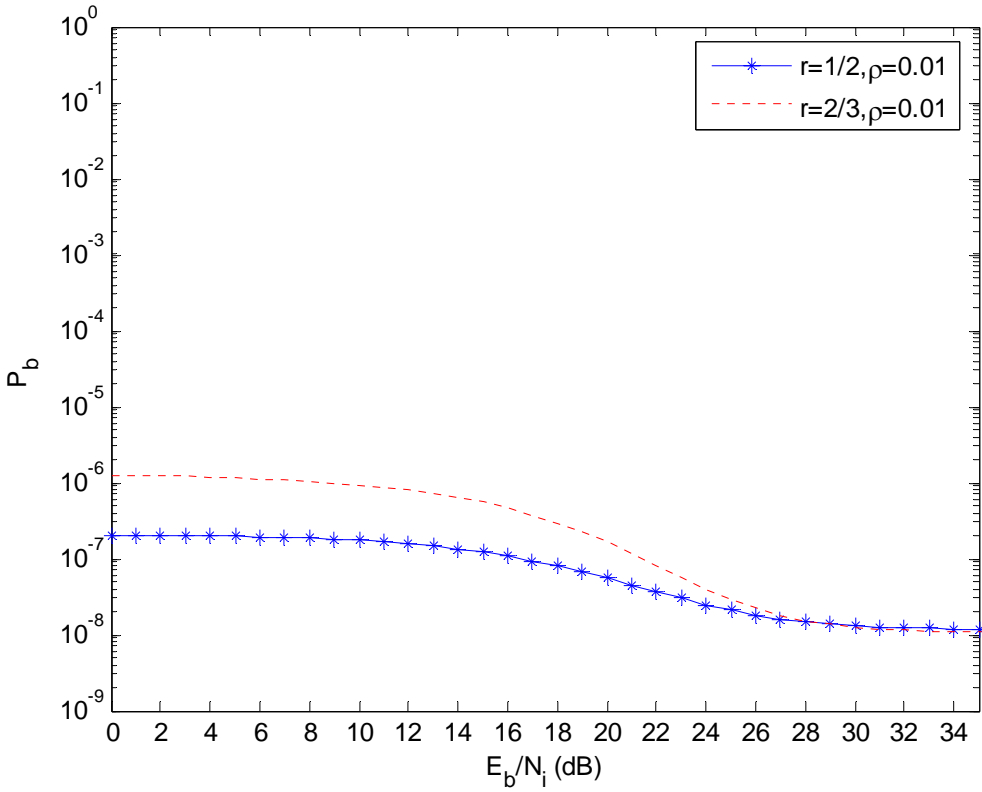


Figure 46. Comparison between QPSK, $r=1/2$ and 8-PSK, $r=2/3$ TCM with $K=4$ for $\rho=0.01$ in PNI with $E_b / N_o = 7.1$ dB and $E_b / N_o = 7.8$ dB, respectively.

4. Comparison between TCM with QPSK, $r=1/2$, $K=1$ and 8-PSK, $r=2/3$, $K=2$

In this subsection we compare the performance between the QPSK, $r=1/2$, $K=1$ and 8-PSK, $r=2/3$, $K=2$ TCM systems. As we see in Figure 47, for $\rho=1$ and $\rho=0.2$, the performance of the two systems is approximately the same for a probability of bit error of 10^{-5} , and the required E_b / N_i is 11.8 dB and 15.5 dB, respectively. For $P_b < 10^{-5}$ and $\rho=1$, the performance of the 8-PSK, $r=2/3$ system is better than that of the QPSK, $r=1/2$ system.

Figure 48 shows that for $\rho=0.01$, the 8-PSK, $r=2/3$ system is better than the QPSK, $r=1/2$ system. For $P_b = 10^{-5}$, the QPSK, $r=1/2$ system requires $E_b / N_i = 19.0$ dB, while the TCM system with 8-PSK, $r=2/3$ requires $E_b / N_i = 17.4$ dB, which yields a difference of 1.6 dB.

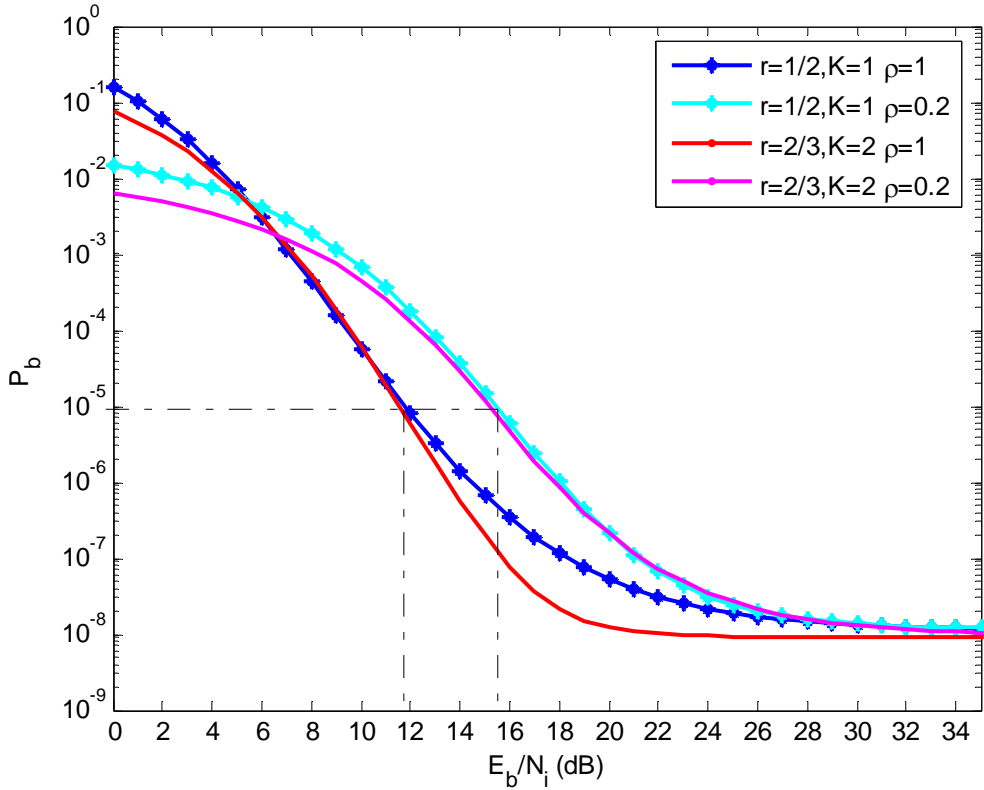


Figure 47. Comparison between QPSK, $r=1/2$, $K=1$ TCM and 8-PSK, $r=2/3$, $K=2$ TCM for $\rho=1$ and $\rho=0.2$ with $E_b / N_o = 10.2$ dB and $E_b / N_o = 12.2$ dB, respectively.

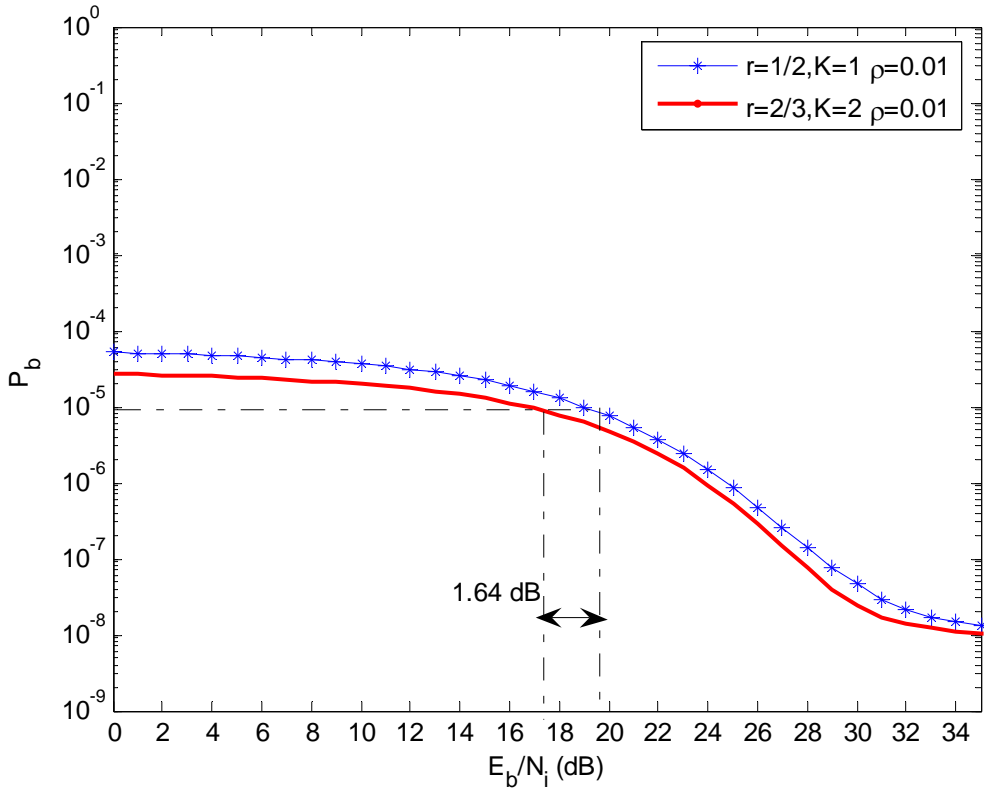


Figure 48. Comparison between QPSK, $r=1/2$, $K=1$ TCM and 8-PSK, $r=2/3$, $K=2$ TCM for $\rho=0.01$ with $E_b/N_o=10.2$ dB and $E_b/N_o=12.2$ dB, respectively.

5. Comparison between TCM with QPSK, $r=1/2$, $K=1$ and 8-PSK, $r=2/3$, $K=3$

In this subsection we compare the performance between the QPSK, $r=1/2$, $K=1$ and 8-PSK, $r=2/3$, $K=3$ TCM systems. As we see in Figure 49, for $\rho=1$ and $\rho=0.2$, the TCM system with 8-PSK, $r=2/3$ and $K=3$ has better performance than the TCM system with QPSK, $r=1/2$ and $K=1$. For $P_b=10^{-5}$ and $\rho=1$, the QPSK, $r=1/2$ system requires $E_b/N_i=11.8$ dB, while the TCM system with 8-PSK, $r=2/3$ requires $E_b/N_i=10.4$ dB, which yields a difference of 1.4 dB. For $P_b=10^{-5}$ and $\rho=0.2$, E_b/N_i is 15.5 dB and 13.4 dB, respectively, and the difference is 2.1 dB. In Figure 50, the two systems are compared for $\rho=0.01$. For $P_b=10^{-5}$, the QPSK, $r=1/2$ system requires $E_b/N_i=19.0$ dB, while for the TCM system with 8-PSK, $r=2/3$, $P_b < 10^{-5}$ for all E_b/N_i . Once again, the overall performance of 8-PSK, $r=2/3$, $K=3$ is better than for QPSK, $r=1/2$, $K=1$.

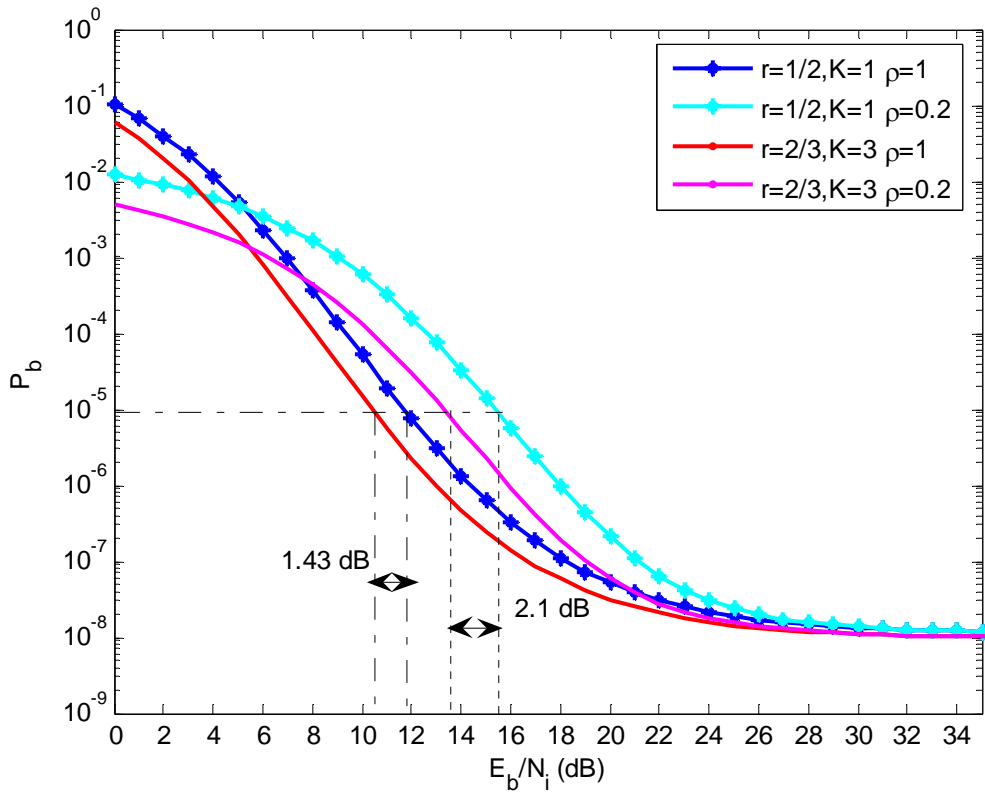


Figure 49. Comparison between QPSK, $r=1/2$, $K=1$ and 8-PSK, $r=2/3$, $K=3$ TCM for $\rho=1$ and $\rho=0.2$ with $E_b / N_o = 10.2$ dB and $E_b / N_o = 8.6$ dB, respectively.

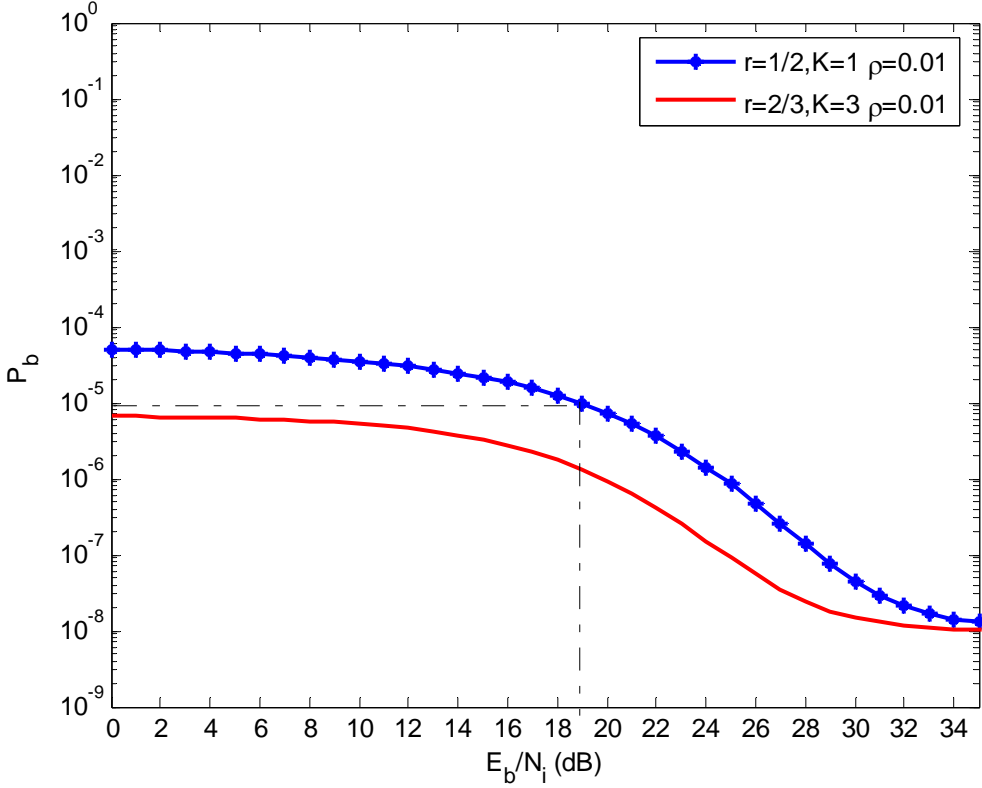


Figure 50. Comparison between QPSK, $r=1/2$, $K=1$ and 8-PSK, $r=2/3$, $K=3$ TCM for $\rho=0.01$ with $E_b / N_o = 10.2$ dB and $E_b / N_o = 8.6$ dB, respectively.

6. Comparison between TCM with QPSK, $r=1/2$, $K=1$ and 8-PSK, $r=2/3$, $K=4$

In this subsection we compare the performance between the QPSK, $r=1/2$, $K=1$ and 8-PSK, $r=2/3$, $K=4$ TCM systems. As we see in Figures 51 and 52, for $\rho=1$ and $\rho=0.2$, respectively, the TCM system with 8-PSK, $r=2/3$ and $K=4$ has better performance than the TCM system with QPSK, $r=1/2$ and $K=1$. For $P_b = 10^{-5}$ and $\rho=1$, the QPSK, $r=1/2$ system requires $E_b / N_i = 11.8$ dB, while the TCM system with 8-PSK, $r=2/3$ requires $E_b / N_i = 8.6$ dB, which yields a difference of 3.2 dB. For $P_b = 10^{-5}$ and $\rho=0.2$, the required E_b / N_i is 15.5 dB and 11.1 dB, respectively, and the difference is 4.4 dB. In Figure 53, the two systems are compared for $\rho=0.01$. For $P_b = 10^{-5}$, the

QPSK, $r=1/2$ system requires $E_b / N_i = 19.0$ dB, while for the TCM system with 8-PSK, $r=2/3$, $P_b < 10^{-5}$ for all E_b / N_i . Once again, the overall performance of the 8-PSK, $r=2/3$, $K=3$ system is better than that of the QPSK, $r=1/2$, $K=1$ system.

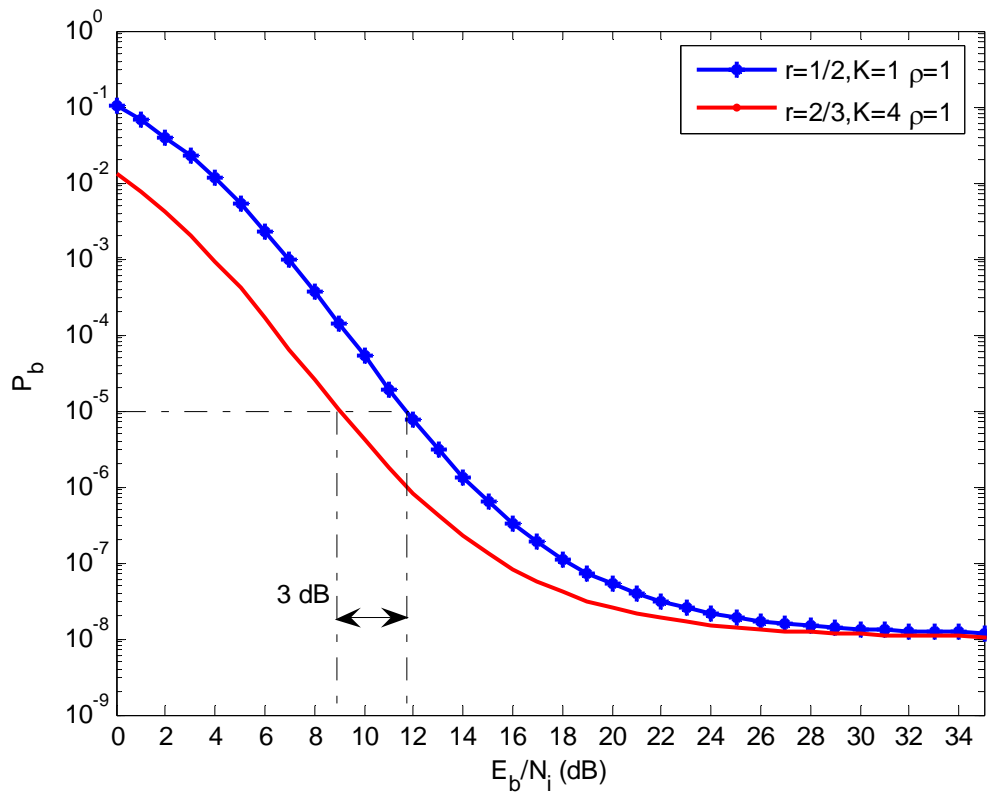


Figure 51. Comparison between TCM with QPSK, $r=1/2$, $K=1$ and 8-PSK, $r=2/3$, $K=4$ for $\rho=1$ with $E_b / N_o = 10.2$ dB and $E_b / N_o = 7.8$ dB, respectively.

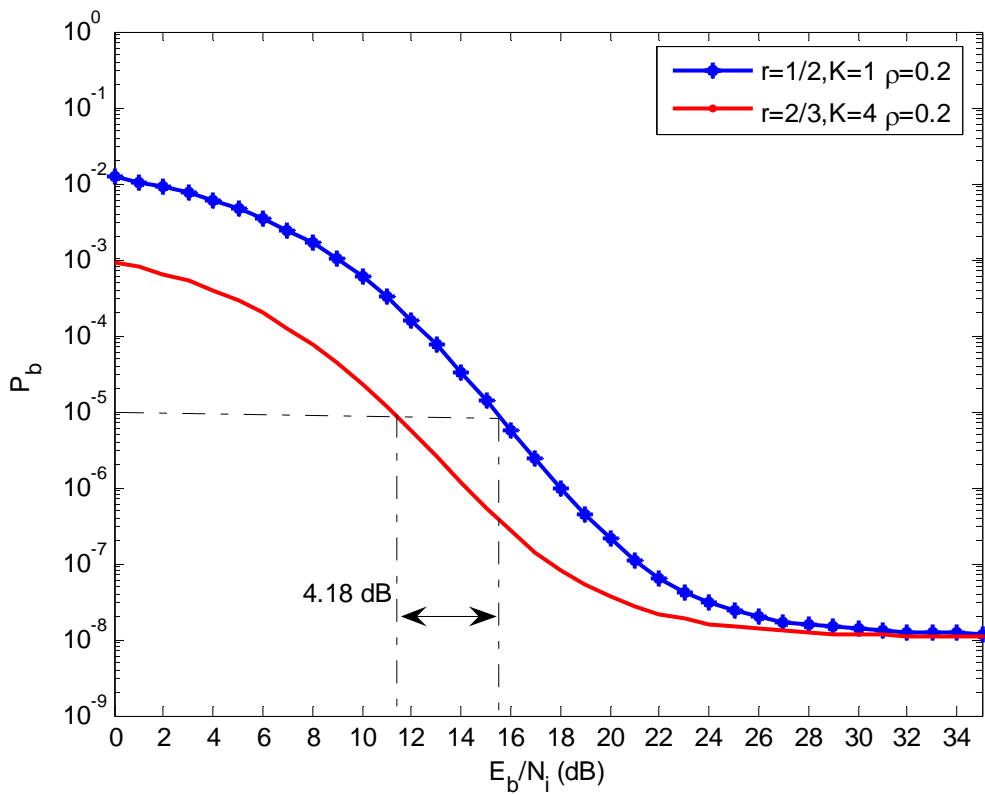


Figure 52. Comparison between TCM with QPSK, $r=1/2$, $K=1$ and 8-PSK, $r=2/3$, $K=4$ for $\rho=0.2$ with $E_b/N_o=10.2$ dB and $E_b/N_o=7.8$ dB, respectively.

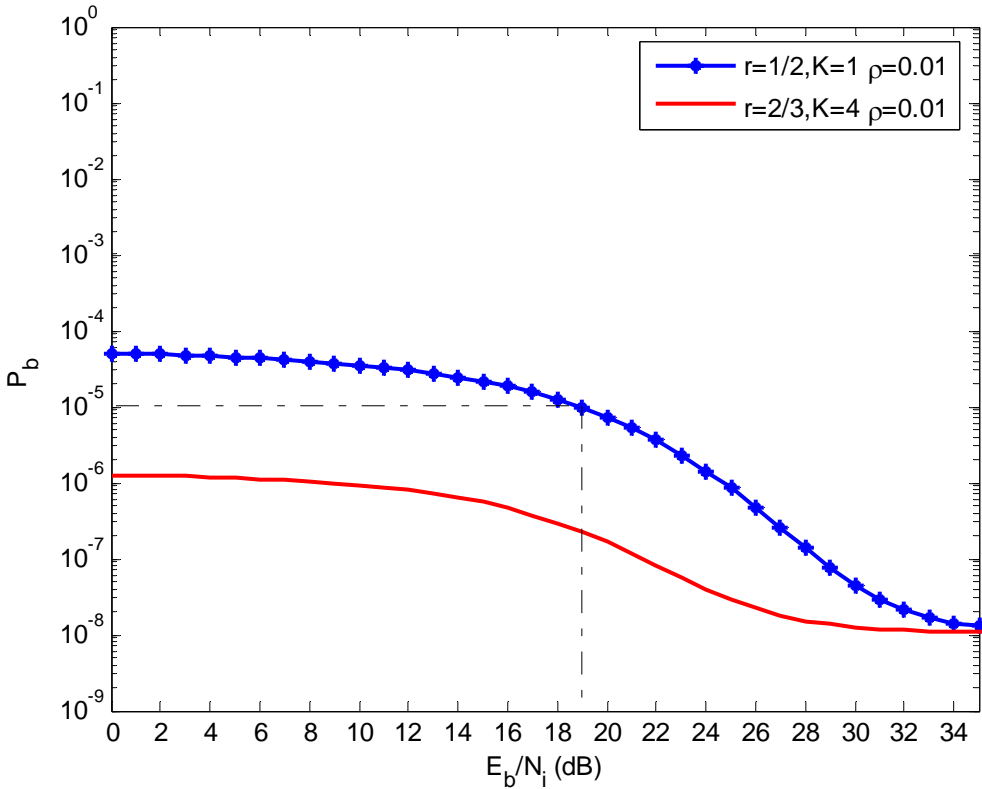


Figure 53. Comparison between TCM with QPSK, $r=1/2$, $K=1$ and 8-PSK, $r=2/3$, $K=4$ for $\rho=0.01$ with $E_b / N_o = 10.2$ dB and $E_b / N_o = 7.8$ dB, respectively.

7. Comparison between TCM with QPSK, $r=1/2$, $K=2$ and 8-PSK, $r=2/3$, $K=3$

In this subsection we compare the performance between the QPSK, $r=1/2$, $K=2$ and 8-PSK, $r=2/3$, $K=3$ TCM systems. As we see in Figure 54, for $\rho=1$ the performance of these two systems is approximately the same; and for a probability of bit error of 10^{-5} , the E_b / N_i required is 10.4 dB. For $\rho=0.2$, the TCM system with QPSK, $r=1/2$ and $K=2$ has better performance than the TCM system with 8-PSK, $r=2/3$ and $K=3$. For $P_b = 10^{-5}$, the QPSK, $r=1/2$ system requires $E_b / N_i = 11.9$ dB, while the TCM system with 8-PSK, $r=2/3$ requires $E_b / N_i = 13.4$ dB, which yields a difference of 1.5 dB. Figure 55 shows that $P_b < 10^{-5}$ for both systems for all E_b / N_i when $\rho = 0.01$.

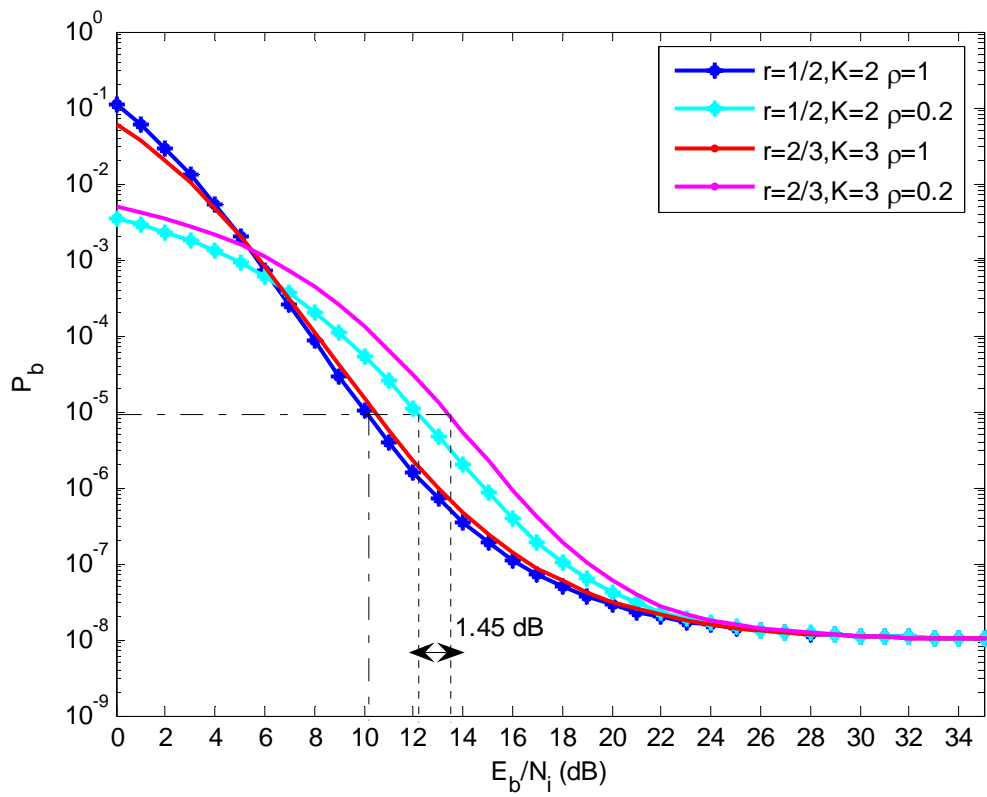


Figure 54. Comparison between TCM with QPSK, $r=1/2$, $K=2$ and 8-PSK, $r=2/3$, $K=3$ for $\rho=1$ and $\rho=0.2$ with $E_b / N_o = 8.1$ dB and $E_b / N_o = 8.6$ dB, respectively.

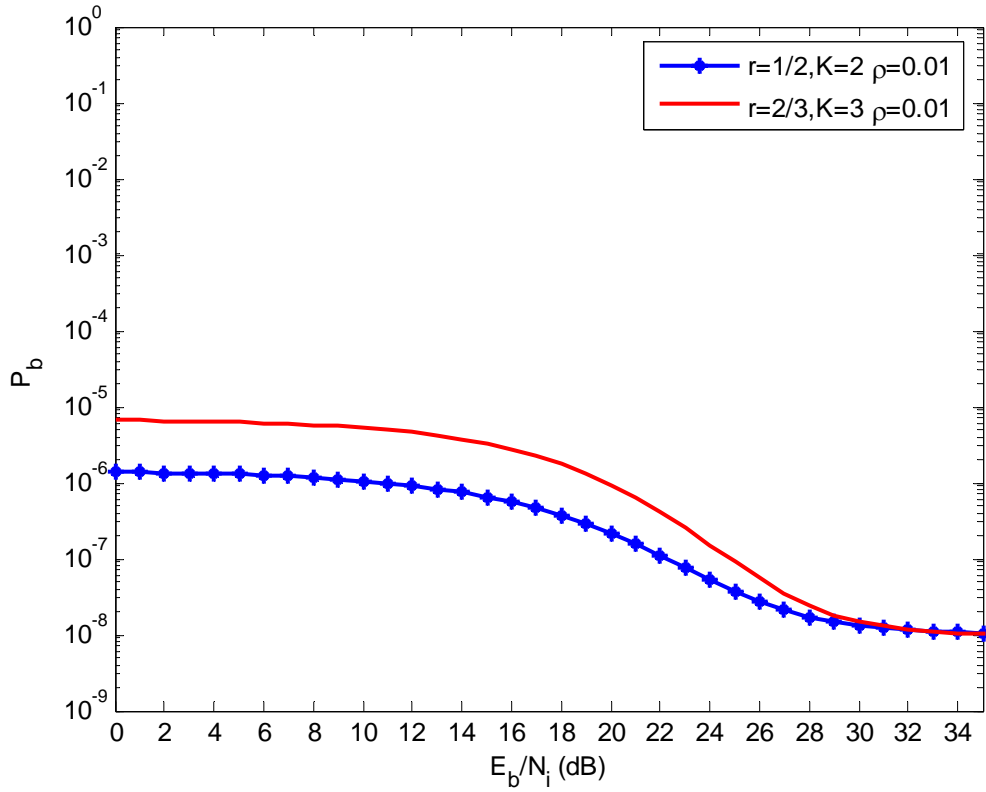


Figure 55. Comparison between TCM with QPSK, $r=1/2$, $K=2$ and 8-PSK, $r=2/3$, $K=3$ for $\rho=0.01$ with $E_b/N_o=8.1$ dB and $E_b/N_o=8.6$ dB, respectively.

8. Comparison between TCM with QPSK, $r=1/2$, $K=2$ and 8-PSK $r=2/3$, $K=4$

In this subsection we compare the performance between the QPSK, $r=1/2$, $K=2$ and 8-PSK, $r=2/3$, $K=4$ TCM systems. As we see in Figures 56 and 57, for $\rho=1$ and $\rho=0.2$, the TCM system with 8-PSK, $r=2/3$ and $K=4$ has better performance than the TCM system with QPSK, $r=1/2$ and $K=2$. For $P_b=10^{-5}$ and $\rho=1$, the QPSK, $r=1/2$ system requires $E_b/N_i=10.3$ dB, while the TCM system with 8-PSK, $r=2/3$ requires $E_b/N_i=8.8$ dB, which yields a difference of 1.5 dB. For $P_b=10^{-5}$ and $\rho=0.2$, the

required E_b / N_i is 11.9 dB and 11.3 dB, respectively, and the difference is 0.6 dB. Figure 55 shows that for $\rho=0.01$ both systems have approximately the same performance and $P_b < 10^{-5}$ for all E_b / N_i .

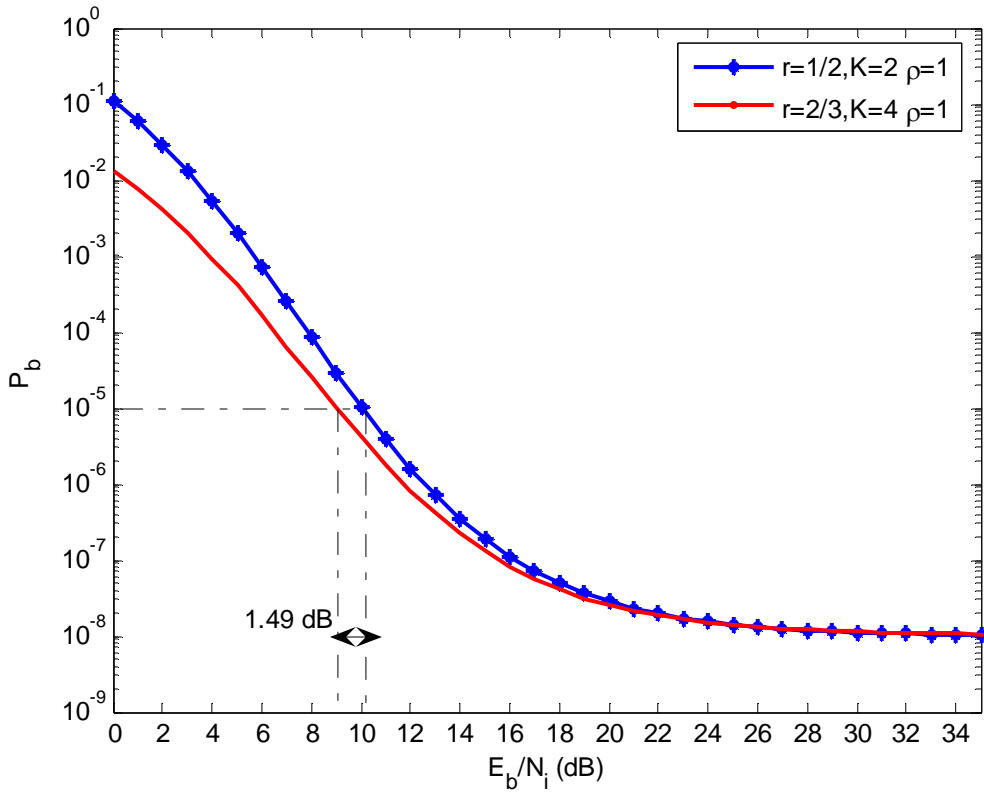


Figure 56. Comparison between TCM with QPSK, $r=1/2$, $K=2$ and 8-PSK, $r=2/3$, $K=4$ for $\rho=1$ with $E_b / N_o=8.1$ dB and $E_b / N_o=7.8$ dB, respectively.

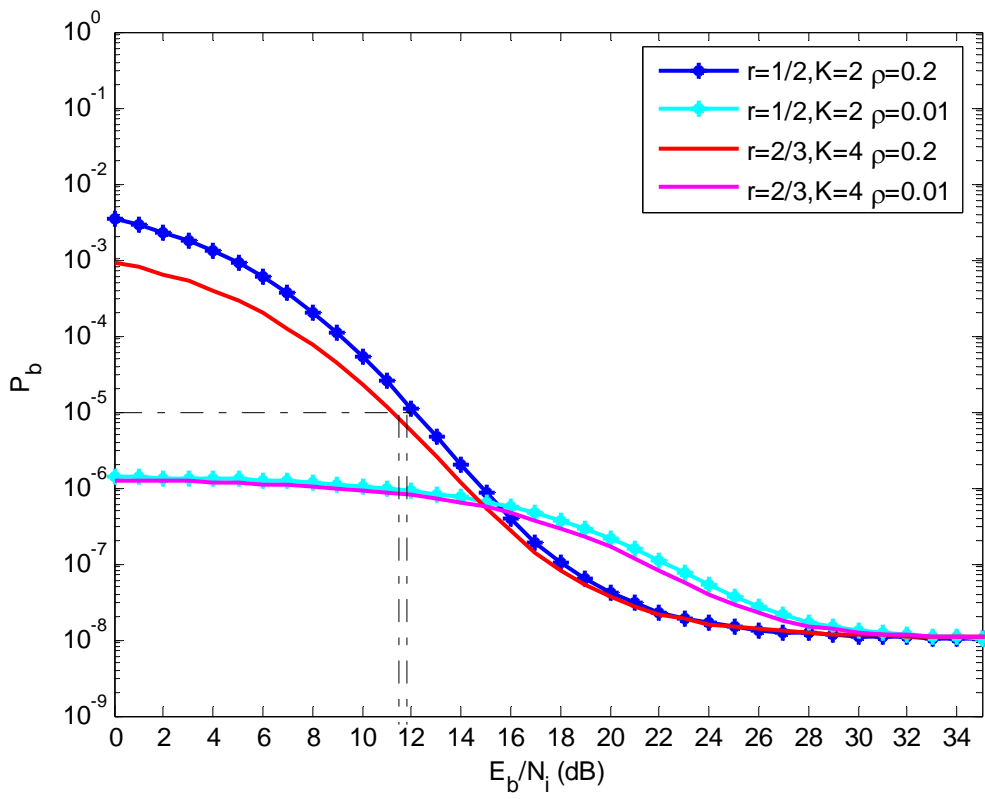


Figure 57. Comparison between TCM with QPSK, $r=1/2$, $K=2$ and 8-PSK, $r=2/3$, $K=4$ for $\rho=1$ with $E_b / N_o=8.1$ dB and $E_b / N_o=7.8$ dB, respectively.

Table 5. Comparison between QPSK, $r=1/2$ and 8-PSK, $r=2/3$ TCM, each having the same number memory elements for $P_b = 10^{-5}$ in PNI.

Encoder	E_b / N_o	ρ	E_b / N_i	Remarks
$r=1/2, K=2$	8.1 dB	$\rho = 1$	10.0 dB	QPSK, $r=1/2$ has better performance than 8-PSK, $r=2/3$ by 1.8 dB.
$r=2/3, K=2$	12.2 dB		11.8 dB	
$r=1/2, K=2$	8.1 dB	$\rho = 0.2$	12.2 dB	QPSK, $r=1/2$ has better performance than 8-PSK, $r=2/3$ by 2.8 dB.
$r=2/3, K=2$	12.2 dB		15.0 dB	
$r=1/2, K=2$	8.1 dB	$\rho = 0.01$	For all E_b / N_i	QPSK, $r=1/2$ has better performance than 8-PSK, $r=2/3$ for all E_b / N_i .
$r=2/3, K=2$	12.2 dB		17.2 dB	
$r=1/2, K=3$	7.4 dB	$\rho = 1$	9.4 dB	QPSK, $r=1/2$ has better performance than 8-PSK, $r=2/3$ by 1.1 dB.
$r=2/3, K=3$	8.6 dB		10.5 dB	
$r=1/2, K=3$	7.4 dB	$\rho = 0.2$	11.9 dB	QPSK, $r=1/2$ has better performance than 8-PSK, $r=2/3$ by 1.6 dB.
$r=2/3, K=3$	8.6 dB		13.5 dB	
$r=1/2, K=3$	7.4 dB	$\rho = 0.01$	19.0 dB	8-PSK, $r=1/2$ has better performance than QPSK, $r=2/3$ for all E_b / N_i .
$r=2/3, K=3$	8.6 dB		For all E_b / N_i	
$r=1/2, K=4$	7.1 dB	$\rho = 1$	10.0 dB	8-PSK, $r=2/3$ has better performance than QPSK, $r=1/2$ by 0.9 dB.
$r=2/3, K=4$	7.8 dB		9.1 dB	
$r=1/2, K=4$	7.1 dB	$\rho = 0.2$	11.2 dB	Both systems have equal performance.
$r=2/3, K=4$	7.8 dB		11.2 dB	
$r=1/2, K=4$	7.1 dB	$\rho = 0.01$	For all E_b / N_i	$P_b < 10^{-5}$ for both systems for all E_b / N_i .
$r=2/3, K=4$	7.8 dB		For all E_b / N_i	

Table 6. Comparison between QPSK, $r=1/2$ with $K=1$ and 8-PSK, $r=2/3$ TCM with $K=2, 3$, and 4 for $P_b = 10^{-5}$ in PNI.

Encoder	E_b / N_o	ρ	E_b / N_i	Remarks
$r=1/2, K=1$	10.2 dB	$\rho = 1$	11.8 dB	Both systems have equal performance.
$r=2/3, K=2$	12.2 dB		11.8 dB	
$r=1/2, K=1$	10.2 dB	$\rho = 0.2$	15.5 dB	Both systems have equal performance.
$r=2/3, K=2$	12.2 dB		15.5 dB	
$r=1/2, K=1$	10.2 dB	$\rho = 0.01$	19.0 dB	8-PSK, $r=2/3$ has better performance than QPSK, $r=1/2$ by 1.6 dB.
$r=2/3, K=2$	12.2 dB		17.4 dB	
$r=1/2, K=1$	10.2 dB	$\rho = 1$	11.8 dB	8-PSK, $r=2/3$ has better performance than QPSK, $r=1/2$ by 1.4 dB.
$r=2/3, K=3$	8.6 dB		10.4 dB	
$r=1/2, K=1$	10.2 dB	$\rho = 0.2$	15.5 dB	8-PSK, $r=2/3$ has better performance than QPSK, $r=1/2$ by 2.1 dB.
$r=2/3, K=3$	8.6 dB		13.4 dB	
$r=1/2, K=1$	10.2 dB	$\rho = 0.01$	19.0 dB	8-PSK, $r=2/3$ has better performance than QPSK, $r=1/2$ for all E_b / N_i .
$r=2/3, K=3$	8.6 dB		For all E_b / N_i	
$r=1/2, K=1$	10.2 dB	$\rho = 1$	11.8 dB	8-PSK, $r=2/3$ has better performance than QPSK, $r=1/2$ by 3.2 dB.
$r=2/3, K=4$	7.8 dB		8.6 dB	
$r=1/2, K=1$	10.2 dB	$\rho = 0.2$	15.5 dB	8-PSK, $r=2/3$ has better performance than QPSK, $r=1/2$ by 4.4 dB.
$r=2/3, K=4$	7.8 dB		11.1 dB	
$r=1/2, K=1$	10.2 dB	$\rho = 0.01$	19.0 dB	8-PSK, $r=2/3$ has better performance than QPSK, $r=1/2$ for all E_b / N_i .
$r=2/3, K=4$	7.8 dB		For all E_b / N_i	

Table 7. Comparison between QPSK, $r=1/2$ with $K=2$ and 8-PSK, $r=2/3$, TCM with $K=3$ and 4 for $P_b = 10^{-5}$ in PNI.

Encoder	E_b / N_o	ρ	E_b / N_i	Remarks
$r=1/2, K=2$	8.1 dB	$\rho = 1$	10.1 dB	Both systems have equal performance.
$r=2/3, K=3$	8.6 dB		10.1 dB	
$r=1/2, K=2$	8.1 dB	$\rho = 0.2$	11.9 dB	QPSK, $r=1/2$ has better performance than 8-PSK, $r=2/3$ by 1.5 dB.
$r=2/3, K=3$	8.6 dB		13.4 dB	
$r=1/2, K=2$	8.1 dB	$\rho = 0.01$	For all E_b / N_i	$P_b < 10^{-5}$ for both systems for all E_b / N_i .
$r=2/3, K=3$	8.6 dB		For all E_b / N_i	
$r=1/2, K=2$	8.1 dB	$\rho = 1$	10.3 dB	8-PSK, $r=2/3$ has better performance than QPSK, $r=1/2$ by 1.5 dB.
$r=2/3, K=4$	7.8 dB		8.8 dB	
$r=1/2, K=2$	8.1 dB	$\rho = 0.2$	11.9 dB	8-PSK, $r=2/3$ has better performance than QPSK, $r=1/2$ by 0.6 dB.
$r=2/3, K=4$	7.8 dB		11.3 dB	
$r=1/2, K=2$	8.1 dB	$\rho = 0.01$	For all E_b / N_i	$P_b < 10^{-5}$ for both systems for all E_b / N_i .
$r=2/3, K=4$	7.8 dB		For all E_b / N_i	

F. SUMMARY

In this chapter, the performance of TCM in PNI with both $r=1/2$ encoding and QPSK modulation and $r=2/3$ encoding with 8-PSK modulation was examined for $K=1, 2, 3$, and 4. The results of the comparison between QPSK, $r=1/2$ and 8-PSK, $r=2/3$ TCM systems with $K=2, 3$, and 4 are summarized in Tables 5, 6 and 7, where the E_b / N_o was selected for $P_b = 10^{-8}$ when $E_b / N_i \gg 1$.

The performance of 8-PSK, $r=2/3$ TCM with $K=2, 3$, and 4 is shown in Tables 3 and 4. As can be seen, the required E_b / N_i decreases as the number of memory elements

increases, and the degradation due to PNI is much less for larger K . The conclusion is that TCM systems have significant resistance to PNI when K is large enough.

A comparison between the two TCM systems investigated, both with the same number of memory elements K , was also made. As can be seen in Table 5, the QPSK, $r=1/2$ system has better performance than the 8-PSK, $r=2/3$ system for $K=2$ and 3, but when the instantaneous interference power increases and fraction of time the PNI is on is reduced ($\rho < 0.2$), the performance of the 8-PSK, $r=2/3$ system is better. For $K=4$, the 8-PSK, $r=2/3$ system has better performance.

The two TCM systems were also compared when the number of memory elements in the 8-PSK, $r=2/3$ system is larger than for the QPSK, $r=1/2$ system. From Table 6 we see that the QPSK, $r=1/2$, $K=1$ system has the same performance as the 8-PSK, $r=2/3$, $K=2$ system when $\rho \geq 0.2$, but for $\rho < 0.2$, the 8-PSK, $r=2/3$, $K=2$ system performs better than the QPSK, $r=1/2$, $K=1$ system.

From Table 6, we see that the 8-PSK, $r=2/3$, $K=2$ system is always better than the QPSK, $r=1/2$, $K=1$ system, and the difference increases as the fraction of time the PNI is on decreases. For $\rho = 1$, the 8-PSK, $r=2/3$, $K=3$ system is better than the QPSK, $K=1$ system by 1.4 dB, and for $\rho = 0.2$ the difference increases to 2.1 dB. When $\rho < 0.01$, the 8-PSK, $r=2/3$, $K=3$ system has $P_b < 10^{-5}$ for all E_b / N_i , while the QPSK, $r=1/2$, $K=1$ system requires $E_b / N_i = 19.0$ dB.

From Table 6, we see that for $\rho = 1$ and $\rho = 0.2$, the 8-PSK, $r=2/3$, $K=4$ system is always better than the QPSK, $r=1/2$, $K=1$ system by 3.2 dB and 4.4 dB, respectively. For $\rho = 0.01$ the 8-PSK, $r=2/3$, $K=4$ system has $P_b < 10^{-5}$ for all E_b / N_i , while the QPSK, $r=1/2$, $K=1$ system requires $E_b / N_i = 19.0$ dB.

The two TCM systems were also compared when $K=2$ and $K=3$ for QPSK, $r=1/2$ TCM and 8-PSK, $r=2/3$ TCM, respectively. From Table 7, for $\rho = 0.2$, the QPSK, $r=1/2$ system has better performance than the 8-PSK, $r=2/3$ system, but for $\rho = 0.01$, both systems have $P_b < 10^{-5}$ for all E_b / N_i .

From Table 7, we see that for $\rho = 1$ and $\rho = 0.2$, the 8-PSK, $r=2/3$, $K=4$ system is always better than the QPSK, $r=1/2$, $K=2$ system by 1.5 dB and 0.6 dB, respectively, but for $\rho = 0.01$, both systems have $P_b < 10^{-5}$ for all E_b / N_i .

In this chapter the QPSK, $r=1/2$ and the 8-PSK, $r=2/3$ systems were examined when, in addition to AWGN, pulse-noise interference is also present. A comparison between the two systems having same number of memory elements as well as one TCM system having more memory elements was made. In the next and final chapter, we review the results obtained in this thesis and make recommendations for future research.

V. CONCLUSIONS AND RECOMMENDATIONS

A. CONCLUSIONS

The performance of TCM with both $r=1/2$ encoding and QPSK modulation and $r=2/3$ encoding with 8-PSK modulation for 1, 2, 3, and 4 encoder memory elements was examined in this thesis. The data rate of the latter system is 50% greater than that of the former given the same channel bandwidth. The effect of both AWGN and PNI were considered.

In order to compute the probability of bit error, only the first term in the upper bound, which is the dominant term for $P_b < 10^{-5}$, was used without affecting the precision of the results. A comparison between TCM systems in AWGN only with the same number of memory elements K was made. The QPSK, $r=1/2$ system always has better performance than the 8-PSK, $r=2/3$ system.

The two TCM systems were also compared when the number of memory elements in the 8-PSK, $r=2/3$ system was larger than for the QPSK, $r=1/2$ system and only AWGN was present. It was found that the QPSK, $r=1/2$, $K=1$ system has better performance than the 8-PSK, $r=2/3$, $K=2$ system for all E_b / N_0 . When we increase the number of memory elements in both encoders by a factor of two, we get an improvement, but for $P_b > 10^{-5}$, the QPSK, $r=1/2$ system still has better performance. For $P_b < 10^{-5}$, the 8-PSK, $r=2/3$ system has a slightly better performance, on the order of 0.5 dB. Finally, when the 8-PSK, $r=2/3$ system has four times as many memory elements as the QPSK, $r=1/2$ system, the 8-PSK, $r=2/3$ system achieves a better performance, on the order of 1.6 dB, for $P_b = 10^{-5}$. In this case, we get both a higher data rate and better performance, but the complexity of the decoder increases significantly.

Similar comparisons between QPSK, $r=1/2$ and 8-PSK, $r=2/3$ TCM systems with both AWGN and PNI were also made. The E_b / N_i required decreases as the number of memory elements increases, and the degradation due to PNI is much less for larger K . Both TCM systems have significant resistance to PNI when K is large, and as K

increases, the degradation of the system due to PNI decreases, increasing the robustness of the system in PNI. Even small K results in some immunity from the degradation caused by PNI.

A comparison between both TCM systems, each having the same number of memory elements, was made. The QPSK, $r=1/2$ system has better performance than the 8-PSK, $r=2/3$ TCM system for $K=2$, but as K increases and ρ decreases, the 8-PSK, $r=2/3$ system outperforms the QPSK, $r=1/2$ system. Hence, increased data rates as well as increased robustness when PNI is present can be simultaneously obtained at the cost of a slight increase in required E_b / N_0 .

Finally, a comparison between the QPSK, $r=1/2$ and the 8-PSK, $r=2/3$ TCM systems was made with the latter system having more memory elements than the QPSK, $r=1/2$ system. The performance of the 8-PSK, $r=2/3$ system is better than that of the QPSK, $r=1/2$ system, and the difference between the two systems increases when the fraction of time the PNI is on decreases.

B. RECOMMENDATIONS

In this thesis, the performance of 8-PSK, $r=2/3$ and QPSK, $r=1/2$ TCM in AWGN as well as both AWGN and PNI for $K=1, 2, 3$, and 4 was investigated. The difficulty of the analysis increases exponentially as K increases, and as a result, the performance of the two TCM systems in both AWGN and PNI was not examined for more than four encoder memory elements per encoder. In order to evaluate the systems for large K , up to eight, simulations should be performed, avoiding the analytical difficulties attendant on TCM where K is large.

Also using simulations, the research should be extended to TCM systems with higher code rates such as $r=3/4$ and $r=4/5$, examining the effects of pulse-noise interference.

The relative immunity of TCM to a hostile noise environment is of great importance, especially in military applications, where the intentional interference of communications systems is often a fact.

LIST OF REFERENCES

- [1] G. Ungerboeck, “Channel coding with multilevel phase signals” *IEEE Trans. Inform. Theory*, vol. IT-28, pp. 55-67, January 1982.
- [2] G. Ungerboeck, “Trellis-Coded Modulation with Redundant Signal Sets. Part I: Introduction,” *IEEE Commun. Mag.*, vol. 25, pp. 5-11, February 1987.
- [3] Ezio Bigliery, Dariush Divsalar, Peter J. McLane, and Marvin K. Simon, *Introduction to Trellis-coded Modulation with applications*, Prentice-Hall, Inc., May 1991.
- [4] Konstantinos Pyloudis, *Low Spectral Efficiency Trellis Coded Modulation* Master’s Thesis, Naval Postgraduate School, Monterey, CA, 2006.
- [5] G. Ungerboeck, “Trellis-Coded Modulation with Redundant Signal Sets. Part II: State of the Art,” *IEEE Commun. Mag.*, vol. 25, pp. 12-21, February 1987.
- [6] Clark Robertson, Notes for EC4580 (Error Correction Coding), Naval Postgraduate School, Monterey, CA, 2001 (unpublished).
- [7] B. Sklar, *Digital Communications: Fundamental and Applications*, 2nd edition, Prentice-Hall, Upper Saddle River, NJ, 2001.
- [8] Daniel J. Costello, and Shu Lin, *Error Control Coding: Fundamental and Applications*, 2nd edition, Prentice-Hall, Upper Saddle River, NJ, 2004.
- [9] J. G. Proakis, *Digital Communications*, 4th edition, McGraw Hill, New York, NY, 2001.

THIS PAGE INTENTIONALLY LEFT BLANK

INITIAL DISTRIBUTION LIST

1. Defense Technical Information Center
Ft. Belvoir, Virginia
2. Dudley Knox Library
Naval Postgraduate School
Monterey, California
3. Chairman, Code EC
Department of Electrical and Computer Engineering
Monterey, California
4. Professor R. Clark Robertson, Code EC/Rc
Department of Electrical and Computer Engineering
Monterey, California
5. Professor Tri Ha, Code EC/Ha
Department of Electrical and Computer Engineering
Monterey, California
6. Embassy of Greece, Office of Naval Attache
Washington, D.C.
7. Ioannis Katzourakis
Athens, Greece